Genetic analysis of Nkx2.2 and Nkx2.9 transcription factors in mouse brain development: specific functions in the hindbrain

Von der Fakultät für Lebenswissenschaften

der Technischen Universität Carolo-Wilhelmina

zu Braunschweig

zur Erlangung des Grades

einer Doktorin der Naturwissenschaften

(Dr. rer. nat.)

genehmigte

D i s s e r t a t i o n

von Wassan Jarrar
aus Amman / Jordanien

1. Referent: Professor a.D. Dr..Hans-Henning Arnold
2. Referent: Professor Dr. Martin Korte
eingereicht am: 19.03.2014
mündliche Prüfung (Disputation) am: 11.06.2014

Druckjahr 2014

Vorveröffentlichungen der Dissertation

Teilergebnisse aus dieser Arbeit wurden mit Genehmigung der Fakultät für Lebenswissenschaften, vertreten durch den Mentor der Arbeit, in folgenden Beiträgen vorab veröffentlicht:

Tagungsbeiträge

“Specification of branchio-visceral motor neurons in the murine hindbrain depends on the transcription factors Nkx2.2 and Nkx2.9”

Wassan Jarrar, Hans-Henning Arnold and Andreas Holz

The 44th annual conference of the German Genetics Society (GfG);

September 23 - 25, 2013

Contents

1. Summary

Nkx2.2 and Nkx2.9 are homologous homeodomain transcription factors with overlapping spatio-temporal expression in the developing central nervous system (CNS). They play a role in dorso-ventral patterning of the CNS. In this study, the function of Nkx2.2 and Nkx2.9 in hindbrain development was analyzed, specifically their role in the formation of branchiovisceral motor neurons (bvMNs).

A redundant function of Nkx2.2 and Nkx2.9 was revealed for the correct formation of branchiovisceral motor neuron progenitors (p3). Loss of both, Nkx2.2 and Nkx2.9 transcription factors led to the transformation of progenitor cell fate from bvMN to somatic motor neurons (sMN) in rhombomeres 4 to 7. Changes in cell fate were less evident in *Nkx2.2*$^{-/-}$ and *Nkx2.9*$^{-/-}$ single mutant embryos. In *Nkx2.2;Nkx2.9* double-null embryos a decrease in bvMN cell numbers and a concomitant increase in sMNs was observed. This decrease in bvMNs was most prominent in the caudal rhombomeres of the hindbrain. In fact, all posterior branchiovisceral motor nuclei of the nucleus ambiguus and dorsal motor nucleus of the vagus were missing in late-gestational stages of *Nkx2.2;Nkx2.9* double-null embryos, while the facial motor nucleus was severely reduced and branchiovisceral motor neurons of the anterior trigeminal nucleus were unaffected.

Genetic labeling of the Nkx2.2 cell lineage through Cre-mediated recombination revealed that all branchiovisceral motor neurons represent descendants of p3 progenitor cells. Lineage tracing provided direct evidence that a ventral-to-dorsal transformation of progenitor cell identity occurred in the absence of Nkx2.2 together with Nkx2.9 transcription factors.

In summary, this study provides evidence that both Nkx2.2 and Nkx2.9 transcription factors are required in a redundant cell autonomous manner to determine the subtype identity of branchiovisceral motor neurons in rhombomeres 4 to 7 of the murine hindbrain.

2. Introduction

The hindbrain is an essential part of the brain that controls key physiological functions. It comprises many important neuronal subtypes including those forming the cranial nerves and serotonergic neurons (Lidov and Molliver, 1982; Cordes, 2001; Guthrie, 2007). The proper function of these different neurons is of high significance for vital functions in the adult organism. Cranial nerves coordinate motor activity and sensory functions (Cordes, 2001; Guthrie, 2007). Serotonergic neurons influence respiration and a variety of behavioral functions (Lucki, 1998). Rhythm generators which control respiration also develop in the hindbrain (Champagnat and Fortin, 1997; Mellen and Thoby-Brisson, 2012). Understanding the molecular mechanism of cranial nerve development is of high relevance and importance for a better understanding of congenital cranial dysinnervation disorders in humans (Guthrie, 2007).

The adult hindbrain is comprised of the pons and medulla oblongata. During early embryonic development, the hindbrain is subdivided into 7 or 8 compartments called rhombomeres (r1-r8) (Lumsden and Keynes, 1989). Various signals along the rostro-caudal and dorso-ventral axis of the rhombencephalon provide unique identity to each rhombomere and lead to the differentiation of diverse types of neurons in each rhombomere.

The initial establishment of rhombomeric compartments is regulated by several pathways which act along the rostro-caudal axis of the hindbrain and include FGF and retinoic acid signaling (reviewed in Alexander et al., 2009). Both signaling pathways initiate the expression of specific *Hox* genes which are highly conserved homeodomain transcription factors that provide patterning information to developing tissues along the rostro-caudal axis (Krumlauf, 1994). In vertebrates, a total of 39 *Hox* genes are organized into four gene clusters which are located on different chromosomes. Based on similarities in their sequence and position in the different clusters, 13 paralogous groups (PG) of *Hox* genes are identified and only the paralogous groups 1 to 4 are expressed in the hindbrain. *Hox* genes of one PG usually have the same anterior boundary of gene expression during early development and this boundary corresponds to rhombomere borders (Murphy et al., 1989; Wilkinson et al., 1989). Importantly, the combined expression of several *Hox* genes in a specific rhombomere determines its positional identity. Loss-of-function studies identified the roles of *Hox* genes in determining segmental identity of specific rhombomeres (Studer

et al., 1996; Rossel and Capechhi, 1999; Barrow et al., 2000). Homeodomain proteins that act upstream of *Hox* genes, such as Kreisler, play also an essential role in determining rhombomere identity (McKay et al., 1994; Manzanares et al., 1999). *Hox* genes can thus be used as markers to determine the identity of rhombomeres.

The rostro-caudal positions of cells together with signals along the dorso-ventral axis specify distinct progenitor domains (Jessell, 2000). Sonic hedgehog (Shh), a morphogen secreted by the notochord and floor plate, forms a concentration gradient along the dorso-ventral axis of the spinal cord with highest morphogen levels ventrally (Ericson et al., 1997; Yamada et al., 1993). *Shh* signaling results in the expression of several homeodomain transcription factors (TF). A subset of these TFs are repressed (Class I proteins; such as Pax6 and Pax7) by Shh signaling while others are activated (Class II proteins; e.g. Nkx6.1 and Nkx2.2) (Briscoe et al., 2000). In response to *Shh* signaling and due to cross-repressive interactions between these homeodomain TFs, boundaries between distinct ventral progenitor domains are formed and different neuronal subtypes are generated along the dorso-ventral axis (Briscoe et al., 2000; Briscoe and Ericson, 1999; Jessell, 2000; Muhr et al., 2001; Shirasaki and Pfaff, 2002). Although this model of a morphogen gradient was established for vertebrate spinal cord, it is thought to also apply for patterning of the hindbrain along the dorso-ventral axis, since for instance cranial and spinal motor neurons are lost in *Shh*–deficient mutant embryos (Litingtung and Chiang, 2000). Loss-of-function experiments revealed that specific transcription factors, such as Lhx3, Lhx4, Pax6 and Nkx2.2, are required for determining the subtype of neurons in the spinal cord and hindbrain (Briscoe et al., 1999; Briscoe and Ericson, 1999; Ericson et al., 1997; Sharma et al., 1998).

The most ventral progenitor domain next to the floor plate is referred to as p3 domain that expresses the TFs Nkx2.2 and Nkx2.9 and gives rise to V3 interneurons in the spinal cord (Briscoe et al., 1999; Pabst et al., 2003). In contrast, Nkx2.2 and Nkx2.9-expressing p3 progenitor cells in hindbrain form branchial and visceral motor neurons (Fig.1) (Briscoe et al., 1999; Ericson et al., 1997; Pabst et al., 2003; Pattyn et al., 2000; Pattyn et al., 2003b). Dorsal to the p3 domain, pMN progenitor cells expressing the Olig2 TF give rise to somatic motor neurons in both, the spinal cord and hindbrain (Fig.1) (Takebayashi et al., 2000; Mizuguchi et al., 2001; Novitch et al., 2001; Zhou and Anderson, 2002). Branchial and visceral motor neurons are characterized by the expression of a combination of transcription factors including the homeodomain protein Paired-like homeobox 2b (Phox2b) which is required for the generation of bvMNs (Hirsch et al., 2007; Pattyn et al.,

2000) (Fig.1, b). In contrast, pMN-derived postmitotic somatic motor neurons are characterized by the specific expression of the homeodomain transcription factor Hb9 (Arber et al., 1999; Thaler et al., 1999) (Fig.1, b). The pan-motor neuronal transcription factor Islet-1 is expressed by all postmitotic motor neurons (Ericson et al., 1992; Pfaff et al., 1996) (Fig.1, b).

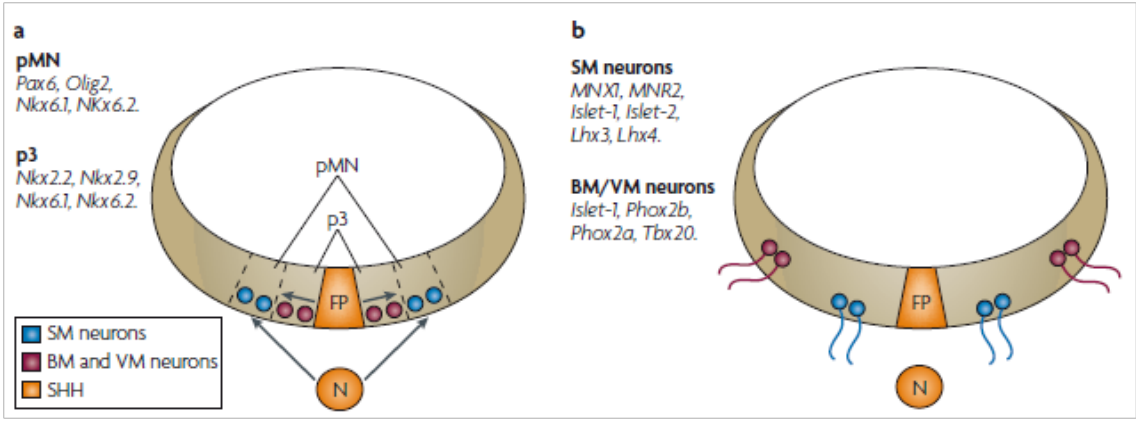

Fig.1: Shh-dependant patterning of cranial motor neurons. The schematic represents a transverse section through the hindbrain (A, B). Shh expression from notochord and floor plate cells forms a gradient that results in the expression of a combination of characteristic transcription factors (as indicated) at different dorso-ventral levels of the hindbrain and in turn leads to the formation of the p3 and pMN progenitor domains (A). BM and VM neurons arise from cells of the p3 progenitor domain and migrate dorsally and extend their axons out of the CNS at common dorsal exit points. In contrast, SM neurons are generated from pMN progenitor cells, reside at ventral positions and exit the CNS ventrally (B). N, notochord; FP, floor plate; SHH, sonic hedgehog; SM, somatic motor; BM, Branchiomotor; VM, visceral motor; CNS, central nervous system. Adapted from (Guthrie, 2007).

The cell bodies (somata) of all three motor neuron subtypes reside in the hindbrain and their axons exit the rhombencephalon and form the motor components of the cranial nerves (Fig.1, Fig.2, Table.1) (Chandrasekhar, 2004; Cordes, 2001; Guthrie, 2007). It is important to realize that branchial and visceral (branchiovisceral) motor neurons (bvMNs) are formed along most of the rostro-caudal axis of the hindbrain (r2-r7) and in the anterior part of the spinal cord (C1- C4/C5) (Pattyn et al., 2000; Pattyn et al., 2003a), while generation of somatic motor neurons (sMNs) is confined to rhombomere 5 and rhombomere 7 as well as to the spinal cord along the entire rostro-caudal axis (Novitch et al., 2001; Arber et al., 1999) (Fig.2, bvMNs in blue and sMNs in red; Table.1). The cell bodies of branchial and visceral motor neurons migrate during early development dorsally and their axons leave the CNS from distinct dorso-lateral exit points present in specific rhombomeres (i.e. r2, r4, r6 and several exit points in r7) and the cervical spinal cord. In contrast, somatic motor

neurons do not migrate over long distances during development and remain close to the midline. Their axons exit the CNS ventrally in rhombomeres 5 and 7 as well as along the rostrocaudal axis of the spinal cord (Fig.1, b; Fig.2) (Sharma et al., 1998; Niederlander and lumsden, 1996).

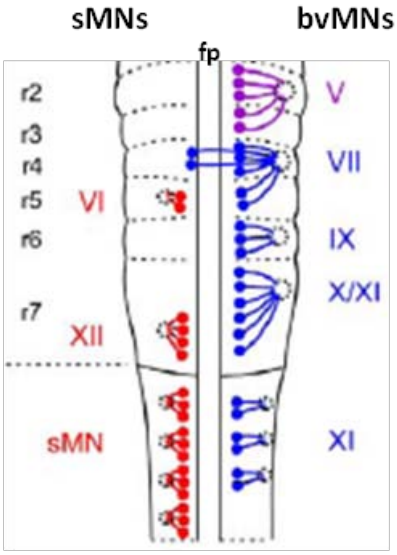

Fig.2: Cranial motor nerve organization. The schematic represents the organization of somatic and branchiovisceral motor neurons within the hindbrain (r2-r7) and cervical spinal cord at E10.5. branchiovisceral motor neurons (bvMNs) are shown in blue and purple while somatic motor neurons (sMNs) are shown in red. The cell bodies of the sMNs are born and reside ventrally near the FP. sMN axons exit the CNS ventrally. In contrast, bvMNs are born ventrally, migrate dorsally and extend their axonal projections to leave the CNS from common dorsal exit points. bvMN axons leave the hindbrain from defined exit points in r2, r4, r6 and several exit points in r7 and the cervical spinal cord. The neurons crossing the midline to the contralateral side represent vestibuloacoustic neurons (VIII). FP: floor plate, sMN: somatic motor neurons, bvMN: branchiovisceral motor neurons, r: rhombomere, Roman numbers denote the motor nerves: V, trigeminal; VI, abducens; VII, facial; IX, glossopharyngeal; X, vagal; XI; accessory with both its cranial and spinal roots; XII, hypoglossal. Modified from (Lieberam et al., 2005). Cranial nerves originating from the midbrain are not illustrated.

The three classes of cranial motor nerves have different synaptic targets; branchial motor nerves innervate muscles derived from the branchial arches, while visceral motor nerves innervate parasympathetic ganglia, smooth muscles and visceral organs. Somatic motor nerves form synapses only on somite-derived skeletal muscles (see Table.1 for details) (Cordes, 2001; Guthrie, 2007). Cell bodies of cranial motor neurons cluster and form a series of motor nuclei at distinct rostro-caudal levels (Fig.2, see Table.1 for names of nuclei) (Chandrasekhar, 2004; Cordes, 2001; Guthrie, 2007). Each motor nucleus is comprised of motor neurons, which originate in individual or different rhombomeres but each motor nucleus contains only a single class (subtype) of motor neurons (Fig.2, Table.1) (Chandrasekhar, 2004; Cordes, 2001; Guthrie, 2007; Jacob et al, 2001).

Cranial nerve	Subtype	Origin	Nucleus	Target tissue
Trigeminal (V)	Branchiomotor	r2, r3	Trigeminal motor	Muscles of mastication
Abducens (VI)	Somatic motor	r5	Abducens	Extraocular muscles (Lateral rectus muscle)
Facial (VII)	Branchiomotor	r4	Facial motor	Muscles of facial expression
	Visceral motor	r5	Superior salivatory	Tear glands, salivary glands
Glossopharyngeal (IX)	Branchiomotor	r6	Nucleus ambiguus	Stylopharyngeus muscle
	Visceral motor	r6	Inferior salivatory	Parotid gland/ Otic ganglion
Vagus (X)	Branchiomotor	r7	Nucleus ambiguus	Laryngeal and pharyngeal muscles
	Visceral motor	r7	Dorsal motor	Non-striated muscle of thoracic and abdominal viscera
Cranial accessory (XI)	Branchiomotor	r7	Nucleus ambiguus	Laryngeal and pharyngeal muscles
Spinal accessory (XI)	Branchiomotor	C1-C4/C5	Accessory nucleus	Sternocleidomastoid and trapezius muscles
Hypoglossal (XII)	Somatic motor	r7	Hypoglossal	Tongue muscles

Table 1: Motor components of cranial nerves, their subtype, their rhombomere of origin, their nuclei and their target tissue. Adapted with modifications from (Cordes, 2001; Chandrasekhar, 2004; Guthrie, 2007). Cranial nerves originating from the midbrain are not listed.

In summary, the subtype of a cranial motor nerve is determined by its rostro-caudal and dorso-ventral position in the brainstem and the molecular composition of transcription factors.

Cell bodies of branchiovisceral motor neurons undergo complex migration patterns during development (Chandrasekhar, 2004). Most branchiovisceral motor neurons migrate dorso-laterally within their rhombomere of origin to reach a position near their axonal exit points. As a characteristic example for most branchiovisceral motor neurons, cell bodies of the trigeminal motor nucleus are born in rhombomere 2 at E10.5 and migrate dorso-laterally during embryonic development (E11.5 - E13.5) to form a cell cluster (Fig.3, grey). All motor neurons of the trigeminal motor nucleus (nV) send their axons into the periphery through a single doso-lateral exit point in close vicinity of the formed motor nucleus. Unlike all other bvMNs, cell bodies of the facial branchiomotor (FBM) neurons undergo a characteristic three-directional migration (Auclair et al., 1996; Garel et al., 2000; Pattyn et

al., 1997; Studer et al., 1996; Song, 2007); they are born in rhombomere 4 between E10.5 and E11.5 and start a unique caudal (tangential) migration along the midline at embryonic day 11.5. Upon their arrival in r6, FBM neurons migrate now laterally and then radially to eventually cluster at the pial surface and form the facial motor nucleus (at about E14.5 all facial motor cell bodies have reached their final position) (Fig.3, black). Another special characteristic of FBM neurons is the fan-shaped structure of their axons which forms during migration (Fig.3, black). This fan-shape results from an extention of FBM axons towards dorso-lateral exit points in r4 at embryonic day E10.5 and the axons exit the CNS and reach their targets even before the first motor neuron cell bodies start their caudal migration. At the time point when the FBM cell bodies start migrating caudally, their axons extend along the cell bodies toward r6 and thereby form the characteristic fan-shape structure (Fig.3, black) (Song, 2007).

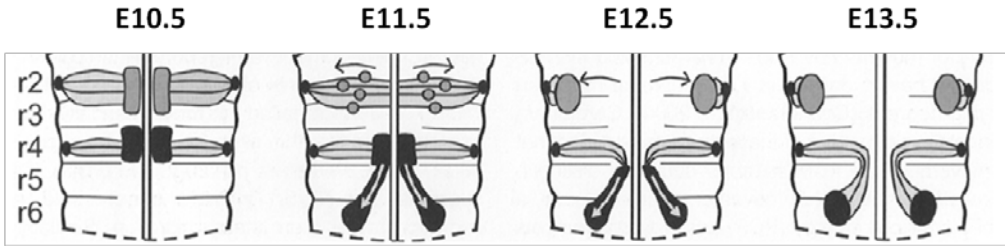

Fig.3: The migration pattern of branchiovisceral motor neurons. A schematic that demonstrates the migration pattern of the trigeminal (grey) and facial (black) motor neurons in open-book preparations of the hindbrain of mouse embryos from E10.5 to E13.5. Trigeminal motor neurons are born in r2 (E10.5) and migrate dorsally (E11.5) to reach their final dorsal position at embryonic stage E12.5. In contrast, branchial facial motor neurons are born in r4 (E10.5 - E11.5) and migrate caudally at about E11.5 to reach their final destination in r6 where they then migrate laterally to form the facial nucleus at E13.5. Note that facial motor neurons start extending their axons at E10.5 towards their dorsal exit point in r4 and the cell bodies migrating caudally leave their axons behind to leave with the other axons from the dorsal exit point. Adapted with modifications from (Song, 2007).

Taken together, rostro-caudal and dorso-ventral patterning provide important positional information to motor neurons and define the identity of cranial motor nerves formed in specific rhombomeres.

Nkx2.2 and Nkx2.9 are structurally related homeodomain transcription factors (Hartigan and Rubenstein, 1996; Pabst et al., 1998). The Shh-dependent spatial and temporal expression patterns of Nkx2.2 and Nkx2.9 overlap from E9.0 until E10.5/E11.0 in the ventral p3 progenitor cells of the spinal cord and hindbrain (Briscoe et al., 1999; Holz et al., 2010; Lek et al., 2010; Pabst et al., 1998; Pabst et al., 2000; Pattyn et al., 2003a).

Cells of the p3 progenitor domain produce postmitotic interneurons, termed V3, in the spinal cord (Briscoe et al., 1999). V3 commissural interneurons contribute to a robust and rhythmic locomotion (Zhang et al., 2008). V3 interneurons of the spinal cord are missing in *Nkx2.2*$^{-/-}$ single mutant embryos and appear to be transformed into somatic motor neurons (Briscoe et al., 1999). However, *Nkx2.9*$^{-/-}$ single mutant embryos show no defects in the formation of V3 interneurons (Pabst et al, 2003). Interestingly, Nkx2.9 expression has almost vanished when V3 interneurons differentiate in wildtype spinal cord (i.e. at about E10.5), while the expression of Nkx2.2 persists longer (Briscoe et al., 1999). These findings suggest that *Nkx2.2*, but not *Nkx2.9*, is required for the differentiation of V3 interneurons in the spinal cord. Despite the ventral-to-dorsal change of cell fate in the absence of *Nkx2.2*, the p3 progenitor domain remains intact in the spinal cord of *Nkx2.2*$^{-/-}$ single mutants (Briscoe et al., 1999, Holz et al 2010). This indicates that the *Nkx2.2* gene is required only for the differentiation of V3 interneurons but is dispensable for the formation of the p3 progenitor cells. This raises the possibility that the expression of the similar transcription factor Nkx2.9 in early p3 progenitors (before E10.5 in the rodent spinal cord) is sufficient to establish the p3 progenitor domain in absence of *Nkx2.2* (Briscoe et al., 1999). To test this hypothesis, double-knockout mice deficient for both *Nkx2.2* and *Nkx2.9* were analyzed. In absence of both Nkx2.2 and Nkx2.9 functionally related TFs, progenitor cells in the p3 domain are misspecified and entirely replaced by somatic motor neuron progenitors (Holz et al., 2010). This result demonstrates that *Nkx2.2* and *Nkx2.9* can function redundantly in the establishment of p3 progenitors in spinal cord.

It is also known that Nkx2.2 and Nkx2.9 TFs play an essential role in the formation and/or maintenance of the floor plate in the spinal cord, since floor plate cells were severely reduced in the spinal cord of *Nkx2.2;Nkx2.9* double-null embryos (Holz et al., 2010; Lek et al., 2010). The influence of *Nkx2.2* and *Nkx2.9* on the floor plate also occurs in a redundant fashion, because loss of both *Nkx2.2* and *Nkx2.9* genes resulted in a stronger defect compared to *Nkx2.2*$^{+/-}$*;Nkx2.9*$^{-/-}$ compound mutants or *Nkx2.2*$^{-/-}$ and *Nkx2.9*$^{-/-}$ single

mutants (single mutants showed no defects in floor plate) (Holz et al., 2010; Lek et al., 2010).

In contrast to the developing spinal cord, p3 progenitors of the hindbrain do not give rise to specific interneurons but rather form branchiovisceral motor neurons (Pattyn et al., 2003a). In the rodent CNS most bvMNs are born between E9.5 and E10.5 with the exception of rhombomere 4 where bvMN generation continues until E11.5. This time period overlaps tightly with the expression patterns of Nkx2.2 and Nkx2.9, which are detectable in p3 progenitors of the wildtype hindbrain from E9.0 until E11.0 (Briscoe et al., 1999; Pabst et al., 1998).

Interestingly, p3-derived postmitotic bvMNs are formed normally in the hindbrain of *Nkx2.2*$^{-/-}$ single mutant embryos. Likewise, *Nkx2.9*$^{-/-}$ single mutant embryos also produce bvMNs, although they show moderate defects in the spinal accessory nerve (XI), which appears thinner and shorter (Pabst et al., 2003). These results strongly suggest that both *Nkx2.2* and *Nkx2.9* genes function redundantly in the formation of bvMNs in the hindbrain.

Subsequent to the generation of bvMNs, serotonergic neurons are also generated from p3 progenitors in the hindbrain except rhombomere 4, which continues to form bvMNs (Briscoe et al., 1999; Pattyn et al., 2003a; Lidov and Molliver, 1982). The first serotonergic neurons can be detected in the hindbrain at E10.75 (Pattyn et al., 2003a). Serotonergic neurons are characterized by the secretion of the neurotransmitter serotonin (also called 5-HT) (Jacobs and Azmitia, 1992; Kiyasova and Gaspar, 2011; Lidov and Molliver, 1982; Richerson, 2004). Anatomical studies showed that serotonergic neurons in the hindbrain send their axonal projections rostrally connecting to midbrain and forebrain, and caudally to connect with the spinal cord (Jacobs and Azmitia, 1992). *Nkx2.2* is required for the formation of serotonergic neurons since 5-HT^{+} neurons are almost completely missing in *Nkx2.2*$^{-/-}$ knockout animals (Briscoe et al., 1999; Pattyn et al., 2003a).

2.1 Aim of this study

The homeodomain transcription factors, Nkx2.2 and Nkx2.9, show spatio-temporally overlapping expression from E9.0 until E11.0 in the murine hindbrain (Briscoe et al., 1999). During this period, most of the branchiovisceral motor neurons (bvMNs) are generated presumably from Nkx2.2 and Nkx2.9 co-expressing p3 progenitor cells of the hindbrain (Briscoe et al., 1999; Ericson et al., 1997; Pabst et al., 2003; Pattyn et al., 2000; Pattyn at el., 2003a; Pattyn et al., 2003b). In *Nkx2.2*$^{-/-}$ single mutant mice, the generation of branchiovisceral motor neurons was reported to be normal (Briscoe et al., 1999), whereas mutants lacking *Nkx2.9* showed partial defects in the spinal accessory nerve (XI) which consists of branchial motor neurons (Pabst et al., 2003; Dillon et al., 2005; Bravo-Ambrosio et al., 2012; this work). The phenotypes of *Nkx2.2*$^{-/-}$ and *Nkx2.9*$^{-/-}$ single mutants are consistent with redundant functions of both transcription factors in the determination of bvMNs. Therefore, it is a major aim of this study to experimentally test the ideas of functional redundancy in hindbrain. To this end, I investigated the consequences of disrupting both the *Nkx2.2* and *Nkx2.9* genes for the development of bvMNs. The following questions were specifically addressed: 1) Does the formation of bvMNs require the gene activity of *Nkx2.2* and *Nkx2.9* and what is the fate of progenitor cells in the p3 domain of hindbrain in the absence of both transcription factors? 2) Are there different effects of the disruption of *Nkx2.2* and *Nkx2.9* genes on cell specification at different axial levels of the rhombencephalon? 3) What is the precise cell lineage relationship of Nkx2.2^{+} progenitor cells during hindbrain development in normal and *Nkx2.2;Nkx2.9* double-null mouse embryos? To assess the cell lineage the *Nkx2.2*^{cre} mouse was generated and examined in detail here. 4) Is the floor plate in hindbrain affected in *Nkx2.2;Nkx2.9* double-null mouse embryos, as it was shown for the spinal cord (Holz et al., 2010)?

3. Results

3.1 Analysis of the formation of branchiovisceral motor neurons in the hindbrain of *Nkx2.2;Nkx2.9* double-null mouse embryos

To understand the fate of p3 cells in the absence of Nkx2.2 and/or Nkx2.9 transcription factors and to test the hypothesis of functional redundancy, the hindbrain of *Nkx2.2* and *Nkx2.9* deficient embryos was analyzed in this work. The analysis was done in detail on the entire rostro-caudal axis of the hindbrain throughout embryonic development. Specifically, branchiovisceral progenitors and their postmitotic motor neuron descendants as well as their axonal projections were examined.

3.1.1 The vagus and accessory nerves are severely reduced in *Nkx2.2*$^{-/-}$*;Nkx2.9*$^{-/-}$ mutant embryos

Cranial motor nerves were analyzed on whole-mounts of mouse embryos at E10.5 by immunostaining using an antibody directed against the neuronal cell adhesion molecule NCAM-L1. Most sensory ganglia and cranial nerves of the branchiovisceral subtype (V, VII/VIII, IX, X, XI) and the somatic hypoglossal nerve (XII) could be visualized in wildtype and various *Nkx2.2* and *Nkx2.9* mutant embryos (Fig.4) (see Table.1 for the nomenclature of the different cranial nerves). The abducens nerve (VI) could not be visualized in whole-mount preparations with this method (Huber and Huettl, 2011). It is important to realize that most cranial nerves contain motor neurons and also sensory components (Cordes, 2001, Huber and Huettl, 2011). Only the two somatic motor nerves (VI, XII) and the branchial accessory nerve (XI) lack any sensory fascicles.

The accessory motor nerve (XI) is comprised of two different components: a spinal root, which extends from motor neurons of the cervical spinal cord (Snider and Palavali, 1990; Wentworth and Hinds, 1978), and a cranial root, which originates from bvMNs of the most posterior part of the rhombencephalon (Gilland and Baker, 1993; Chandrasekhar, 2004) (Fig.4, A). The spinal root fibers exit the CNS dorsolaterally at the cervical region C1 to C4/ C5 and join together as they ascend rostrally, forming the so-called spinal accessory nerve (SAN) (Bravo-Ambrosio and Kaprielian, 2011; Schubert and Kaprielian, 2001; Snider and Palavali, 1990) (Fig.4, A). When the SAN reaches the caudal hindbrain it descends and moves near the vagus nerve (X) on its path to target the sternocleidomastoid and trapezius muscles in the neck (Gottschall et al., 1980; Brichta et al., 1987; Kandel, 2000).

In contrast, axons of the cranial root of the accessory nerve exit in close proximity to caudal motor nerves of the vagus (X). They ascend rostrally together with the spinal accessory roots before joining the vagus nerve (X) to innervate the pharynx and larynx muscles (Ryan et al., 2007; Ong et al., 2010).

As reported before, cranial nerve morphology in the *Nkx2.2*$^{-/-}$ single mutant was completely normal in comparison to the wildtype embryo (Fig.4, A, B). In *Nkx2.9*$^{-/-}$ mutants, the spinal accessory nerve (SAN) appeared much thinner and shorter in accordance with previously published reports (Pabst et al., 2003; Dillon et al., 2005) (Fig.4, C). In *Nkx2.2*$^{+/-}$*;Nkx2.9*$^{-/-}$ compound embryos, containing only one functional *Nkx2.2* gene but lacking both *Nkx2.9* alleles, a more pronounced reduction in length and thickness of the accessory nerve was observed (Fig.4, D). Finally, in embryos totally devoid of *Nkx2.2* and *Nkx2.9*, complete loss of the accessory nerve, both cranial and spinal roots, was observed (Fig.4, E). In addition, a severe reduction of the vagus nerve was noticed (Fig.4, E). It is of interest to note that the defect of the vagus nerve was also apparent in *Nkx2.9*$^{-/-}$ single mutant embryos (Pabst et al., 2003; Fig.4, C) and in *Nkx2.2*$^{+/-}$*;Nkx2.9*$^{-/-}$ compound mutant embryos albeit less severe (Fig.4, D). The more rostral branchiovisceral nerves (V, VII/VIII, IX) as well as the somatic hypoglossal motor nerve (XII) seemed unaffected in all analyzed genotypes (Fig.4). Since the NCAM-L1 antibody fails to distinguish between motor and sensory axons, the observed nerve staining in *Nkx2.2;Nkx2.9* double-null mutants is likely to include sensory ganglia of the vagus (Fig.4, E). It is also known that the facial and glossopharyngeal nerves contain sensory fibers and ganglia (Barlow, 2002; Cordes, 2001; Huber and Huettl, 2011).

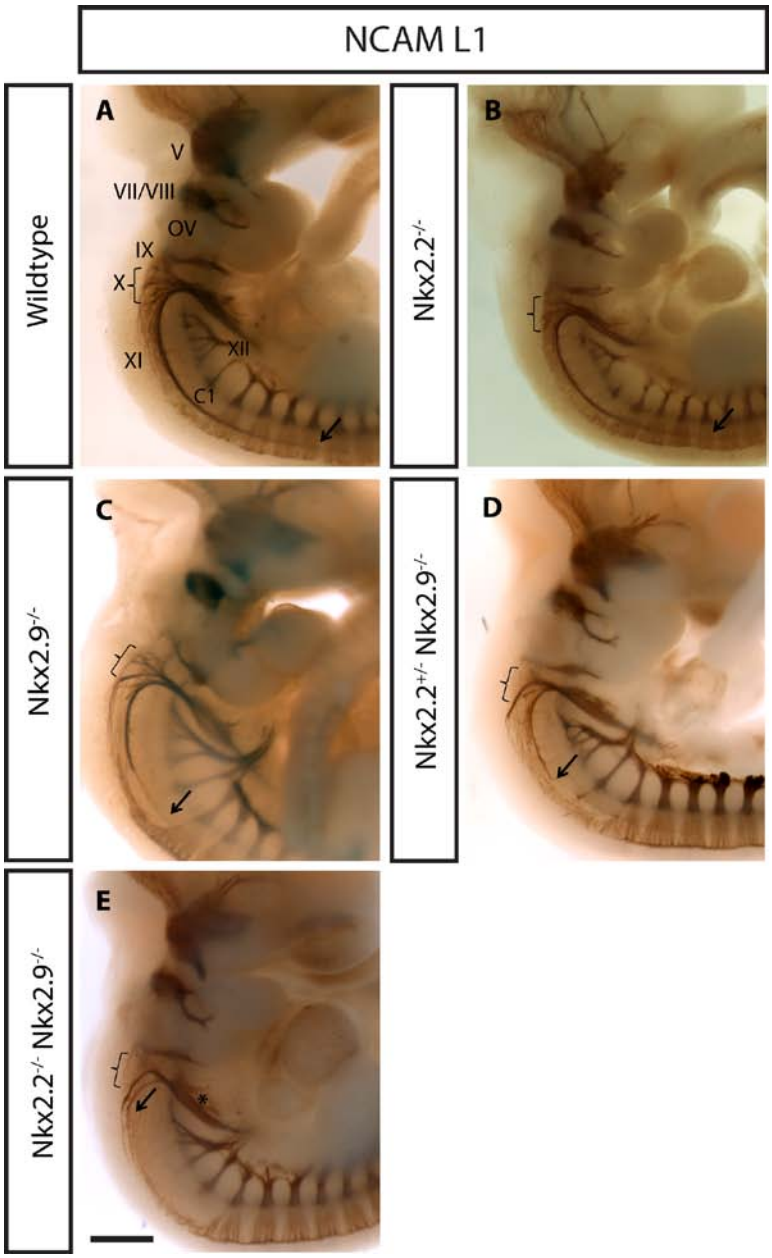

Fig.4: Severe defects in the vagus nerve (X) and the accessory nerve (XI) of *Nkx2.2;Nkx2.9* double-null mice. A whole-mount immunostaining with an antibody directed against the NCAM-L1 antigen in wildtype (A), *Nkx2.2*$^{-/-}$ (B), *Nkx2.9*$^{-/-}$ (C), *Nkx2.2*$^{+/-}$*;Nkx2.9*$^{-/-}$ (D) and *Nkx2.2;Nkx2.9* double-null mutant (E) embryos at E10.5 was performed. Note the thinner and shorter accessory nerve in *Nkx2.9*$^{-/-}$ mutants (C, arrow marks the caudal end of the accessory nerve) in comparison to the wildtype (A, arrow) and the *Nkx2.2*$^{-/-}$ mutant embryos (B, arrow). The roots of the vagus nerve seemed to be also mildly affected in the *Nkx2.9*$^{-/-}$ mutants (C, bracket marks the region from which the roots of the vagus normally arise). The defects of the accessory nerve and the vagus nerve were enhanced in the *Nkx2.2*$^{+/-}$*;Nkx2.9*$^{-/-}$ compound mutant embryos (D, arrow and brackets) while in the *Nkx2.2;Nkx2.9* double-null mutant embryo the roots of vagus nerve were severely reduced and the accessory nerve was completely missing (E, arrow and brackets). The organization of the remaining cranial nerves in mutant embryos (B, C, D, E) was indistinguishable to the wildtype embryos (A). The asterisk in (E) marks the staining of sensory fibers of the vagus. The depicted data is representative to Wildtype (n = 4), *Nkx2.2*$^{-/-}$ (n = 2), *Nkx2.9*$^{-/-}$ (n = 6), *Nkx2.2*$^{+/-}$*;Nkx2.9*$^{-/-}$ (n = 6), *Nkx2.2*$^{-/-}$*;Nkx2.9*$^{-/-}$ (n = 5). Cranial nerves are designated in roman numerals: V,trigeminal nerve; VII,facial nerve; VIII,vestibuloacoustic nerve; IX, glossopharyngeal nerve; X,vagus nerve; XI, accessory nerve; XII,hypoglossal nerve. OV: otic vesicle. C1: first cervical nerve. Scale bar 500 µm.

Similar to the results of NCAM-L1 staining, the pan-neuronal neurofilament antibody (Dodd et al., 1988) also revealed severe reduction of the vagus nerve (X) and the accessory nerve (XI) in *Nkx2.2;Nkx2.9* double-null mutant embryos (Fig.5, D). Similar defects were observed in *Nkx2.9*$^{-/-}$ single and *Nkx2.2*$^{+/-}$*;Nkx2.9*$^{-/-}$ compound mutant embryos but to a lesser degree (Fig.5, B, C). Taken together, these observations of cranial nerve defects in *Nkx2.2;Nkx2.9* mutant mice (Fig.4 and Fig.5) seem to apply to branchiovisceral motor nerves, i.e. the vagus nerve and the accessory nerve, but not to somatic motor nerves.

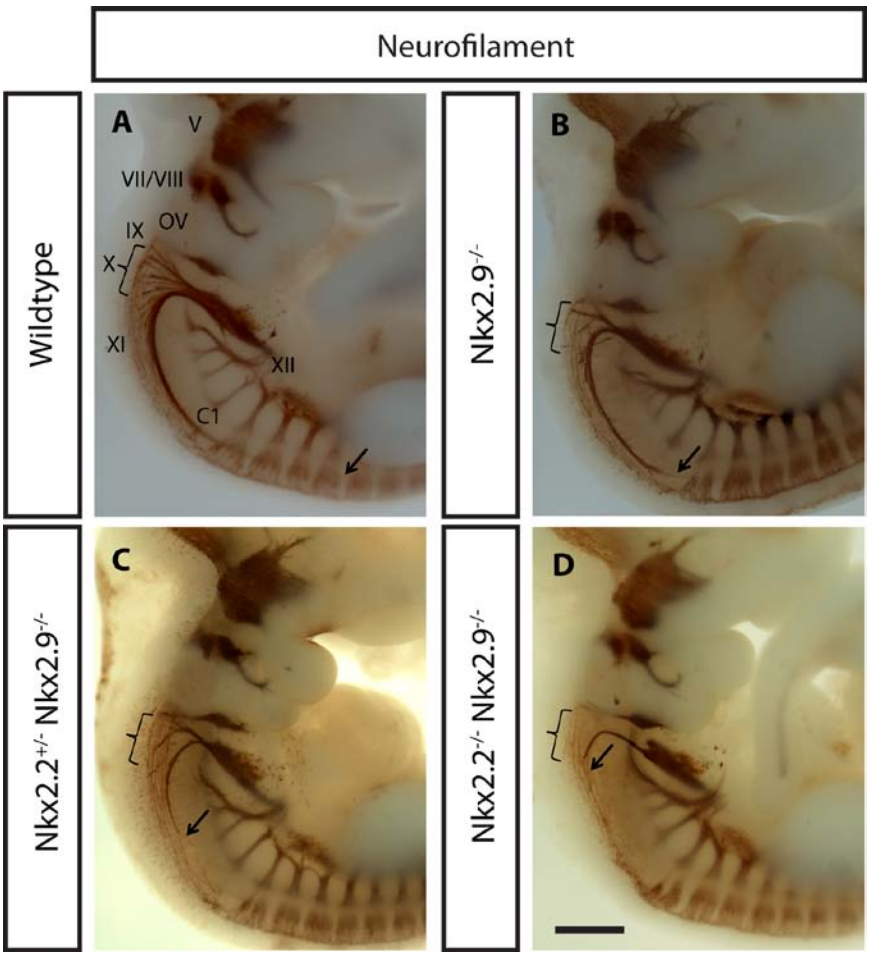

Fig.5: Neurofilament staining revealed defects in the vagus nerve (x) and the accessory nerve (XI) of *Nkx2.2;Nkx2.9* double-knockout embryos. Whole-mount immunostainings with a widely used antibody directed against the neurofilament antigen confirmed the previous results. The results obtained in wildtype (A) *Nkx2.9*$^{-/-}$ (B), *Nkx2.2*$^{+/-}$*;Nkx2.9*$^{-/-}$ (C) and *Nkx2.2;Nkx2.9* double-null mutant (D) embryos at E10.5 are highly similar to the former findings. The partial defects in the vagus nerve and accessory nerve are evident in the *Nkx2.9*$^{-/-}$ mutants (arrow and bracket in B), are more severe in *Nkx2.2*$^{+/-}$*;Nkx2.9*$^{-/-}$ compound mutants (arrow and bracket in C) and the nerve roots are almost absent in *Nkx2.2;Nkx2.9* double-null mutant embryos (arrow and bracket in D). The depicted data is representative to wildtype (n = 2), *Nkx2.9*$^{-/-}$ (n = 13), *Nkx2.2*$^{+/-}$*;Nkx2.9*$^{-/-}$ (n = 5), *Nkx2.2*$^{-/-}$*;Nkx2.9*$^{-/-}$ (n = 6). The arrow marks the caudal end of the accessory nerve and the bracket marks the region from which the roots of the vagus normally arise. Cranial nerves are designated in roman numerals: V,trigeminal nerve; VII,facial nerve; VIII, vestibuloacoustic nerve IX; glossopharyngeal nerve; X,vagus nerve; XI, accessory nerve; XII,hypoglossal nerve. C1: first cervical nerve. OV: otic vesicle. Scale bar 500 µm.

3.1.2 Phox2b-expressing branchiovisceral motor neurons are drastically reduced in *Nkx2.2;Nkx2.9* double-null embryos

It is of importance to realize that bvMNs are formed almost along the entire antero-posterior axis of the hindbrain from rhombomeres r2 to r7. In addition, this motor neuron subtype is also present in the most rostral part of the spinal cord (C1- C4/C5) (Pattyn et al., 2000; Pattyn et al., 2003a). The formation of branchiovisceral motor neurons along the antero-posterior axis of the hindbrain was analyzed in the various *Nkx2.2;Nkx2.9* mutant and control mice.

To identify bvMNs in the murine hindbrain, immunohistochemistry was performed on whole-mounts of E10.5 mouse embryos with an antibody directed against the homeodomain transcription factor Phox2b that is required for the generation of bvMNs (Hirsch et al., 2007; Pattyn et al., 2000). Phox2b serves as reliable marker for mature bvMNs and late progenitor cells before they become postmitotic (Dubreuil et al., 2000; Dubreuil et al., 2002; Pattyn et al., 2000). “Openbook preparations” of hindbrains stained for Phox2b were obtained by cutting the neural tube along the roof plate and flat-mounting the rhombencephalon for subsequent imaging (Fig.6).

As seen in the wildtype, Phox2b^{+} branchiovisceral motor neurons are born in abundance at embryonic stage E10.5 along both sides of the ventral midline of the rhombencephalon (Fig.6, A, black arrowhead). The stronger accumulation of Phox2b seen in rhombomeres 2 and 4 corresponds to precursors of the branchial trigeminal (V) and facial (VII) motor neurons, respectively (Pattyn et al., 1997). It is important to note that most of the cells of the medial and dorsal Phox2b^{+} columns represent cell populations which are distinct from motor neurons. These cells are born in the dorsal half of the hindbrain in close proximity to the roof plate (Dauger et al., 2003; Gaufo et al., 2003; Gray et al., 2008; Sieber et al., 2007; Thoby-Brisson et al., 2009) (Fig.6, A, red and green arrowhead). Hence, bvMNs that have already completed their dorsal migration at this time of development (Pattyn et al., 2000) cannot be distinguished from the dorsally born cell populations.

When compared to wildtype control, *Nkx2.2*$^{-/-}$ and *Nkx2.9*$^{-/-}$ single knockout mice as well as *Nkx2.2*$^{+/-}$*;Nkx2.9*$^{-/-}$ compound mutants showed no differences in Phox2b-expression in the hindbrain (Fig.6, B, C, D). However, *Nkx2.2;Nkx2.9* double-knockout mutants exhibited clearly reduced ventral expression of Phox2b. Significantly, this decline was more pronounced in the posterior part of the hindbrain (Fig.6, E). A reduction of Phox2b-

expressing branchial motor neurons of the facial nerve at rhombomere 4 was also evident (Fig.6, E, asterisk). In rhombomere 2, no difference in the Phox2b expression pattern was detected in mutant embryos regardless of the genotype. Taken together, these observations suggest that in the absence of both Nkx2.2 and Nkx2.9 transcription factors Phox2b^{+} bvMNs which are born ventrally are decreased in cell number. It appears that bvMNs of caudal rhombomeres are more affected and that this loss of Phox2b expression occurs in a graded fashion along the A/P axis.

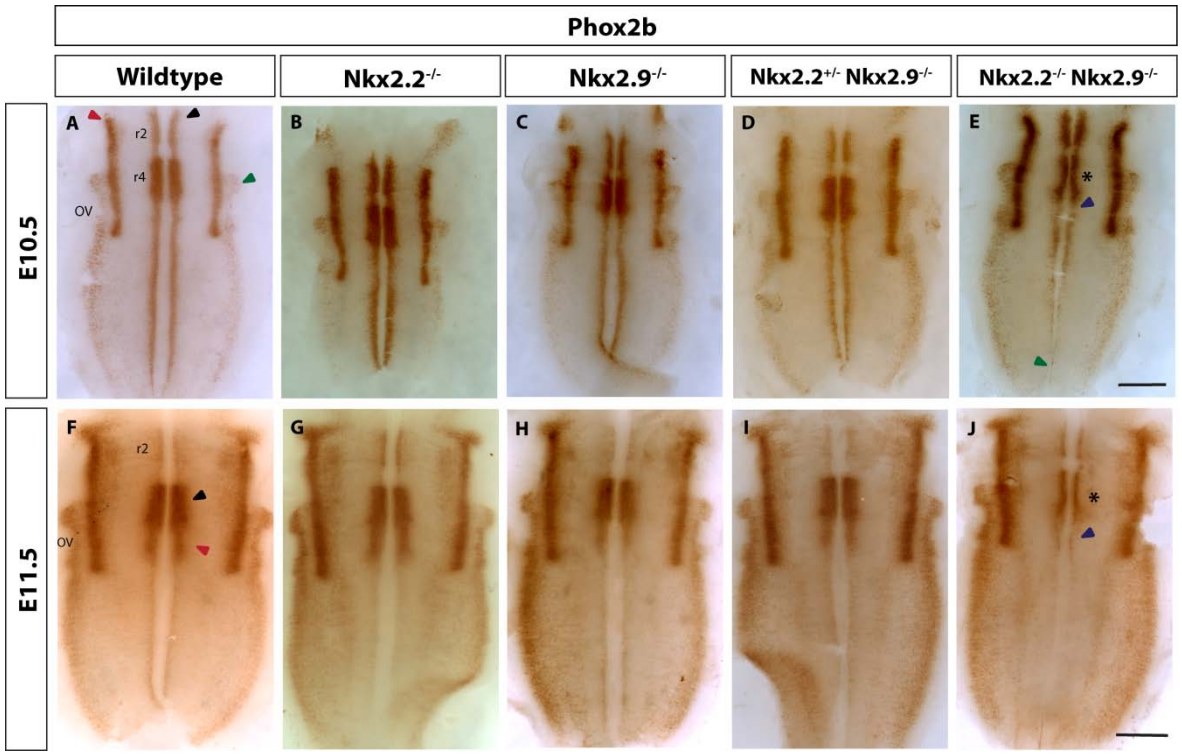

Fig.6: A gradual reduction of Phox2b-expressing branchiovisceral motor neurons along the antero-posterior axis of the hindbrain with the most pronounced defects in posterior rhombomeres. Top view on openbook preparations of the hindbrain wildtype (A, F), *Nkx2.2*$^{-/-}$ (B, G), *Nkx2.9*$^{-/-}$ (C, H), *Nkx2.2*$^{+/-}$*;Nkx2.9*$^{-/-}$ (D, I) and *Nkx2.2;Nkx2.9* double-knockout (E, J) embryos at E10.5 (A - E) and E11.5 (F - J). After performing a whole-mount immunohistochemical detection of Phox2b-expressing branchiovisceral precursors and postmitotic motor neurons, the neural tube covering the entire rhombencephalon was dissected, cut open at its dorsal roof plate, and flattened with its dorsal side up. The anterior end of the hindbrain points in all panels to the top. The ventral columns (black arrowhead in A) correspond to bvMNs, which are born exclusively at this location and will migrate dorsally after they exit the cell cycle at around E10.5-E11 (Dubreuil et al., 2000; Dubreuil et al., 2002). The ventral accumulation of Phox2b expression close to the anterior end of the rhombencephalon represents the trigeminal and the branchial facial motor neurons located in r2 and r4, respectively. The medial (A, red arrowhead) and dorsal (A, green arrowhead) Phox2b^{+} stripes of cells are populations which have nothing to do with bvMNs (see below for a detailed description). Note that using this assay no changes in Phox2b-expression in *Nkx2.2*$^{-/-}$ and *Nkx2.9*$^{-/-}$ as well as *Nkx2.2*$^{+/-}$*;Nkx2.9*$^{-/-}$ compound mutants were detectable in comparison to wildtype animals (A-D). Embryos lacking both Nkx2.2 and Nkx2.9 transcription factors, however, showed a severe decrease in the expression of Phox2b starting at the level of rhombomere 4 (E, asterisk) and extending to the caudal parts of the hindbrain (E, green arrowhead). In the wildtype, at E11.5, the branchial motor neurons of the facial are still generated (F, black arrowhead) and they start migrating into rhombomere 5 (F, red arrowhead). Notice that the majority

of Phox2b-expressing bvMNs along the AP axis already migrated dorsally like the motor neurons of the trigeminal in rhombomere 2 (hence less staining ventrally and more along the dorso-ventral axis). In embryos lacking *Nkx2.2* and *Nkx2.9*, a drastic decrease in the expression of Phox2b at the level of rhombomere 4 was evident (J, asterisk). In addition, Phox2b expression was faint in rhombomere 5 (J, blue arrowhead) and almost absent ventrally in more caudal parts of the hindbrain (J). The medial stripe of Phox2b expression which starts rostrally at the level of r2 and is demarcated caudally at the r6/r7 boundary represents progenitors of dorsal DB2 domain (A, red arrowhead) from which RTN neurons and other neuronal types originate (Gray et al., 2008; Thoby-Brisson et al., 2009; Sieber et al., 2007). The dorsal column of Phox2b expression extends from the r3/r4 boundary until the posterior end of the hindbrain and corresponds to the dorsal DA3 progenitor domain which gives rise to noradrenergic visceral sensory interneurons of the nucleus of the solitary tract (NTS) and area postrema (AP) (A, green arrowhead) (Dauger et al., 2003; Gaufo et al., 2003; Gray et al., 2008; Sieber et al., 2007). The illustrated data of E10.5 embryos is representative to: Wildtype (n = 5), *Nkx2.2*$^{-/-}$ (n = 3), *Nkx2.9*$^{-/-}$ (n = 2), *Nkx2.2*$^{+/-}$*;Nkx2.9*$^{-/-}$ (n = 5), *Nkx2.2*$^{-/-}$*;Nkx2.9*$^{-/-}$ (n = 4) and of the E11.5 embryos is representative to: Wildtype (n = 2), *Nkx2.2*$^{-/-}$ (n = 2), *Nkx2.9*$^{-/-}$ (n = 3), *Nkx2.2*$^{+/-}$*;Nkx2.9*$^{-/-}$ (n = 2), *Nkx2.2*$^{-/-}$*;Nkx2.9*$^{-/-}$ (n = 4). OV: otic vesicle. Scale bar: 500µm.

In order to test the possibility whether the initial decrease in bvMNs in *Nkx2.2;Nkx2.9* double-knockout mutant mice might be compensated by increased generation of bvMNs at later stages of development, I also analyzed the expression of Phox2b in a later embryonic stage at E11.5 (Fig.6, F - J). During development, branchiovisceral motor neurons are known to undergo complex migrations (Chandrasekhar, 2004). At E11.5, most branchiovisceral motor neurons are postmitotic and are migrating dorsally (Pattyn et al., 2000; Song et al., 2006). Accordingly, at this time point the intensity of the ventral Phox2b signal was decreased significantly along the entire A/P-axis in comparison to the earlier developmental stage at E10.5 (Fig.6, A). For instance, in the anterior rhombomere 2 of wildtype embryos, ventral Phox2b^{+} cells disappeared almost completely, likely due to the dorsal migration of r2-derived trigeminal motor neurons (Fig.6, F - J). An exception to this common migration behavior of branchiovisceral motor neurons can be seen in rhombomeres 4 and 5, where facial motor neurons of the branchial subtype are born in r4 and migrate caudally through r5 (Fig.6, F) to reach rhombomere 6 at the age of E12.5 (Auclair et al., 1996; Garel et al., 2000; Pattyn et al., 1997; Studer et al., 1996). In agreement with my previous observations at E10.5 (Fig.6, A - E), the expression pattern of Phox2b was not appreciably different in wildtype, *Nkx2.2*$^{-/-}$ and *Nkx2.9*$^{-/-}$ single as well as *Nkx2.2*$^{+/-}$*;Nkx2.9*$^{-/-}$compound mutant embryos (Fig.6, F - I). However, the ventral Phox2b^{+} expression domain was severely affected in *Nkx2.2;Nkx2.9* double-null mutant embryos along the A/P-axis with the exception of trigeminal motor neurons in rhombomere 2, which were present and seemed to migrate normally (Fig.6, J). Interestingly, in rhombomere 4 the reduction in Phox2b-expressing branchial precursors of the facial

nucleus was more obvious at E11.5 than at E10.5 (Fig.6, E, J). It is likely that the faint expression of Phox2b in rhombomere 5 represents branchial motor neurons of the facial nucleus migrating caudally together with a few residual bvMNs that originate in r5. However, at E11.5 Phox2b expression posterior to rhombomere 5 was almost extinguished in the ventral domain of mutants lacking both Nkx2.2 and Nkx2.9 transcription factors (Fig.6, J). Together, these data strongly indicate the loss of bvMNs in *Nkx2.2;Nkx2.9* double-null mutant embryos causing a motor neuron defect that is not compensated during subsequent development.

3.1.3 Transformation of bvMN into sMN fate in *Nkx2.2;Nkx2.9* double-knockout mouse embryos

Using triple-immunofluroscent stainings, the molecular phenotype of the potentially affected motor neuron subtypes was analyzed in control and *Nkx2.2;Nkx2.9* mutant animals in rhombomeres r2 to r7. pMN-derived somatic motor neurons (sMNs) are generated in the hindbrain exclusively in rhombomeres 5 and 7 (Novitch et al., 2001; Arber et al., 1999). In rhombomere 7, sMNs of the hypoglossal motor nerve and bvMNs contributing to the vagal and cranial accessory motor nerves are generated (Gilland and Baker, 1993). Postmitotic sMNs specifically express the homeodomain factor Hb9 (Arber et al., 1999; Thaler et al., 1999). The pan-motor neuronal transcription factor Islet-1 is produced by all postmitotic motor neurons (Ericson et al., 1992; Pfaff et al., 1996). Using this information, I identified postmitotic somatic motor neurons by co-expression of Hb9 and Islet1 and postmitotic bvMNs by co-expression of Phox2b and Islet1 in the ventral half of the hindbrain in wildtype embryos (Fig.7, A). According to published results (Ericson et al., 1997; Pattyn et al., 2000; Song et al., 2006), postmitotic Phox2b^{+}/Islet1^{+} bvMNs migrate from ventral to dorsal positions (Fig.7, A, B) and form a cell cluster close to their dorso-lateral exit points. In contrast, postmitotic sMNs do not leave their original ventral position and project axons from the CNS at distinct ventral exit points (Ericson et al., 1997; Sharma et al., 1998). In the *Nkx2.2*$^{-/-}$ mutant, a slight but significant and consistent decrease in numbers of Phox2b^{+}/Islet1^{+} bvMNs was observed (Fig.7, C). This phenotype appeared to be slightly stronger in *Nkx2.9*$^{-/-}$ single mutant embryos (Fig.7, E). The numbers of Hb9^{+}/Islet1^{+} sMNs appeared increased in both *Nkx2.2*$^{-/-}$ and *Nkx2.9*$^{-/-}$ single mutants (Fig.7, C, E). The observed changes in the number of both motor neuronal subpopulations, bvMNs and sMNs, suggest a possible transformation of fate. In *Nkx2.2*$^{+/-}$*;Nkx2.9*$^{-/-}$ compound mutants expressing only one functional copy of the *Nkx2.2* gene, changes of the

neuronal subtype were clearly stronger (Fig.7, G). In double mutant mouse embryos lacking both *Nkx2.2* and *Nkx2.9*, bvMNs were almost completely absent, whereas the numbers of sMN cells were significantly increased, and they were located ectopically in the normal territory of bvMNs (Fig.7, I).

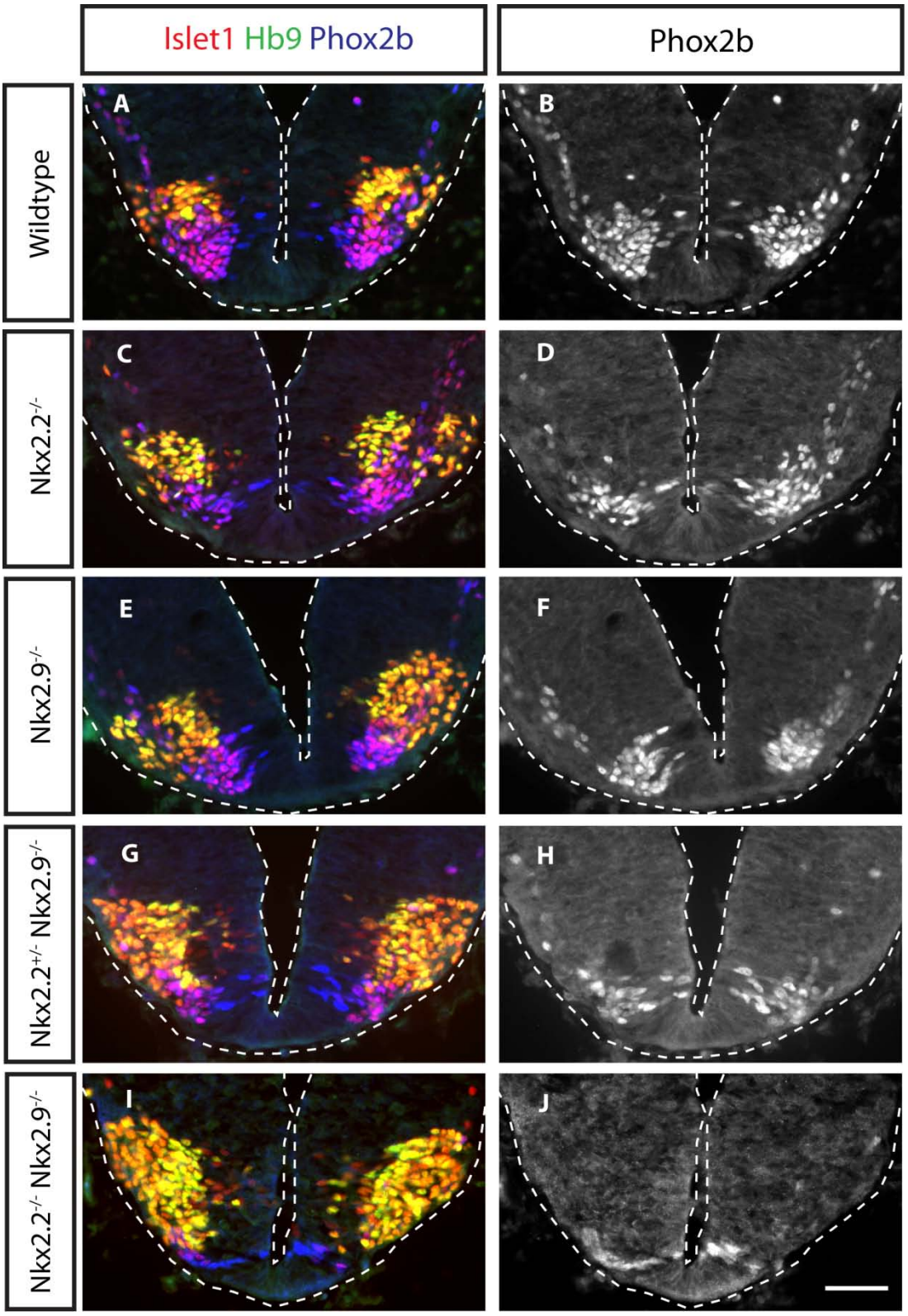

Fig.7: A significant reduction in the number of branchiovisceral motor neurons accompanied by an increase in the number of somatic motor neurons is observed in rhombomere 7 of embryos lacking the Nkx2.2 and Nkx2.9 transcription factors. An immunohistochemical detection of Phox2b (blue), Hb9 (green) and Islet1 (red) was performed on transverse sections of rhombomere 7 of wildtype (A), *Nkx2.2*$^{-/-}$ (C), *Nkx2.9*$^{-/-}$ (E), *Nkx2.2*$^{+/-}$*;Nkx2.9*$^{-/-}$ (G) and *Nkx2.2*$^{-/-}$*;Nkx2.9*$^{-/-}$ (I) embryos at E10.5. For better evaluation, Phox2b expression is also displayed alone as a black and white image (B, D, F, H, and J). Note the progressive reduction in Phox2b^{+}/Islet1^{+} bvMN cells (appearing violett in the merged image) in embryos with less copies of the *Nkx2.2* and *Nkx2.9* genes (C-J) . In contrast, a gradual increase in Hb9^{+}/Islet1^{+} sMN cell numbers (yellow cells) is observed in Nkx2 mutants (C-J) when compared to the wildtype animals (A, B). The images show the ventral parts of the hindbrain, with the ventral end directed to the bottom and dotted lines demarcating the hindbrain tissue boundaries. For each genotype three to five embryos were analyzed. Scale bar: 50 µm.

Quantification of both ventrally located motor neuron subpopulations and the ANOVA test confirmed the statistically significant loss of the bvMNs in all mutant hindbrains at the level of rhombomere 7 (Fig.8, A). Likewise, the increase in sMNs was also significant in *Nkx2.9*$^{-/-}$, *Nkx2.2*$^{+/-}$*;Nkx2.9*$^{-/-}$ and *Nkx2.2*$^{-/-}$*;Nkx2.9*$^{-/-}$ mutant animals. The total number of postmitotic motor neurons expressing Islet1 was not significantly different in all examined mutants compared to wildtype mice (Fig.8, B).

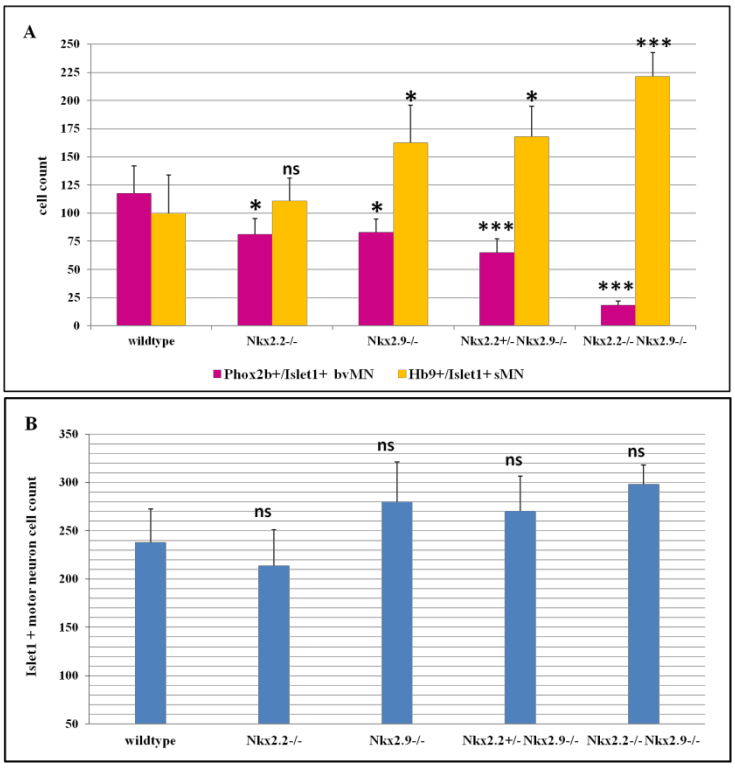

Fig.8: A statistically- significant reduction in the number of bvMNs which was accompanied by significant increase in the number of sMNs was detected in rhombomere 7 of *Nkx2.2;Nkx2.9* mutants. (A) Ventrally-residing Phox2b^{+}/Islet1^{+} bvMNs and Hb9^{+}/Islet1^{+} sMNs were counted in controls and mutant embryos. Notice the gradual decrease in the number of bvMNs and the concurrent increase in the number of Hb9^{+}/Islet1^{+} sMNs in mutants containing a lower number of *Nkx2.2;Nkx2.9* gene copies. Data are expressed as mean ±SD. For statistical evaluation an ANOVA

test was employed and its result was indicated in the figure as follows: ns: not significant (i.e. p >0.05), significant *: p < 0.05, highly significant ***: p <0.0001. For each genotype, three to five embryos were analyzed and various serial sections of r7 were utilized for cell quantification (wildtype (n=27), *Nkx2.2*$^{-/-}$ (n=21), *Nkx2.9*$^{-/-}$ (n=29), *Nkx2.2*$^{+/-}$*;Nkx2.9*$^{-/-}$ (n=24), *Nkx2.2*$^{-/-}$*/Nkx2.9*$^{-/-}$ (n=31), n represents the total number of sections analyzed). (B) Islet1 expressing postmitotic motor nuclei residing ventrally were counted and differences in Islet1^{+} cells in all mutants, regardless of the analyzed genotype, were statistically not significant in comparison to the wildtype animals.

In summary, these results strongly suggest but do not prove that in the absence of Nkx2.2 together with Nkx2.9 branchiovisceral motor neurons are converted to the fate of somatic motor neurons.

Besides rhombomere 7, rhombomere 5 represents the only other area of the hindbrain in which both, somatic and branchiovisceral motor neurons arise. Specifically, bvMNs of the facial motor nerve and sMNs of the abducens motor nerve are born in rhombomere 5 (Chandrasekhar, 2004; Fritzsch, 1996; Sharma et al., 1998). The analysis of motor neuron subtypes at rhombomere 5 provided very similar results as in rhombomere 7. The clear reduction of Phox2b/Islet1 co-expressing branchiovisceral motor neurons was accompanied by the substantial increase of postmitotic Hb9^{+}/Islet1^{+} somatic motor neurons in *Nkx2.2;Nkx2.9* double-null mutants (Fig.9).

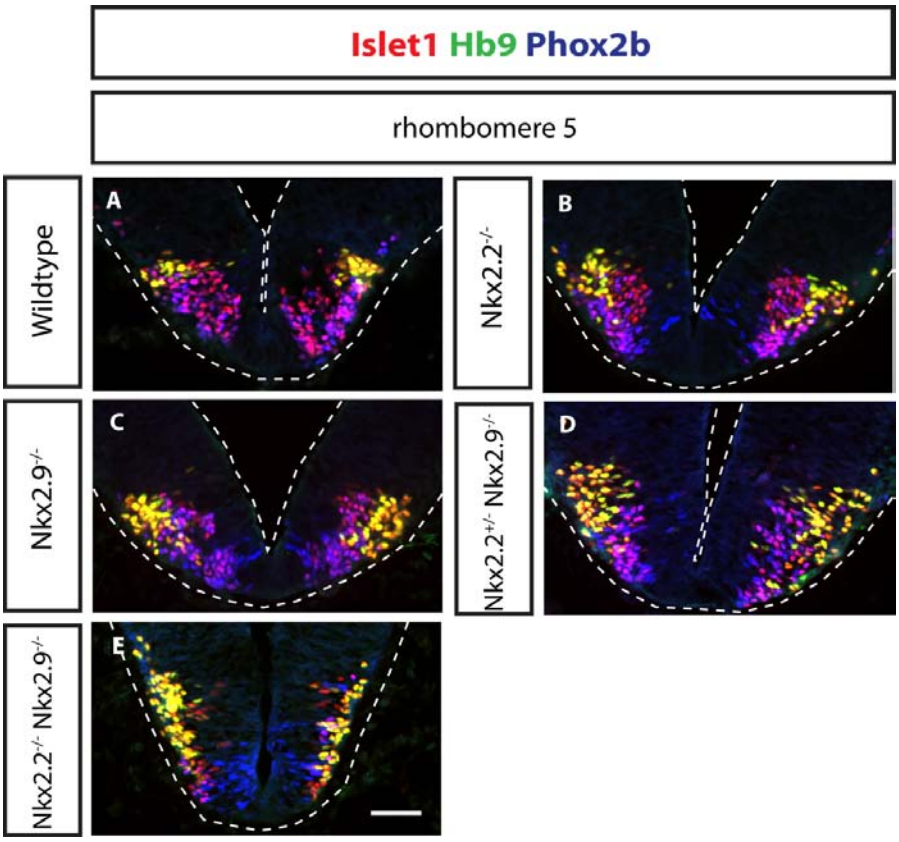

Fig.9: In rhombomere 5, the numbers of branchiovisceral motor neurons were significantly reduced in mice lacking the *Nkx2.2* and *Nkx2.9* genes at E10.5. Similar to findings of motor neuron subtype identity in r7, the decrease in bvMN cells in rhombomere 5 coincides with an increase in the number of somatic motor neurons in *Nkx2.2;Nk2x.9* double-null mutants. The Islet1, HB9, and Phox2b antigens were visualized by immunoflourescent stainings in the wildtype and several different *Nkx2* mutant genotypes as indicated. All images display the ventral parts of the hindbrain. The dotted lines demarcate the boundaries of hindbrain tissue. Highly comparable data was obtained by analyzing 3 to 5 embryos of each genotype. Scale bar: 50 µm.

3.1.3.1 Somatic motor neurons arise ectopically in rhombomere 4 and rhombomere 6 of *Nkx2.2;Nkx2.9* double-knockout embryos

Generation of motor neurons was also analyzed in those regions of the hindbrain that usually are devoid of sMNs and form exclusively branchiovisceral motor neurons (this work; Arber et al., 1999; Novitch et al., 2001; Pattyn et al., 2000; Pattyn et al., 2003b). In the wildtype hindbrain sMNs are lacking in rhombomeres 2 to 4 and in rhombomere 6 (Fig.10). However, these hindbrain areas give rise to Phox2b/Islet-1-expressing bvMNs, contributing to the trigeminal (V), facial (VII), and glossopharyngeal (IX) nerves (Fig.10, A, F, K).

In the anterior rhombomeres 2 and 3, a mild but consistent reduction in the numbers of postmitotic Phox2b^{+}/Islet1^{+} bvMNs was observed in all *Nkx2.2;Nkx2.9* mutants with the strongest effect in embryos lacking both *Nkx2.2* and *Nkx2.9* genes (Fig.10, A-E). However, rhombomeres 4 and 6 of *Nkx2.2;Nkx2.9* double-null embryos showed a drastic reduction of postmitotic bvMNs (Fig.10, J and O), while other *Nkx2.2* and *Nkx2.9* mutant genotypes showed intermediate numbers of bvMNs. *Nkx2.2$^{-/-}$* single mutant embryos exhibited almost no defects (Fig.10, G, L). A slight reduction of bvMNs was apparent in *Nkx2.9$^{-/-}$* single and *Nkx2.2$^{+/-}$;Nkx2.9$^{-/-}$* compound mutants (Fig.10, H, M, I, N). Surprisingly, ectopic sMNs were detected in rhombomeres 4 and 6 of *Nkx2.2$^{+/-}$;Nkx2.9$^{-/-}$* compound and *Nkx2.2;Nkx2.9* double-null mutant embryos (Fig.10, I, N, J, O). In these rhombomeres, r4 and r6, few ectopic sMNs were also visible in mutant animals that lacked only *Nkx2.9* (Fig.10, H, M).

Taken together, most ectopic somatic motor neurons were detected in mutants lacking both *Nkx2.2* and *Nkx2.9* genes.

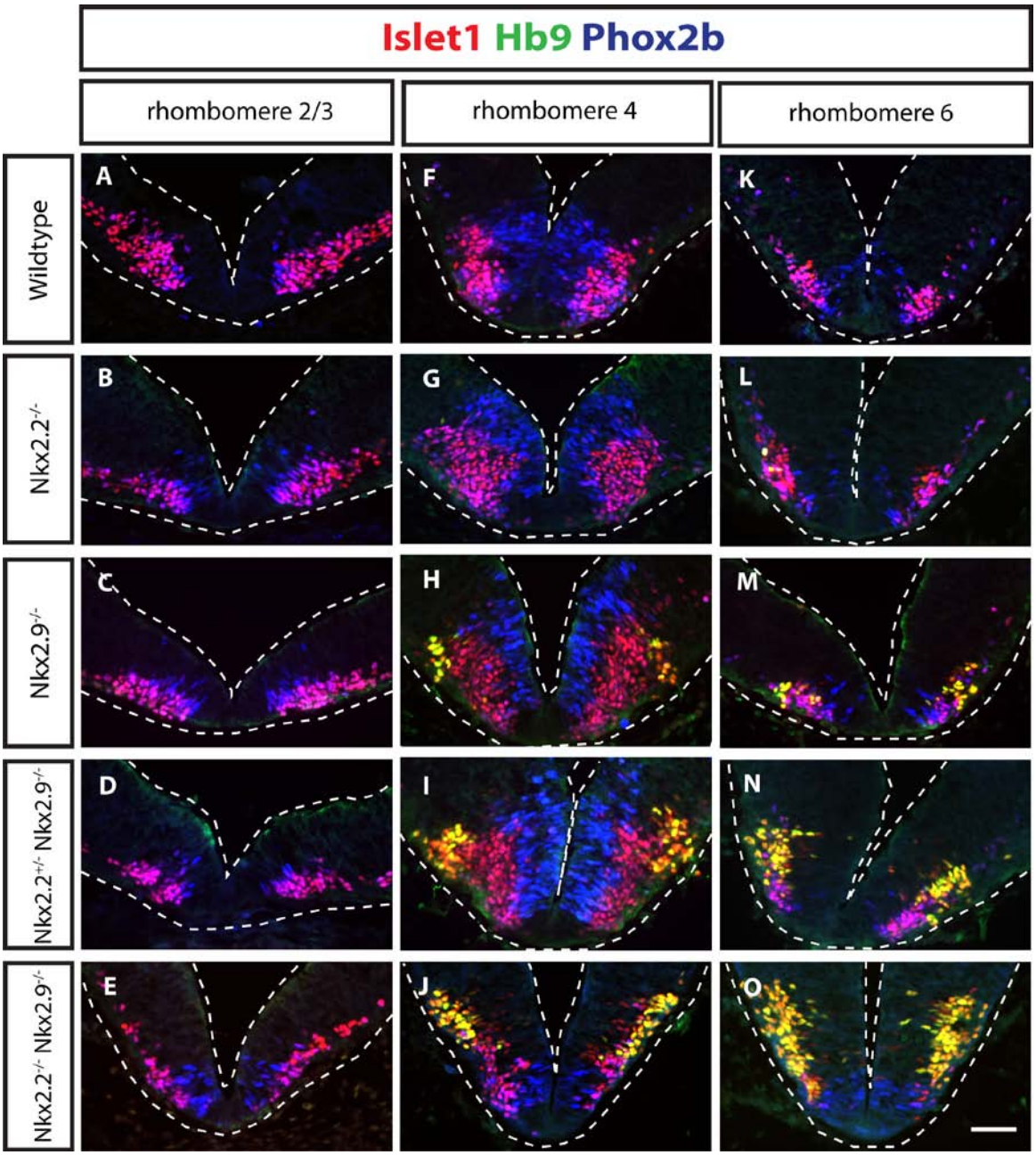

Fig.10: Ectopic presence of somatic motor neurons in rhombomere 4 and 6 of *Nkx2.2;Nkx2.9* mutants. An Immunohistochemistry using antibodies directed against Phox2b (blue), Hb9 (green) and Islet1 (red) was performed on transverse sections of rhombomere r2-r3 (A - E), r4 (F - J), r6 (K - O) of wildtype (A, F, K, n= 4), *Nkx2.2*$^{-/-}$ (B, G, L, n= 3), *Nkx2.9*$^{-/-}$ (C, H, M, n= 3), *Nkx2.2*$^{+/-}$*;Nkx2.9*$^{-/-}$ (D, I, N, n= 4) and *Nkx2.2*$^{-/-}$*;Nkx2.9*$^{-/-}$ mutant (E, J, O, n= 6) embryos at E10.5. A gradual reduction in Phox2b^{+}/Islet1^{+} bvMN cells (violett) is detected in *Nkx2.9*$^{-/-}$ single (H, M) and *Nkx2.2*$^{+/-}$*;Nkx2.9*$^{-/-}$ compound mutants (I, N) while a strong reduction in bvMNs is observed in *Nkx2.2*$^{-/-}$*;Nkx2.9*$^{-/-}$ mutant embryos (J, O) in comparison to *Nkx2.2*$^{-/-}$ single mutant (G, L) and wildtype embryos (F, K). This defect coincides with an atypical presence of Hb9^{+}/Islet1^{+} sMN cells (yellow cells) in *Nkx2.9*$^{-/-}$, *Nkx2.2*$^{+/-}$*;Nkx2.9*$^{-/-}$ and *Nkx2.2;Nkx2.9* double null mutant embryos (H - J, M - O). In *Nkx2.2*$^{-/-}$, the reduction of bvMNs is accompanied by the detection of very few ectopic Hb9^{+}/Islet1^{+} cells in rhombomere 6 (L). All images depict the ventral parts of the hindbrain (pointing to the bottom). The dotted lines demarcate tissue boundaries. Scale bar: 50 µm.

Since the drastic reduction of bvMNs was observed in r4 of *Nkx2.2;Nkx2.9* double-null embryos, a defect that coincided with the ectopic presence of sMNs at rostro-caudal positions that usually are devoid of this cell type, I analyzed whether these changes are the result of an alteration in rhombomere identity. Whole-mount immunostaining was performed on E10.5 embryos using an antibody directed against the Hox gene Hoxb1, the expression of which becomes restricted to rhombomere 4 in the E9.5 mouse embryo. It was demonstrated that this Hox gene is essential for the generation of facial branchial motor neurons (Bell et al., 1999; Gaufo et al., 2000; Goddard et al., 1996; Studer et al., 1996). Hoxb1 expression in the *Nkx2.2;Nkx2.9* double-null mutant was however, indistinguishable from wildtype animals, indicating that the positional identity of r4 has been maintained (Fig.11).

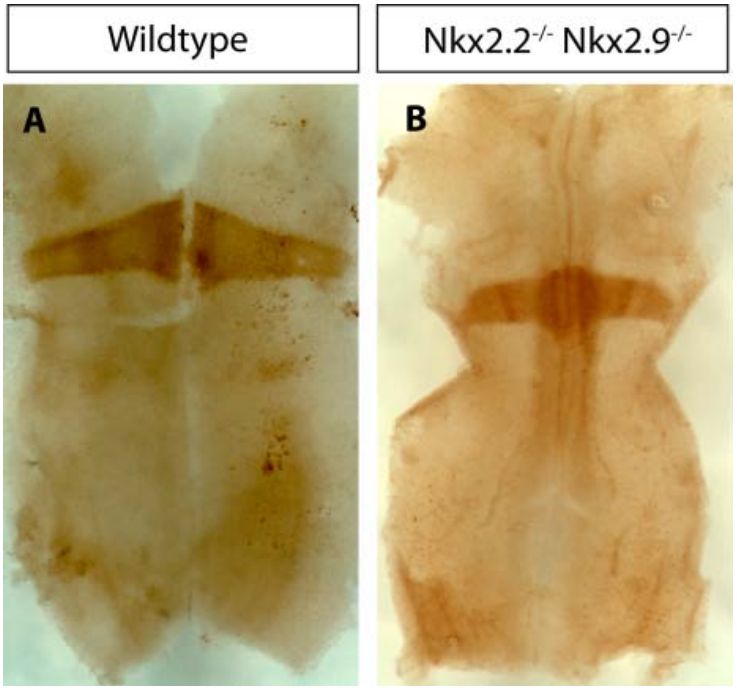

Fig.11: The identity of rhombomere 4 is not altered in mutants lacking *Nkx2.2* and *Nkx2.9*. A whole-mount immunohistochemistry using an anti-Hoxb1 antibody was performed on wildtype (A) and *Nkx2.2;Nkx2.9* double-knockout mutant (B) embryos at E10.5. Depicted are openbook preparations of the hindbrain. Notice that there are no changes in the expression pattern of Hoxb1, a Hox gene that is known to provide segmental identity to r4 (Guthrie et al., 1992).

In summary, these data showed a drastic loss of branchiovisceral motor neurons almost along the entire rostro-caudal axis of the hindbrain of *Nkx2.2;Nkx2.9* double-null mice. Most interestingly, regions of the hindbrain (i.e. r4 and r6) that usually lack somatic motor neurons in the wildtype showed the ectopic presence of $HB9^{+}$/$Islet^{+}$ cells in mutants, strengthening the idea that Nkx2.2 and Nkx2.9 together promote the cell fate of bvMNs and prevent sMN fate during the early development of the murine hindbrain.

3.1.3.2 Most motor nuclei of branchiovisceral cranial nerves are lost in late-gestational *Nkx2.2;Nkx2.9* double-knockout mutant mice

In late gestational embryos, at E15.5, bvMNs and sMNs arrange into discrete motor nuclei (see introduction, Table.1) which can be visualized by in-situ hybridizations using the antisense peripherin RNA probe on serial transverse sections through the brainstem (pons and medulla oblongata) of wildtype and *Nkx2.2* and *Nkx2.9* mutant embryos. The peripherin gene encodes an intermediate filament protein which is expressed in all peripherally projecting neurons including the nuclei of cranial nerves (Escurat et al., 1990).

After cell migrations during E11.5-E12.5, branchiovisceral motor neurons reach their final destination and form distinct nerve nuclei (Cordes, 2001; Guthrie, 2007). Using the peripherin RNA probe, the nuclei of the trigeminal (nV), facial (nVII), vagal (dmnX) motor nerves and the nucleus ambiguus (nA) were detected in wildtype embryos (Fig.12, A, K, P). I also identified the abducens (nVI) and hypoglossal (nXII) nuclei, both of which are formed exclusively by somatic motor neurons and are located close to the ventricle (Fig.12, F, P).

In *Nkx2.2*$^{-/-}$ and *Nkx2.9*$^{-/-}$ single mutant embryos no obvious differences in size or position of bvM and sM nuclei were seen in comparison to wildtype embryos (Fig.12, B, G, L, Q, C, H, M, R). In *Nkx2.2*$^{+/-}$*;Nkx2.9*$^{-/-}$ compound mutant embryos, however, the most posterior motor nucleus, the nucleus ambiguus (nA) was consistently reduced in size, although the other branchiovisceral motor nuclei appeared normal (Fig.12, D, N, white box in S). Moreover, all posterior branchiovisceral motor nuclei such as the nA and dmnX were entirely lacking in *Nkx2.2;Nkx2.9* double-null mutants (Fig.12, T, black arrow and white box, respectively). The facial motor nucleus (nVII) was significantly smaller than normal (Fig.12, O). Significantly, the anterior trigeminal nucleus (nV) in *Nkx2.2;Nkx2.9* double-null mice showed essentially no difference in size compared to wildtype mice (Fig.12, E).

In sharp contrast to the branchiovisceral motor nuclei, the somatic motor nuclei, abducens (nVI) and hypoglossal (nXII), were present and even somewhat bigger in size in *Nkx2.2;Nkx2.9* double-knockout animals (Fig.12, J, white arrow in T). Enlargement of the abducens nucleus was also detectable in *Nkx2.9*$^{-/-}$ single and *Nkx2.2*$^{+/-}$*;Nkx2.9*$^{-/-}$ compound mutants, although less pronounced (Fig.12, H- I).

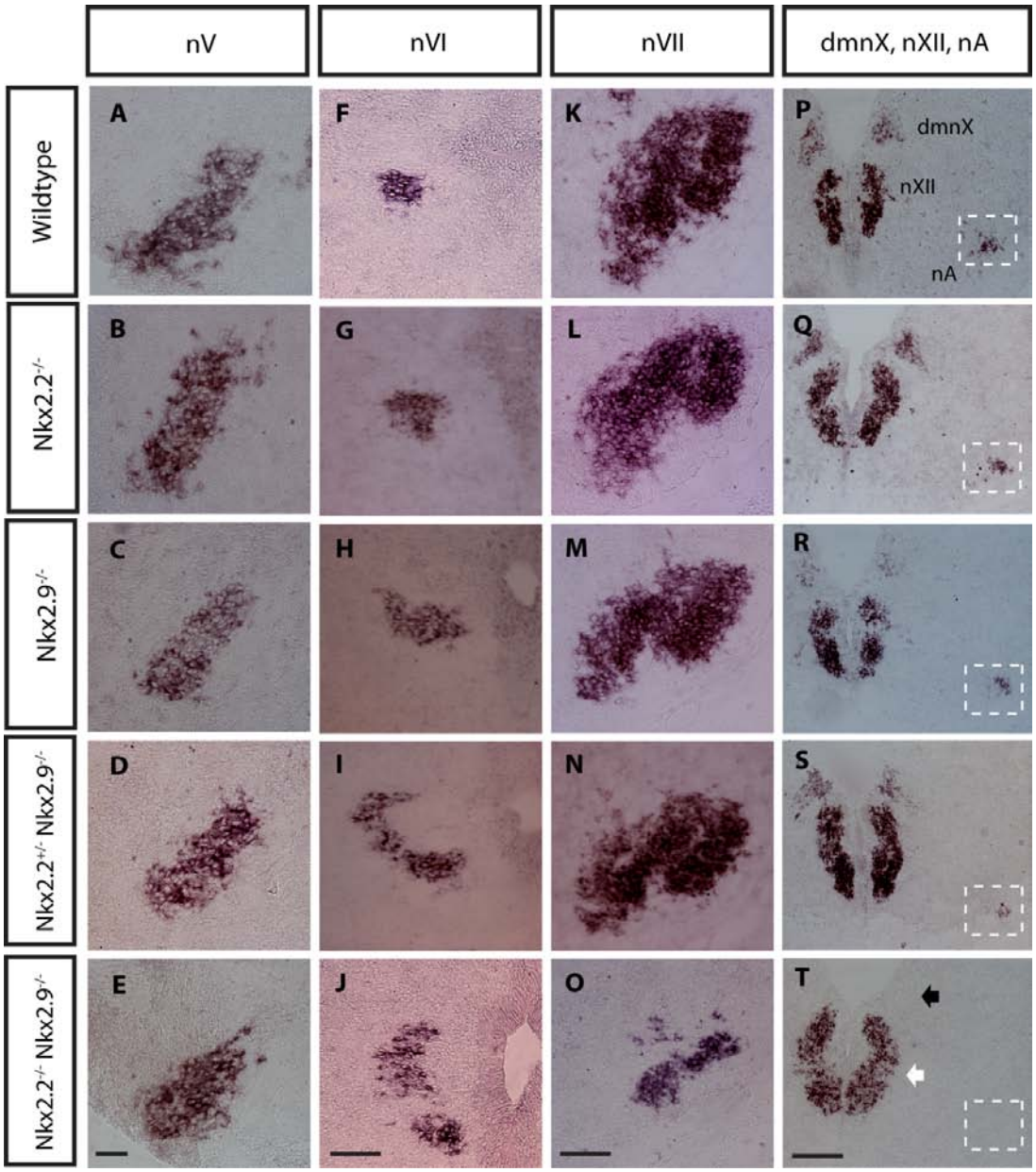

Fig.12: bvM nuclei are reduced or missing while sM nuclei are increased in size in *Nkx2.2;Nkx2.9* double-null mutant embryos at E15.5. *In situ* hybridization using a Peripherin riboprobe was performed on transverse sections of the brainstem of wildtype (A, F, K, P; n= 3), *Nkx2.2*$^{-/-}$ (B, G, L, Q; n=2), *Nkx2.9*$^{-/-}$ (C, H, M, R; n=3), *Nkx2.2*$^{+/-}$*;Nkx2.9*$^{-/-}$ (D, I, N, S; n=3) and *Nkx2.2;Nkx2.9* double-null mutant (E, J, O, T; n=5) embryos at E15.5. The sections are shown in an anterior (left) to posterior direction (right). In absence of Nkx2.2 and Nkx2.9 transcription factors, the dmnX and nA bvM nuclei were undetectable along the entire A/P axis (T; black arrow and white box). The facial motor nucleus was drastically reduced in size in the *Nkx2.2*$^{-/-}$*;Nkx2.9*$^{-/-}$ embryos (O), while the trigeminal bvM nucleus was only slightly reduced (E). In contrast, the abducens and hypoglossal sM nuclei were increased in size in *Nkx2.2;Nkx2.9* double-knockout animals (J, T; white arrow). Most motor nuclei appeared normal in *Nkx2.2*$^{-/-}$ (B, G, L, Q) and *Nkx2.9*$^{-/-}$ (C, H, M, R) single mutant animals. Only a slight increase in the abducens sM nucleus was consistently observed in the *Nkx2.9*$^{-/-}$ (H) and compound *Nkx2.2*$^{+/-}$*;Nkx2.9*$^{-/-}$ (I) mutant embryos. In the *Nkx2.2*$^{+/-}$*;Nkx2.9*$^{-/-}$ mutants, a slight decrease in the size of the nA nucleus was also shown (S; white box), while all remaining branchiovisceral motor nuclei (D, N, S) were indistiguishable from wildtype embryos (A, K, P). Motor nuclei are labeled in roman numerals: nV,trigeminal nucleus; nVII, facial nucleus ; nVI; abducens nucleus; nA; nucleus ambiguous, dmnX: dorsal motor nucleus of the vagus, nXII, hypoglossal nucleus. Scale bars: (A - E); 50 µm, (F – O); 100 µm, (P – T); 200 µm.

In summary, the data obtained so far indicate that the formation of branchiovisceral motor nerves is strongly affected in *Nkx2.2;Nkx2.9* double-knockout embryos. Moreover, it becomes apparent that the size of sM nuclei is increased at late gestational stages, particularly visible of the abducens nucleus. Later in development, severe effects on the population of motor neurons were only significant in mutants lacking both Nkx2.2 and Nkx2.9 transcription factors. *Nkx2.2*$^{-/-}$ and *Nkx2.9*$^{-/-}$ single as well as *Nkx2.2*$^{+/-}$*;Nkx2.9*$^{-/-}$ compound mutant mice showed only minor (if any) defects in motor neurons forming the cranial nerves. The facial nucleus, although significantly smaller than in control mice was still present in the absence of both functional *Nkx2.2* and *Nkx2.9* genes (Fig.12, O). This motor nucleus is comprised of branchial motor neurons which are born earlier in development (E10.5 - E11.5) in rhombomere 4 and migrate in a complex movement along the A/P and the D/V axes to eventually cluster in rhombomere 6 (E12.5 - E14.5) (Garel et al., 2000; Song, 2007; Fig.12, K). In fact, the remaining branchiovisceral motor neurons detected in rhombomere 4 at E10.5 of the *Nkx2.2;Nkx2.9* double-knockout (Fig.10, J) are likely to undergo the described cell migration and seem to form a peripherin^{+} diminished motor nucleus at the normal location of the facial nucleus in r6 (Fig.12, O). To confirm that these Peripherin^{+} cells are indeed branchiovisceral motor neurons, their molecular phenotype was determined (Fig.13). Motor neurons contributing to the wildtype facial nucleus can be identified by the co-expression of Phox2b, Islet-1, and Nkx6.1 (Fig.13, A) (Ericson et al., 1992; Pattyn et al., 1997; Pfaff et al., 1996; Müller et al., 2003). The residual Peripherin^{+} cells in *Nkx2.2;Nkx2.9* double-null mutants at the presumed location of the facial nucleus did co-express these marker proteins (Fig.13, B), suggesting that these cells are normal bvMNs.

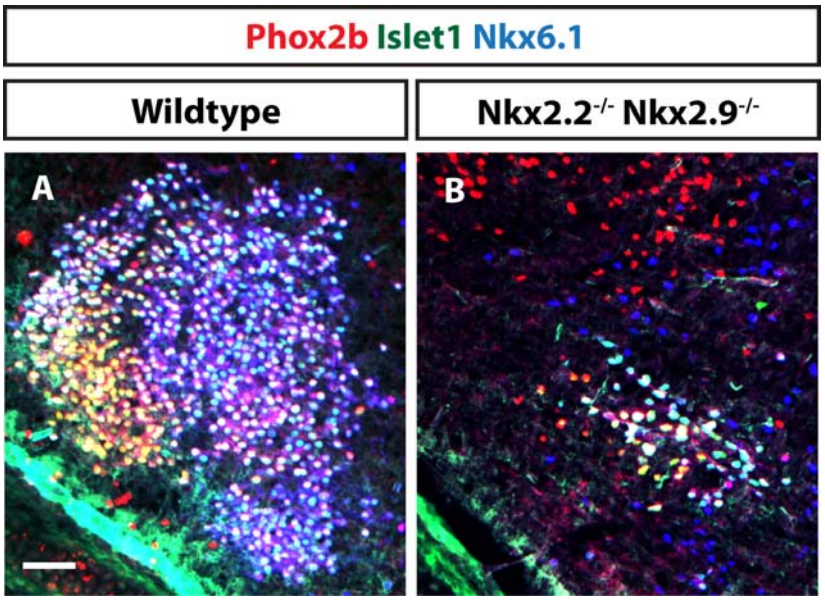

Fig.13: Motor neurons of the defective facial nucleus co-express characteristic markers of postmitotic bvMNs in *Nkx2.2;Nkx2.9* double-null mutant mice. The facial motor nucleus was visualized by immunofluorescent staining of brainstem coronal sections of wildtype (A) and *Nkx2.2;Nkx2.9* double-knockout mutant embryos (B) at E15.5. Branchial facial motor neurons co-express the nuclear marker proteins Phox2b (red) (Pattyn et al., 1997), Islet1 (green) (Ericson et al., 1992; Pfaff et al., 1996) and Nkx6.1 (blue) (Müller et al., 2003) with variable intensities. Triple positive cells (white) mark the facial motor nucleus in the wildype (A) (notice that some cells of the nulceus are yellow because they express only a low level of Nkx6.1). Though at reduced numbers, such triple-positive cells (white) were also clearly found at r6 level in the *Nk2.2;Nkx2.9* double-knockout mutants (B). Scale bar: 50 µm.

3.1.4 P3 progenitor cells undergo ventral-to-dorsal transformation of fate in *Nkx2.2;Nkx2.9* double-null mouse embryos

The transcription factors Nkx2.2 and Olig2 are expressed in the p3 and pMN progenitor domains, respectively (Briscoe et al., 1999; Takebayashi et al., 2000; Mizuguchi et al., 2001; Novitch et al., 2001). Nkx2.2 is able to repress Olig2 expression (Novitch et al, 2001) and suppress the generation of sMNs (Briscoe et al., 1999). The bHLH transcription factor Olig2 in turn continues to be expressed in pMN progenitors and plays a key role in specifying somatic motor neurons (Novitch et al., 2001; Mizuguchi et al., 2001; Zhou and Anderson, 2002). Using these proteins as cell markers, the formation of motor neuron progenitors in *Nkx2.2;Nkx2.9* mutant embryos was investigated in detail.

In caudal wildtype rhombomeres (r5, r7) at the age of E10.5, Olig2-expressing pMN progenitors abut dorsally to the p3 domain and form a clearly demarcated boundary with Nkx2.2-expressing progenitors (Fig.14, A, F). In agreement with published data (Briscoe et al., 1999; Pabst et al., 2003), the p3 progenitor domain in *Nkx2.2*$^{-/-}$ and *Nkx2.9*$^{-/-}$ single mutants was conserved and comparable to wildtype (Fig.14, B, C, G, H). In the *Nkx2.9*$^{-/-}$ single mutant, a mild increase of Olig2^{+} cells was detected (Fig.14, C, H). *Nkx2.2*$^{+/-}$*;Nkx2.9*$^{-/-}$ compound mutants containing only one functional *Nkx2.2* gene showed a marked increase in Olig2^{+} cells accompanied with the reduction in Nkx2.2^{+} p3 progenitor cells (Fig.14, D, I). In *Nkx2.2;Nkx2.9* double-null embryos, the Olig2^{+} domain significantly expanded ventrally including the entire p3 domain (Fig.14, E, J). This ventral expansion of sMN progenitors into the territory of the p3 progenitor domain in the absence of Nkx2.2 and Nkx2.9 factors was further indicated by the unusual co-expression of Olig2 with the FoxA2 transcription factor (Fig.15, B). FoxA2 is expressed by the floor plate (Ruiz i Altaba et al., 1995). In the wildtype co-expression of Nkx2.2 and FoxA2 is observed in lateral floor plate cells at E10.5 (Fig.15, A, violet cells), while in *Nkx2.2;Nkx2.9* double-

null mutants these cells co-express Olig2 and FoxA2 illustrating the significant expansion of sMN progenitors (Fig.15, B, light blue cells). These data clearly indicate that p3 progenitor cells were replaced by Olig2^{+} pMN progenitors in *Nkx2.2;Nkx2.9* double-null embryos.

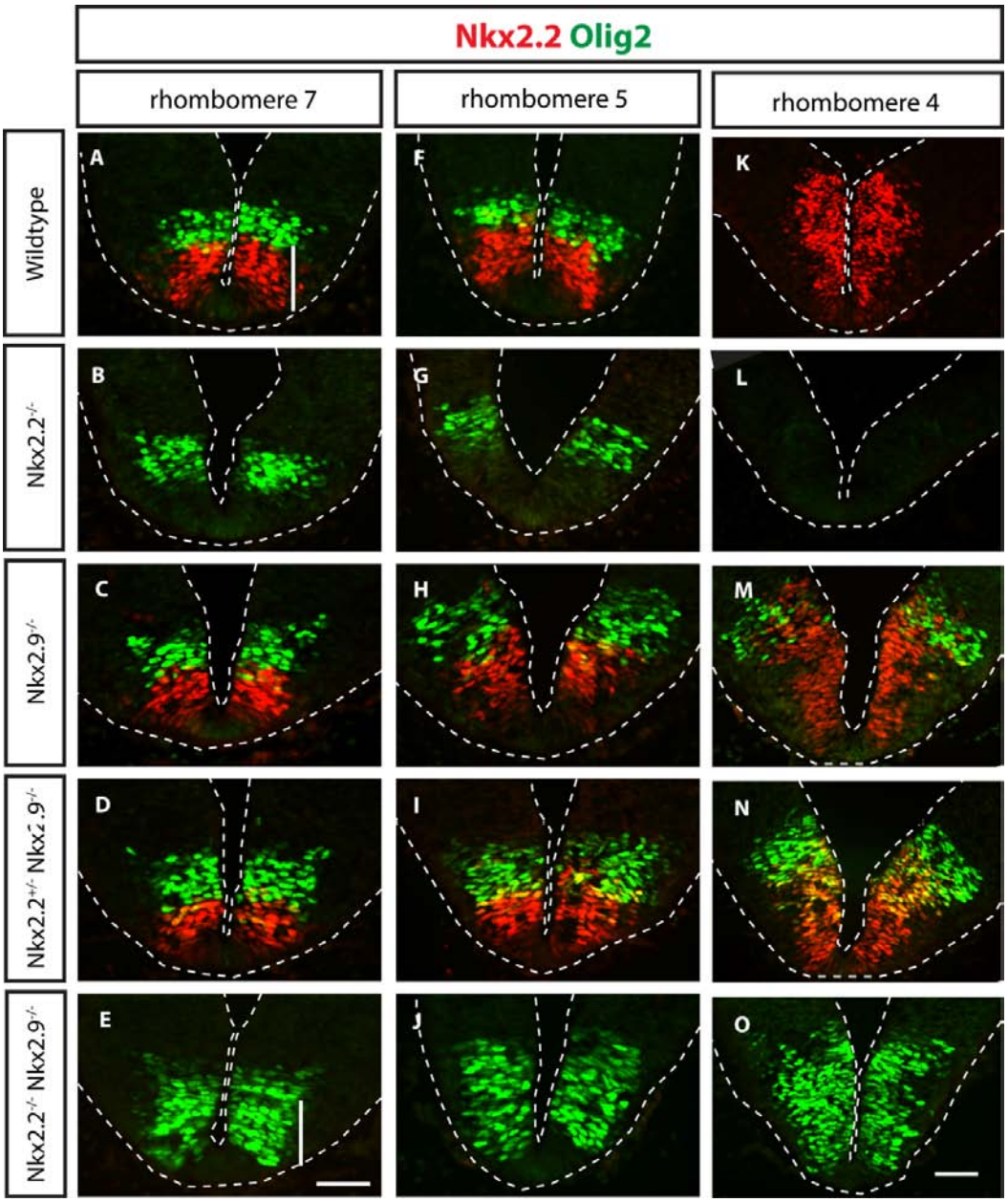

Fig.14: Olig2-expressing pMN progenitors expand ventrally in the hindbrain of embryos lacking both *Nkx2.2;Nkx2.9* genes. Olig2 (green) and Nkx2.2 (red) positive cell nuclei were identified by immunofluorescent labeling of transverse sections of rhombomere 7 (A – E), rhombomere 5 (F – J) and rhombomere 4 (K - O) at E10.5. Wildtype and *Nkx2.2;Nkx2.9* mutant tissue was used as indicated in the figure. Note that in caudal rhombomeres 5 and 7of the wildtype (n=5), Nkx2.2-expressing p3 progenitors are located ventrally to Olig2^{+} pMN progenitors (A, F). The p3 progenitor territory of *Nkx2.2*$^{-/-}$ mutants (n=3) was conserved and the pMN progenitor cells showed no differences when compared to wildtypes (B, G). A mild increase in Olig2^{+} cells was observed in rhombomeres 7 and 5 of *Nkx2.9*$^{-/-}$ (n=3) single mutants (C, H). In contrast, *Nkx2.2*$^{+/-}$*;Nkx2.9*$^{-/-}$ (n=5) mutants showed a reproducible increase in Olig2^{+} pMNs and a

concomitant decrease in Nkx2.2^{+} p3 progenitor cell numbers (D, I). In *Nkx2.2;Nkx2.9* double-knockouts (n=5), Olig2^{+} pMN progenitors expanded ventrally and occupied the entire region of the normal wildtype p3 domain (vertical white bar in E, J). In rhombomere 4 of *Nkx2.2;Nkx2.9* double-null mutants, a rhombomere devoid of Olig2^{+} pMN progenitors in the wildtype (K, n=6), Olig2^{+} ectopic cells which occupied the entire presumptive p3 territory were detected (O, n=6). Even in *Nkx2.9*$^{-/-}$ single (n=3) and *Nkx2.2*$^{+/-}$*;Nkx2.9*$^{-/-}$ (n=4) compound mutants, an ectopic expression of Olig2^{+} cells which was more pronounced in *Nkx2.2*$^{+/-}$*;Nkx2.9*$^{-/-}$ compound mutants was detected (M, N). Notice the presence of cells co-expressing Olig2 and Nkx2.2 in *Nkx2.2*$^{+/-}$*;Nkx2.9*$^{-/-}$ compound mutants, containing one functional *Nkx2.2* allele (N). On the contrary, *Nkx2.2*$^{-/-}$ single mutants (n=3) showed no ectopic expression of Olig2 in rhombomere 4 (L). All images represent ventral parts of the hindbrain and the dotted lines indicate hindbrain tissue boundaries. The white horizontal scale bar in E is representative for images (A- J) while the scale bar in O is representative for images (K - O) and both scale bars correspond to 50µm.

Similar results were obtained in rhombomeres 4 and 6 which are usually devoid of Olig2^{+} pMN cells in wildtypes (Fig.14, K, data not shown). In *Nkx2.2;Nkx2.9* double-knockout mouse embryos, ectopic Olig2^{+} cells were detected occupying the entire p3 region (Fig.14, O, data not shown). In anterior rhombomeres r2 and r3 of *Nkx2.2;Nkx2.9* double-null embryos no or only few ectopic Olig2^{+} cells were observed (data not shown). Ectopic Olig2^{+} cells were also seen in rhombomeres 4 and 6 in *Nkx2.9*$^{-/-}$ single and *Nkx2.2*$^{+/-}$*;Nkx2.9*$^{-/-}$compound mutant animals (Fig.14, M, N, data not shown). In contrast, *Nkx2.2*$^{-/-}$ single mutants contained no ectopic Olig2^{+} pMN progenitors in r4 and r6 rhombomeres compared to wildtype embryos (Fig.14, L, not shown). These data (Fig.14, K - O) suggest that the ectopic Hb9^{+} sMNs detected at the same levels in *Nkx2.2;Nkx2.9* mutants (Fig.10) are derived from early progenitors that changed their fate expressing Olig2 instead of Nkx2.2 and Nkx2.9 transcription factors (Fig.14).

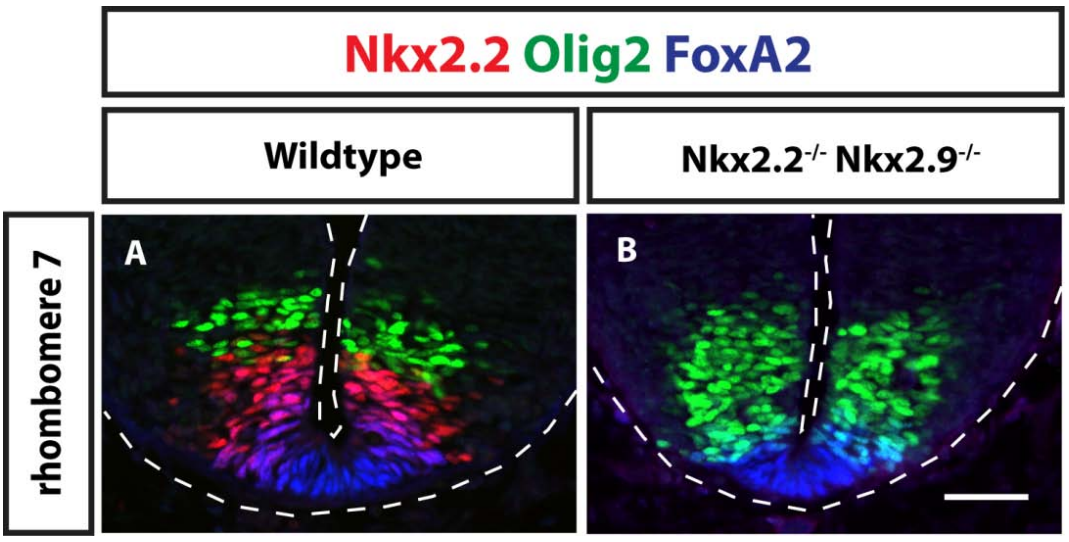

Fig.15: Olig2-expressing pMN progenitors expand ventrally in rhombomere 7 of embryos lacking both *Nkx2.2* and *Nkx2.9* genes. Immunohistochemistry using antibodies directed against Olig2 (green), Nkx2.2 (red), and FoxA2 (blue) was performed on transverse sections of rhombomere 7 in wildtype (A, n=4) and *Nkx2.2;Nkx2.9* double-null mutant (B, n=5) embryos at E10.5. In the wildtype, pMN, p3 and floor plate cells are marked by the expression of Olig2, Nkx2.2 and FoxA2, respectively. Lateral floor plate cells co-express Nkx2.2 and FoxA2 (violett cells in A). In embryos lacking *Nkx2.2* and *Nkx2.9*, Olig2-expression expands ventrally, covering the entire p3 progenitor territory and reaching to the lateral floor plate region (co-expression of Olig2 and FoxA2 is detected; turquoise cells in B). The images illustrate the ventral parts of the hindbrain with dotted lines demarcating hindbrain tissue margins. Scale bar: 50 µm.

The loss of Nkx2.2 and Nkx2.9 transcription factors could lead to premature death of p3 progenitor cells in *Nkx2.2;Nkx2.9* double-null mutant embryos. As a result, pMN cells expressing Olig2 might expand into the territory of p3 progenitors. Therefore, I examined whether apoptotic cells were present in the ventral areas of the hindbrain by performing immunostaining for activated caspase 3, an accepted marker for apoptotic cells (Gown and Willingham, 2002). No indication for significant apoptosis was obtained irrespective of the genotype tested (Fig.16). This supports the hypothesis that p3 progenitor cells undergo a fate switch when *Nkx2.2* and *Nkx2.9* gene functions are ablated.

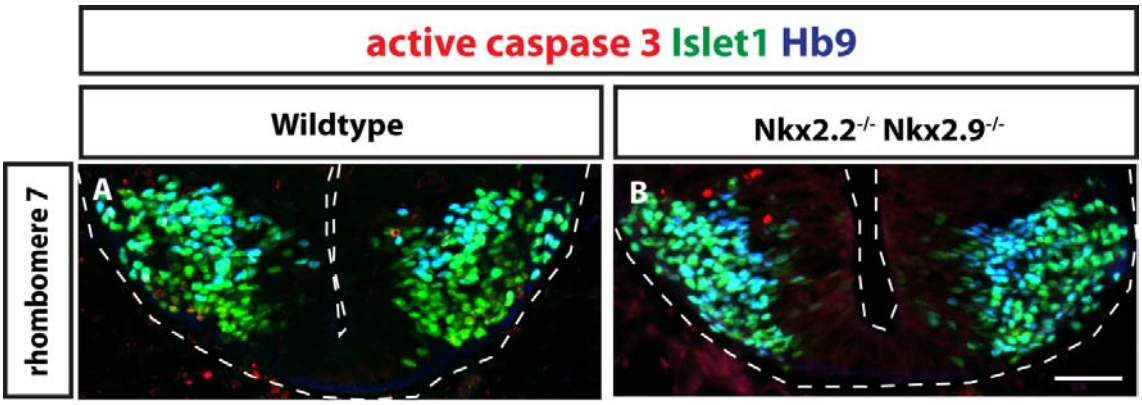

Fig.16: No evidence for apoptosis of p3 progenitors in hindbrains lacking both *Nkx2.2;Nkx2.9* genes. Only very few (if any) apoptotic cells, visualized by activated caspase-3 immunofluorecent staining (red), were detected in the p3 domain of wildtype (A, n=4) and *Nkx2.2;Nkx2.9* double-knockout mutants (B, n=3). A staining for Islet1 (green) and Hb9 (blue) was conducted to define the boundary between progenitors and postmitotic neurons in ventral hindbrain sections of rhombomere 7. The dotted lines reveal the hindbrain tissue boundaries. Scale bar: 50 µm.

Nkx6.1 and Nkx6.2 represent two homologous transcription factors that are expressed early during development of the ventral neural tube within the pMN and p3 progenitor domains. Both genes remain expressed in differentiated bvMNs and play important roles in the proper migration and axonal pathfinding of bvMNs (Sander et al., 2000; Müller et al., 2003; Vallstedt et al., 2001). Very similar to the results obtained in hindbrain of *Nkx2.2;Nkx2.9* mutants (Fig.14, K-O), ectopic expression of Olig2 in anterior

rhombomeres was also detected in mutant embryos devoid of both, Nkx6.1 and Nkx6.2 (Pattyn et al., 2003b). Therefore, it was of interest to analyze the influence (if any) of the *Nkx2.2;Nkx2.9* genes on the expression of Nkx6 transcription factors in the hindbrain. The expression pattern of Nkx6.1 revealed no changes in the *Nkx2.2;Nkx2.9* double-null mutant compared to wildtype embryos neither in rostral (r4) nor in caudal (r7) rhombomeres (Fig.17). This finding suggests that the correct expression of Nkx6.1 in the hindbrain is regulated independently of Nkx2.2 and Nkx2.9. These observations are similar to results obtained in the embryonic spinal cord of *Nkx2.2;Nkx2.9* double-null embryos (Holz et al., 2010). The unchanged expression pattern of Nkx6.1 in *Nkx2.2;Nkx2.9* double-null embryos suggests that the Olig2 expression pattern along the A/P axis is controlled directly by Nkx2.2 and Nkx2.9 and not via a potential loss or missexpression of Nkx6.1.

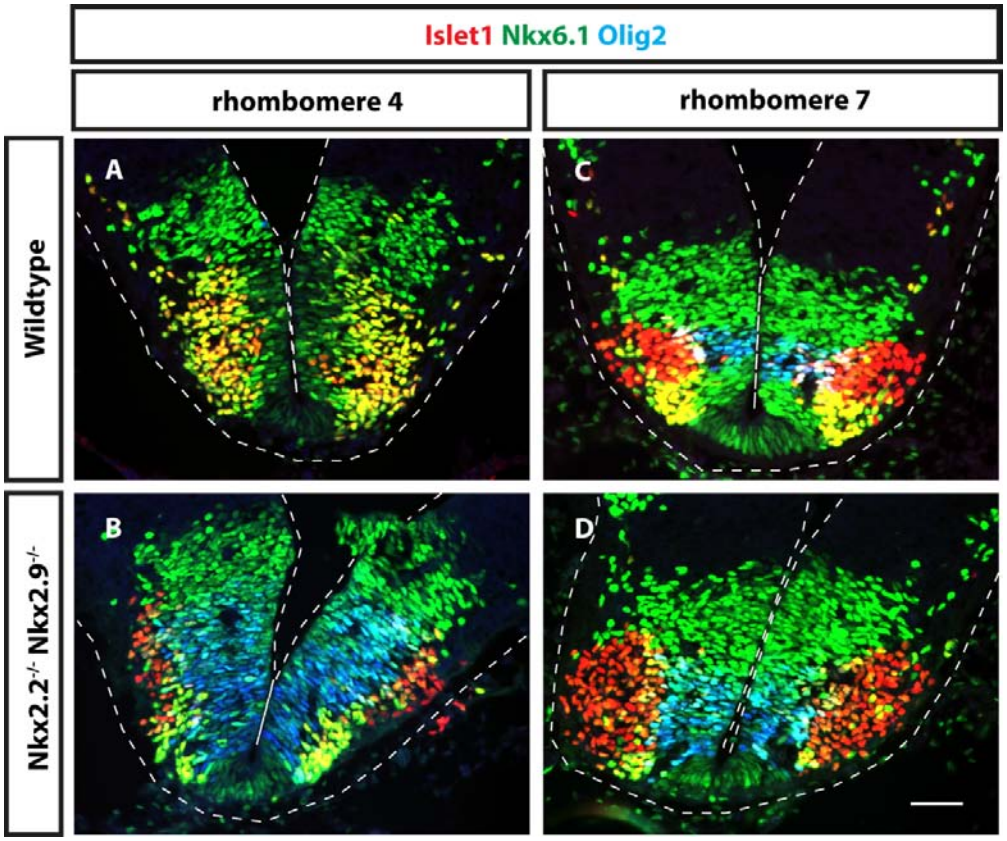

Fig.17: The Nkx6.1 expression domain remains unaltered in embryos lacking both *Nkx2.2;Nkx2.9* genes. No differences were detected in the distribution of Nkx6.1^{+} cell nuclei (green) between wildtypes (n=2, A and C) and *Nkx2.2;Nkx2.9* double-null mutants (n=2, B and D). The hindbrain of E10.5 embryos of both genotypes was compared at rhombomere 4 and 7 levels as indicated. In contrast, co-detection of Olig2 (blue) to visualize pMNs and Islet-1 (red) to reveal postmitotic motor neurons demonstrated severe defects in the motor neuronal cell lineages in *Nkx2.2;Nkx2.9* null mutants as decribed above (see also Figures 7, 10 and 14 for comparison). For instance, notice that Islet1^{+}/Nkx6.1^{+HIGH} cells (appearing yellow in the merged panel A, C) represent the bvMNs that are significantly decreased in cell numbers in *Nkx2.2;Nkx2.9* double-knockout mutants (B,D). Islet1^{+}/Nkx6.1^{+LOW} sMN cells (appearing solid red in the panels) are ectopically present in r4 (B) and increased in numbers in r7 (D) after *Nkx2.2* and *Nkx2.9* gene ablation. Scale bar: 50 µm.

Altogether, the results strongly support the hypothesis that Nkx2.2 and Nkx2.9 transcription factors control the cell fate of motor neuron progenitor cells in the murine hindbrain. They also support the idea that both transcription factors act redundantly at least in part and therefore one of both factors is sufficient to maintain normal cell fate in the p3 progenitor domain of the hindbrain. Thus, the functions of both Nkx2.2 and Nkx2.9 transcription factors in the p3 domain seem to be highly analogous in hindbrain and spinal cord, although different neuronal subtypes arise from p3 of spinal cord and hindbrain (Holz et al., 2010; see discussion for more details).

3.1.5 Tracing the p3 cell lineage in absence of Nkx2.2 and Nkx2.9 transcription factors

All defects in *Nkx2.2;Nkx2.9* double-null mouse embryos indicated that p3 progenitors undergo a ventral-to-dorsal transformation of cell fate. However, a direct proof that bvMNs indeed transform into sMNs is still missing. To prove this hypothesis, the *Nkx2.2*^{cre} mouse was used which was generated by Dr. Andreas Holz in the group of Prof. Dr. Hans-Henning Arnold.

3.1.5.1 The *Nkx2.2*^{cre} mouse

The *Nkx2.2*^{cre} mouse was used to analyze the p3 cell lineage in more detail. In this transgenic mouse line, the prokaryotic *Cre recombinase* open reading frame (ORF) replaces the entire ORF of the endogenous *Nkx2.2* gene (Fig.18).

The Cre/loxp site-specific recombinase system is a very powerful research tool which can be used for cell-specific gene disruption. Furthermore, employing suitable reporter mouse strains this experimental tool allows the accurate genetic labeling of cell lineages and their analysis (Orban et al., 1992). Here, the *Nkx2.2*^{cre} mouse was used to mark Nkx2.2-expressing progenitor cells and follow their progeny in detail. Since the *Nkx2.2*^{Cre} construct also results in the deletion of the *Nkx2.2* open reading frame, this genetic tool would allow studying cell lineage decisions in the presence and absence of *Nkx2.2* function.

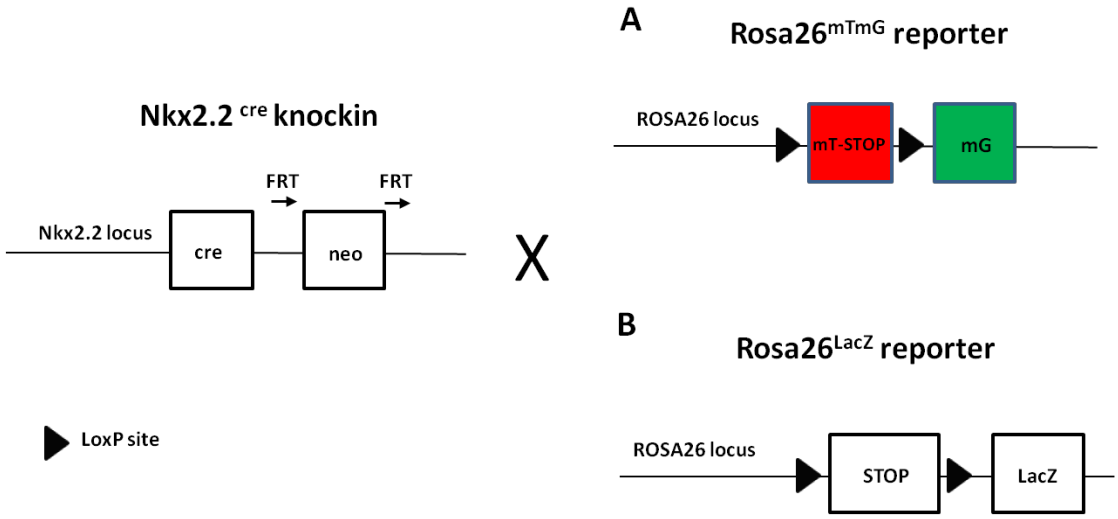

Fig.18: The *Nkx2.2*^{Cre} knockin mouse line was crossed with reporter mouse lines for lineage analysis studies. This schematic represents the strategy of crossing the *Nkx2.2*^{cre} knockin mouse line (generated in the group of Prof.Dr.Hans-Henning Arnold by Dr. Andreas Holz) with the *Rosa26*^{mTmG} reporter mouse line (A) (Muzumdar et al., 2007) and the *Rosa26*^{LacZ} reporter mouse line (B) (Soriano, 1999). The *Nkx2.2*^{cre} knockin allele was generated by deleting and replacing the open reading frame of the endogenous *Nkx2.2* gene by the open reading frame encoding the prokaryotic Cre recombinase protein, therefore resulting in a complete *Nkx2.2* null allele. In addition, a neomycin positive selection cassette was added to the targeting construct as indicated. Note that the neomycin gene was flanked by FRT sites of identical orientation to allow the subsequent removal of this genetic element by crossing resulting mouse lines with germ-line expressing FLIP recombinase mouse strains. In the *Rosa26*^{mTmG} reporter mouse line construct (A), two ORFs are inserted in the *Rosa26* locus; the ORF enconding membrane-targeted dimer Tomato (mT) (which is flanked by two loxP sites which are used by the Cre recombinase to excise the mT ORF upon recombination) and the ORF encoding membrane-targeted GFP (mG) which is only expressed when recombination takes place. In the *Rosa26*^{LacZ} reporter mouse line construct, a neomycin cassette followed by four pA sequences and flanked by two loxP sites is inserted into the *Rosa26* locus. In addition, a *LacZ* gene sequence is inserted downstream to the neo cassette and b-galactosidase is only expressed in cells where Cre-mediated recombination takes place. ORF: open reading frame, pA: polyadenylation sequence, Cre: Cre recombinase, neo: neomycin resistance gene, FRT: flippase recognition target site.

In order to ensure the reliability of the *Nkx2.2*^{cre} mouse, the specificity of the *Nkx2.2 cre* activity was determined by crossing the *Nkx2.2 cre* allele (*Nkx2.2* $^{cre/+}$) with *Rosa26*^{mTmG} reporter mice (Muzumdar et al., 2007) (Fig.18, A). This reporter mouse strain bears a genetically modified *Rosa26* locus that encodes a dispensable murine gene which is constitutively active in all tissues at all developmental time points (Soriano, 1999). Two open reading frames have been inserted under the control of *Rosa26* gene regulatory elements in *Rosa26*^{mTmG} mice (Muzumdar et al., 2007) (Fig.18, A): first, an ORF encoding membrane-targeted dimerTomato (mT). This upstream open reading frame is followed by a potent transcriptional stop element (i.e. containing several copies of polyadenylation (pA) signals). Importantly, the mT ORF together with the multiple pA sites is flanked by

loxP sites which are recognized by Cre recombinase and mediate site-specific DNA recombination. Second, downstream of the mT ORF and its loxP sites, an additional ORF encoding the membrane-targeted green fluorescent protein (mG or mGFP) has been inserted. The upstream mT genetic region functions as a so-called 'Stop-flox' element. In the absence of Cre-mediated recombination (i.e. the native state) membrane-targeted tomato protein is produced constitutively in all cells of the organism, whereas GFP protein is not expressed due to the potent polyadenylation signals downstream of the mT ORF. Upon Cre-mediated recombination, however, the entire 'Stop-flox' cassette is removed leaving behind a single loxP site and the now transcriptionaly activated membrane-targeted GFP protein (Muzumdar et al., 2007).

Briefly, in this experimental setup all cells of the mouse are red before the expression of Cre protein and turn green after Cre production and site-specific DNA recombination. All descendants of genetically recombined cells, i.e. cells that once have activated the Nkx2.2 gene but do not necessarily express it anymore at the time of analysis will be green permanently.

3.1.5.1.1 Branchiovisceral cranial motor nerves are descendants of the Nkx2.2 cell lineage

To assess the specificity of the *Nkx2.2 cre* allele, Cre-mediated GFP expression in whole-mount embryos of the $Nkx2.2^{cre\Delta neo/+};Rosa26^{mTmG/+}$ genotype was documented (Fig.19). Consistent with the well-characterized expression pattern of Nkx2.2 at E10.5, GFP reporter expression was detected along the entire AP axis of the ventral CNS (Price et al., 1992; Briscoe et al., 1999; Pabst et al., 2000). In contrast, $Nkx2.2^{+/+};Rosa26^{mTmG/+}$ control littermates did not show any GFP expression (not shown).

Specifically, all motor parts of the branchiovisceral cranial nerves were identified by the expression of the membrane-bound GFP reporter. For example, reporter expression was detected only in the mandibular branch (V3) of the trigeminal nerve, but not in the purely sensory ophthalmic (V1) and maxillary parts (V2) (Fig.19; A, white arrow). It is known that the mandibular branch (V3) is the only trigeminal branch which contains both motor and sensory nerves, while the other two branches are pure sensory nerves (Schneider-Maunoury et al., 1997; Zhang et al., 2000). Axons of the branchial accessory nerve (XI), which exit from the posterior hindbrain and cervical spinal cord dorso-laterally, are also labeled (Fig.19, A) and can be visualized in great detail after clearing the embryo with

BABB (see Methods, section 5.2.6.2) (Fig.19, B). On the contrary, the hypoglossal nerve (XII), which is a pure somatic motor nerve, failed to exhibit GFP expression (Fig.19, A, asterisk). In accordance with previous work (Sussel et al., 1998), Nkx2.2 driven cre was also expressed in the developing pancreas (Fig.19; A; black arrow). In some embryos, the neomycin selection cassette had been genetically removed from the targeted *Nkx2.2* locus by mating the ancestry of this animal with FLIP recombinase-expressing transgenic strains. No differences in the specificity of Cre-mediated recombination was observed in embryos either containing (n=4) or lacking (n=10) the neomycin selection cassette of the recombinant gene.

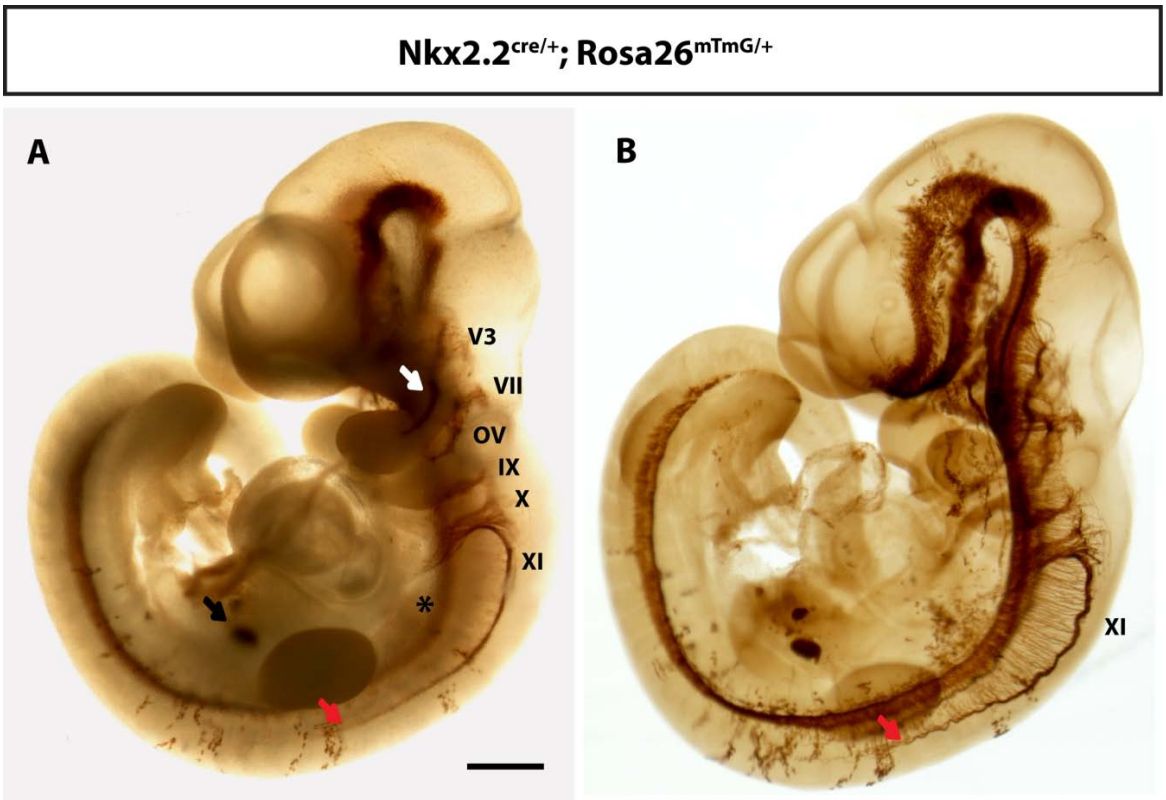

Fig.19: *Nkx2.2*^{Cre} knockin mice allow the genetic labeling of branchio-visceral motor neurons. A whole-mount GFP immunostaining was performed on *Nkx2.2*$^{creΔneo/+}$;*Rosa26*$^{mTmG/+}$ embryos at E10.5. Membrane-tagged GFP antigen was detected using an appropriate anti-GFP antibody combined with a horseradish peroxidase coupled secondary antibody. Displayed is the distribution of GFP visualized by DAB oxidation before (A) and after (B) the same embryo was cleared. Note that mGFP expression is detected along almost the entire rostro-caudal axis in the ventral CNS. GFP staining was also detected in all motor parts of the branchiovisceral cranial nerves reaching into peripheral tissue; the V3 motor branch of the trigeminal nerve (V) is indicated by the white arrow (A), the facial motor nerve (VII), glossopharyngeal motor nerve (IX) and vagus motor nerve (X) as well as the cranial and spinal roots of the accessory motor nerve (XI) are also labeled and their positions are indicated. The caudal boundary of the accessory motor nerve is marked by the red arrow in A and B. However, the hypoglossal somatic motor nerve (XII) is not labeled and the expected position of this ventrally exiting nerve is marked by the asterisk (A). Reporter expression was also detected in the developing pancreas (black arrow, A). After clearing the embryo in B, the projections of all motor nerves were more obvious. For instance, notice the dorsally-projecting axons of the accessory nerve (XI) in B. Scale bar in A: 500µm.

3.1.5.1.2 Specific reporter expression in the Nkx2.2-expressing p3 progenitors

To further assess the specificity of the *Nkx2.2*^{Cre} mouse, GFP-reporter expression was analyzed in p3 progenitor cells at an early embryonic stage (E10.5) in the posterior hindbrain (Fig.20). Reporter expression was specific for the p3 domain as visualized by the co-staining of membrane-targeted GFP and nuclear Nkx2.2 proteins by the same progenitor cells (Fig.20). In addition, a clear boundary was observed between the GFP expression domain and the dorsally abutting Olig2^{+} pMN-progenitors (Fig.20). Hence, Cre-mediated reporter recombination by the *Nkx2.2*^{Cre} mouse strain appears to recapitulate faithfully the endogenous *Nkx2.2* gene activity in hindbrain. It should be emphasized that in this (Fig.20), and many other, triple stainings the red fluorescent channel that also detects the mTomato protein was used. The mTomato is expressed in non-recombined cells. Interference with the detection of nuclear proteins, like Olig2 or other antigens, were not observed. This is possibly due to abundant antigen expression and the utilization of an apparently very potent secondary antibody reagent that is much stronger than the membrane-targeted tomato signal and therefore renders it almost undetectable.

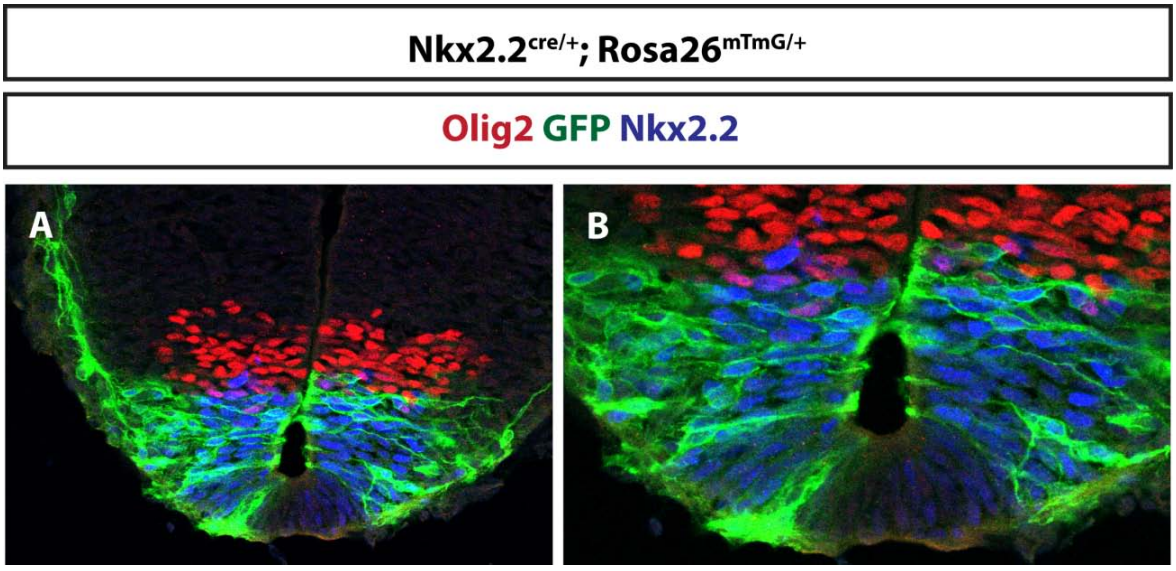

Fig.20: The membrane-targeted GFP and Nkx2.2 overlap in their expression domains. Confocal microscopy was used to visualize the precise distributions of GFP (green), Nkx2.2 (blue) and Olig2 (red) proteins in a transverse section of the posterior hindbrain (r7) obtained from an *Nkx2.2*$^{cre/+}$*;Rosa26*$^{mTmG/+}$ embryo at E10.5. This high-resolution technology allowed the unambiguous demonstration of GFP expression in the membrane of cells showing a co-staining of Nkx2.2 in their nuclei (B). In contrast, membrane-tagged GFP protein was not expressed by somatic motor neuron progenitors, the nuclei which expressed Olig2 transcription factor. Note the GFP^{+} cells that are migrating dorsally (A) and likely represent bvMNs (compare to Fig.21 below). Consistently in these experiments, a few Nkx2.2^{+} p3 progenitors did not express mGFP in their membrane. It is likely that this is due to differences in the kinetics of Cre-mediated recombination and resulting GFP expression compared to the endogenous Nkx2.2 expression by the uncompromised *Nkx2.2* locus.

3.1.5.1.3 Identification of postmitotic branchiovisceral motor neurons and their axonal projections by Nkx2.2^{Cre} mediated reporter expression

For further characterization of the *Nkx2.2$^{Cre/+}$;Rosa26^{mTmG}* mouse strain, I turned my attention to postmitotic motor neurons. It is widely believed that bvMNs derive from p3 progenitors in the mammalian hindbrain. However, direct proof for this hypothesis is missing. Using the novel *Nkx2.2^{Cre}* tool to genetically (i.e. permanently) label Nkx2.2 descendants it should be possible to follow the fate of the p3 cell lineage and provide evidence for the progenitor-product relationship.

That branchiovisceral motor neurons are indeed descendants of the Nkx2.2 cell lineage, can be directly seen in sections through r7 from embryos which were heterozygous for both the *Nkx2.2^{Cre}* and the *Rosa26^{mTmG}* allele. The expression of GFP, Islet1 and Hb9 was visualized by immnuofluorescence (Fig.21). Reporter expression was detected in the post-mitotic Islet1^{+}/HB9^{-} bvMNs that have not yet migrated dorsally to their presumed exit points but clustered laterally to the p3 progenitors. Some Islet1^{+}/HB9^{-} branchiovisceral motor neurons were already migrating dorsally and their cell processes were also GFP positive at least in part (Fig.21, see arrow). In contrast, postmitotic Islet1^{+}/HB9^{+} somatic motor neurons aligned at a more dorso-lateral position and did not express the GFP reporter (Fig.21).

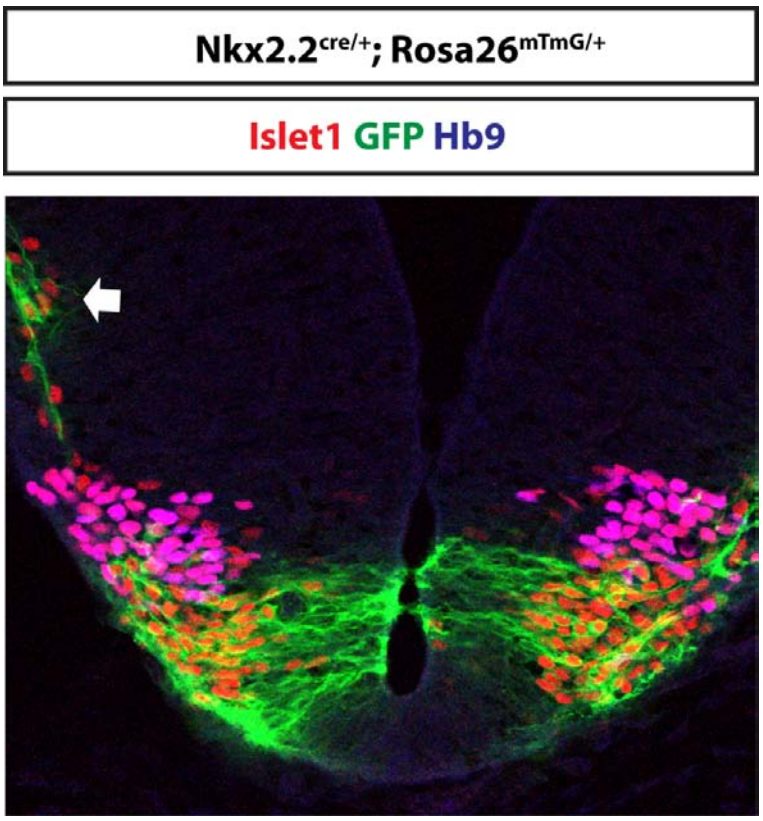

Fig.21: Postmitotic bvMNs are derived from the Nkx2.2 cell lineage. Immunofluorescent visualization of Islet1 (red), GFP (green) and Hb9 (blue) by confocal microscopy on a transverse section of the posterior hindbrain (r7) of an *Nkx2.2$^{cre/+}$;Rosa26$^{mTmG/+}$* E10.5 embryo. Using confocal imaging, membrane-tagged GFP was detected in the postmitotic Islet1^{+}/Hb9 $^{-}$ bvMNs which clustered laterally to the GFP^{+} p3 progenitor domain. GFP-expression was also observed close to the ventricle, presumably corresponding to p3 progenitors (see Fig.20 for Nkx2.2 and GFP co-expression). Some of the Islet1^{+}/Hb9 $^{-}$ bvMNs were already migrating dorsally and expressed GFP in their cell membranes and cell processes (see arrow). GFP reporter expression, however, remained undetectable in the Islet^{+}/Hb9^{+} sMNs.

I next analyzed *Nkx2.2$^{cre/+}$;Rosa26$^{mTmG/+}$* embryos along the entire rostro-caudal axis of the rhombencephalon to clarify whether indeed all bvMNs were descendants of the Nkx2.2-lineage. The cell fate analysis was performed at E10.5 a time when most bvMNs have already been formed (Pattyn et al., 2003a) and begin migrating dorso-laterally (Ericson et al., 1997). Also at this time their axons start growing out and exit the CNS from well-defined dorso-lateral exit points (Sharma et al., 1998; Niederlander and lumsden, 1996).

In rhombomere 2, trigeminal bvMNs and cells in the p3 progenitor territory (ventricular zone) expressed GFP (Fig.22, A, B). Trigeminal bvMNs migrating towards their dorso-lateral exit points were also detected (Schneider-Maunoury et al., 1997; Studer et al., 1996). In addition, the first trigeminal axons outside of the hindbrain could be seen (Fig.22, A, B, white arrow) beginning to form the trigeminal cranial motor nerves (see V3 in Fig.19).

In addition, facial branchiomotor neurons (FBM) extended their axons towards their future exit points at r4 which is the rhombomere of their origin (Fig.22, C, D, white arrow) (Auclair et al., 1996; Garel et al., 2000; Goddard et al., 1996; Studer et al., 1996). At the same level axons most likely corresponding to the vestibuloacoustic neurons (VIII) extended across the ventral midline (Bruce et al., 1997; Tiveron et al., 2003) (Fig.22, C', red arrow). Furthermore, visceral motor neurons of the facial nerve, which are born in r5, have started to migrate dorsally (Fig.22, E, F) and send their axons anteriorly into r4 sharing the exit point with axonal projections of the branchiomotoric facial nerve (Fig.22, C, white arrow) (Goddard et al., 1996; Garel et al., 2000).

Likewise, GFP-positive motor neurons originating in r6 translocate dorsolaterally and send their axons out of the CNS to form the motor part of the glossopharyngeal nerve (IX) (Fig.22, G, H; Fig.19).

In the anterior region of rhombomere 7, where bvMNs are born that contribute to the vagus nerve (X), GFP-expression in Phox2b/Islet1-positive cells migrating dorso-laterally and GFP-expressing axons extending dorsally within the neural epithelium to dorsal exit points were identified (Sharma et al., 1998; Niederlander and lumsden, 1996). Remarkably, GFP-expressing axons invading sensory ganglia were also detected, characteristic for branchiovisceral motor trajectories (Jacob et al., 2000; Zhang et al., 2000) (Fig.22, I, J).

Reporter expression was also seen in motor neurons of the cranial root of the accessory nerve which are generated in the posterior part of rhombomere 7 and migrate dorso-laterally sending their axons to the so-called lateral exit points (LEP) and after leaving the CNS turning rostrally to join with other accessory axons in the accessory nerve (Dillon et al., 2005; Bravo-Ambrosio et al., 2012) (Fig.22, K, L; Fig.19).

In contrast, GFP reporter expression was not detected in Islet1^{+} /Phox2b^{-} sMNs and the corresponding medial domain of their origin (pMN) (Novitch et al., 2001; Mizuguchi et al., 2001) in rhombomeres 5 and 7 (Fig.22, E, F, I – L).

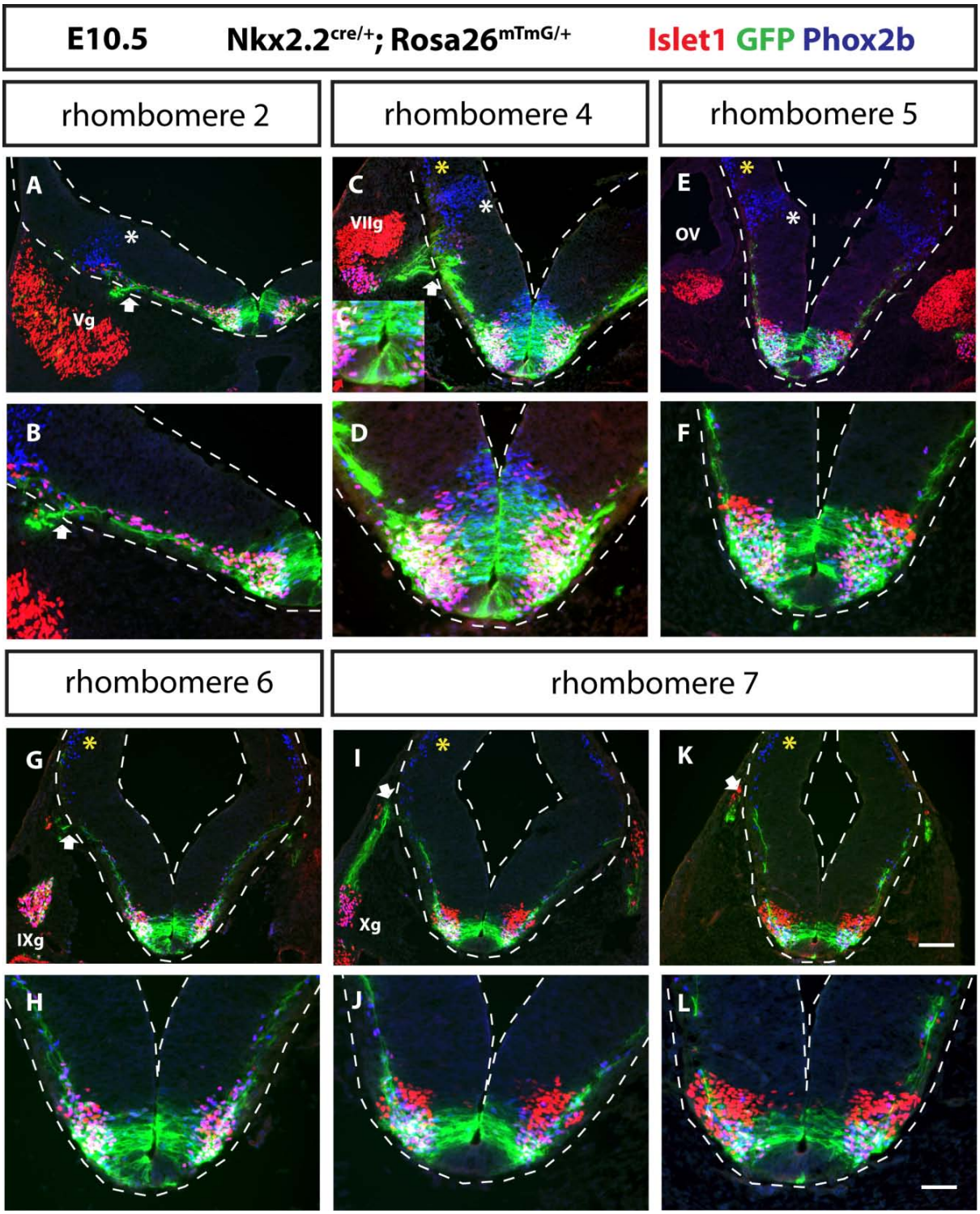

Fig.22: bvMNs generated along the entire rostro-caudal axis of hindbrain belong to the Nkx2.2-lineage. An immunostaining on transverse sections in r2 (A, B), r4 (C, D), r5 (E, F), r6 (G, H), rostral region of r7 (I, J), caudal region of r7 (K, L) of the hindbrain of an *Nkx2.2*$^{cre/+}$*;Rosa26*$^{mTmG/+}$ embryo (n=3) at E10.5, using antibodies directed against Islet1 (red), GFP (green) and Phox2b (blue). Islet1^{+}/Phox2b^{+} bvMNs of the trigeminal (A, B), facial (C-F), glossopharyngeal (G, H), vagus (I, J) and accessory (K, L) motor nerves were born ventrally and expressed GFP in their cell membrane. In addition, vestibuloacoustic neurons (VIII), born in r4, send their axons across the midline (C', red arrow). GFP-expression was also detected in migrating bvMNs and in their dorsally-projecting axons. GFP^{+} axons left the CNS at defined exit points (white arrow) in r2 (A, B), r4 (C), r6 (G), and r7 (I, K). GFP^{+} motor axons of the vagus nerve

exited the hindbrain and invaded the nodose sensory ganglion (Xg) before they project to their final peripheral targets (I). The GFP-expression visible close to the ventricle corresponds to p3 progenitors, which in these images could not be specifically visualized by additional immunostainings. GFP reporter expression was excluded from Islet1^{+}/Phox2b^{-} sMNs (red cells) and from the pMN domain which lies medial to the sMNs at rhombomere 5 level (E, F) and rhombomere 7 level (I – L). The dorso- lateral Phox2b^{+} cells (white asterisk in r2 (A), r4 (C), r5 (E)) represents the DB2 progenitor domain while the more dorsal Phox2b-expressing cells (yellow asterisk in r4 to r7 (C, E, G, I, K)) are the progenitors of the DA3 domain, both of which are generated in the dorsal half of the hindbrain and are not derived from the Nkx2.2-lineage. The dotted lines demarcate hindbrain tissue margins. Scale bar: 100 µm in A, C, E, G, I and K, 50 µm in B, D, F, H, J and L. Vg: Trigeminal ganglion, VIIg: geniculate ganglion, IXg: petrose ganglion, Xg: nodose ganglion, OV: otic vesicle.

Altogether, the Cre activity of the *Nkx2.2^{Cre}* mouse line appeared to be highly specific in the hindbrain and marked all branchiovisceral motor neurons. In addition, the GFP reporter expression allowed to precisely monitor the distinct cell bodies of motor nuclei and their axonal projections. Furthermore and highly consistent with previous reports (Niederlander and lumsden, 1996; Schneider-Maunoury et al., 1997), I demonstrated that these axonal trajectories left the hindbrain at defined exit points to form the characteristic motor branches of the trigeminal (r2), facial (r4), glossopharyngeal (r6), vagus and cranial accessory (r7) nerves . In summary, these data revealed that the *Nkx2.2^{Cre};Rosa26^{mTmG}* mouse line is a suitable tool to study neuronal cell fate including the axonal projections of branchiovisceral motor neurons.

As development progresses, most of the migrating cells have reached their final location and clustered to form distinct motor nuclei by E14.5 (Cordes, 2001; Guthrie, 2007). To examine the formation of these motor nuclei, the *Nkx2.2^{Cre}* mouse line was crossed to the *Rosa26^{LacZ}* reporter line (Fig.18, B), that upon Cre mediated DNA recombination expresses the prokaryotic β-galactosidase enzyme (Soriano, 1999). β-galactosidase accumulates in the cytoplasm of recombined cells and therefore is suited to analyze the formation of motor nuclei. However, this reporter line may not be suitable for the analysis of axonal projections.Transverse sections of brainstem from *Nkx2.2$^{cre/+}$;Rosa26$^{LacZ/+}$* embryos revealed that expression of markers for branchiovisceral motor neurons and the β-galactosidase coincided in all branchiovisceral motor nuclei. The trigeminal motor and facial motor nuclei co-expressed the marker Islet1 for postmitotic motor neurons together with β-galactosidase (Fig.23, A, B). Similarly, neurons in the dMNx and the nucleus ambiguus which were identified by Phox2b expression also produced the β-galactosidase reporter protein (Fig.23, C, D).

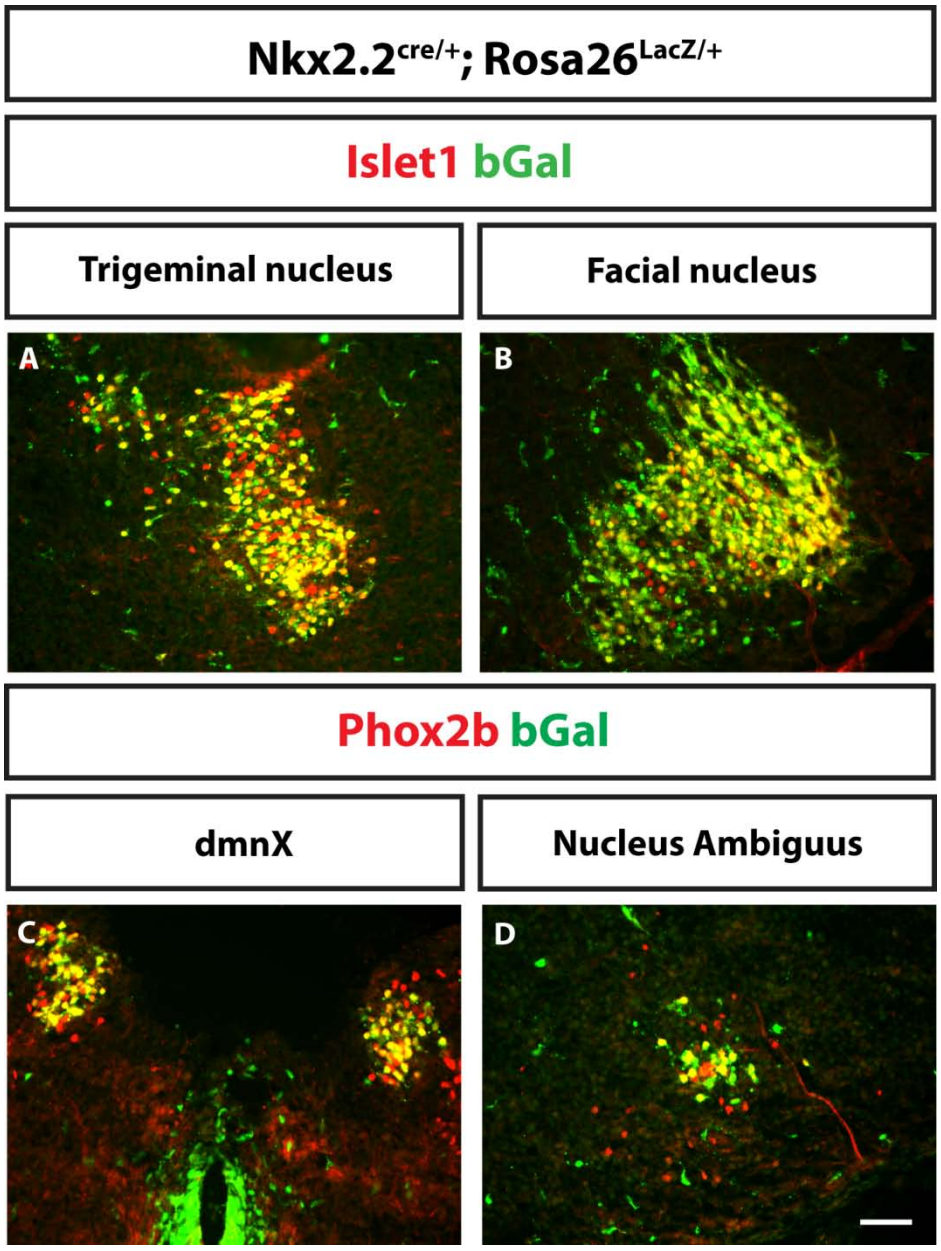

Fig.23: Branchiovisceral motor nuclei only contain neurons that are derived from the Nkx2.2 cell lineage. Transverse sections through the brainstem of *Nkx2.2$^{cre/+}$;Rosa26$^{\beta Gal/+}$* embryos were immunostained with an antibody directed against β-galactosidase antigen at E14.5 (A-D, green). In addition, these sections were also used to detect the bvMN markers Islet (A, B) and Phox2b (C, D). As indicated, the panels show that the trigeminal and facial nuclei co-express Islet1 and the β-galactosidase protein where, despite of the different cellular distributions of the antigens, positive cells often appear yellow in the merged images that were documented using conventional epifluorescence microscopy. The dorsal motor nucleus of the vagus (dmnX) and the Nucleus ambiguus both co-express Phox2b and β-galactosidase. Taken together, these data demonstrate that motor neurons forming these branchiovisceral motor nuclei all originate from the Nkx2.2-cell lineage. The GFP$^+$ (green) cells surrounding the ventricle in C, most probably correspond to oligodendrocyte precursors which is a cell population also known to be formed from Nkx2.2$^+$ p3 progenitors starting at about E13.5 (Qi et al., 2001) Scale bar: 50µm.

In contrast, the somatic motor neurons of the abducens and hypoglossal nuclei clustering ventrally (Novitch et al., 2001; Mizuguchi et al., 2001) did not express β-galactosidase and were therefore not part of the Nkx2.2-lineage (Fig.24).

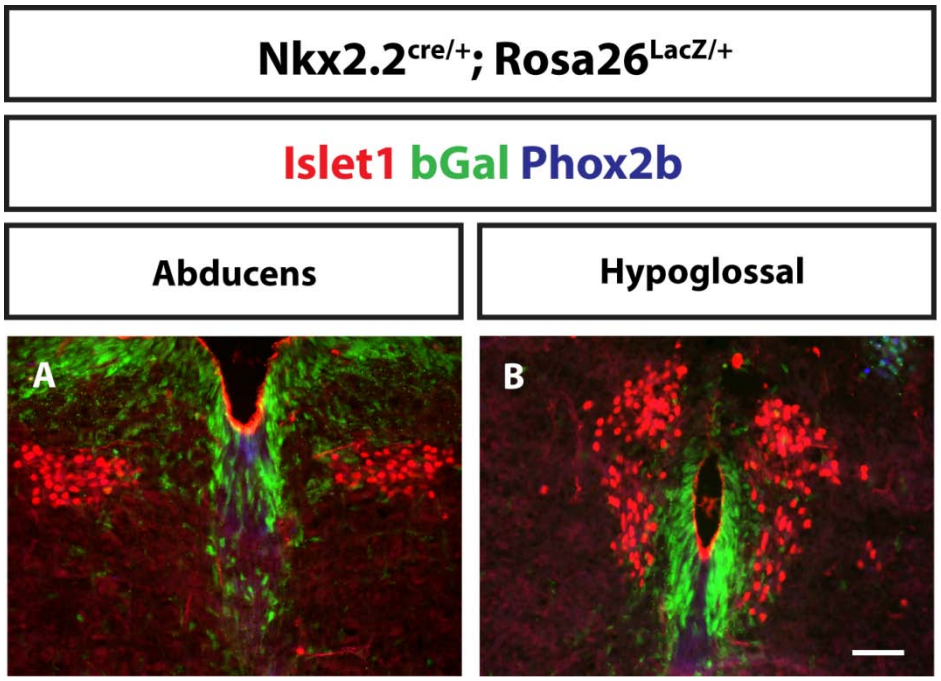

Fig.24: Somatic motor nuclei are not derived from the Nkx2.2-cell lineage. Transverse sections through the brainstem of *Nkx2.2*$^{cre/+}$;*Rosa26*$^{bGal/+}$ embryos were immunostained with antibodies recognizing β-galactosidase (green), Islet1 (red) and Phox2b (blue) antigens at E14.5. Note that Islet1^{+}/Phox2b^{-} somatic motor neurons which are located close to the midline, the position where they were originally born, are negative for b-galactosidase expression. The GFP^{+} (green) cells surrounding the ventricle in A and B, most probably correspond to oligodendrocyte precursors which is a cell population also known to be formed from Nkx2.2^{+} p3 progenitors starting at about E13.5 (Qi et al., 2001) Scale bar: 50µm.

Collectively, the analysis of the *Nkx2.2*^{Cre} mouse line clearly demonstrated that all branchiovisceral motor neurons are descendants of the Nkx2.2-lineage. Furthermore, this mouse model with appropriate reporter strains provided a powerful experimental system for cell lineage tracing throughout development of the hindbrain.

3.1.5.2 bvMNs transform into sMN cell fate in mouse embryos lacking *Nkx2.2* and *Nkx2.9*

The *Nkx2.2*^{Cre} genetic tool also allows monitoring the fate of p3 cells in the absence of Nkx2.2 and Nkx2.9 transcription factors. For this purpose, *Nkx2.2*^{Cre}*; Rosa26*^{mTmG} mice were crossed to the *Nkx2.2* and *Nkx2.9* knockout animals and their offspring was subsequently analyzed in detail. Specifically, the fate of the p3 cells was analyzed in the *Nkx2.2*$^{cre/-}$*; Nkx2.9*$^{-/-}$*; Rosa26*$^{mTmG/+}$ genotype which is devoid of both Nkx2.2 and Nkx2.9 transcription factors and can be directly compared to *Nkx2.2*$^{cre/+}$*; Nkx2.9*$^{+/+}$*; Rosa26*$^{mTmG/+}$ controls.

It was shown previously that in *Nkx2.2;Nkx2.9* double-null mutant mice, Olig2^{+} progenitor cells of somatic motor neurons occupy the normal p3 territory (Fig.14). These data suggest that a change from p3 fate to pMN fate in the ventral hindbrain occurs in the absence of Nkx2.2 and Nkx2.9 transcription factors. Using the *Nkx2.2*^{Cre} reporter system, the fate-switch hypothesis was tested.

Analysis of rhombomere 7 of E10.5 *Nkx2.2*$^{cre/-}$*; Nkx2.9*$^{-/-}$*; Rosa26*$^{mTmG/+}$ embryos revealed a significant ventral expansion of Olig2^{+} cells into the p3 territory (Fig.25, B). This data is entirely compatible with my results obtained in age-matched *Nkx2.2;Nkx2.9* double-null animals (Fig.14). A far more interesting finding using the *Nkx2.2*^{Cre} mouse was that the Olig2^{+} somatic motor neuron progenitor population located ectopically in the p3 region expressed the membrane-bound GFP protein in absence of *Nkx2.2* and *Nkx2.9* (Fig.25, B). This result then provides the formal proof of an early cell fate change, switching p3 progenitors from branchiovisceral to somatic motor neurons when *Nkx2.2* and *Nkx2.9* gene functions are lost. Furthermore, the analysis of r7 sections with postmitotic motor neuron markers in *Nkx2.2;Nkx2.9* double-null mutant embryos revealed GFP expression in the cell membrane of Hb9^{+} neurons which settled in a ventral position that is characteristical for bvMNs (Fig.25, D). Taken together these observations provide clear evidence that in mouse embryos lacking both *Nkx2.2* and *Nkx2.9* genes, presumptive bvMN progenitors are transformed into Olig2^{+} somatic motor progenitors (Fig.25, B) which continue to differentiated Hb9-expressing sMNs irrespective of their aberrant ventral position in the hindbrain (Fig.25, D).

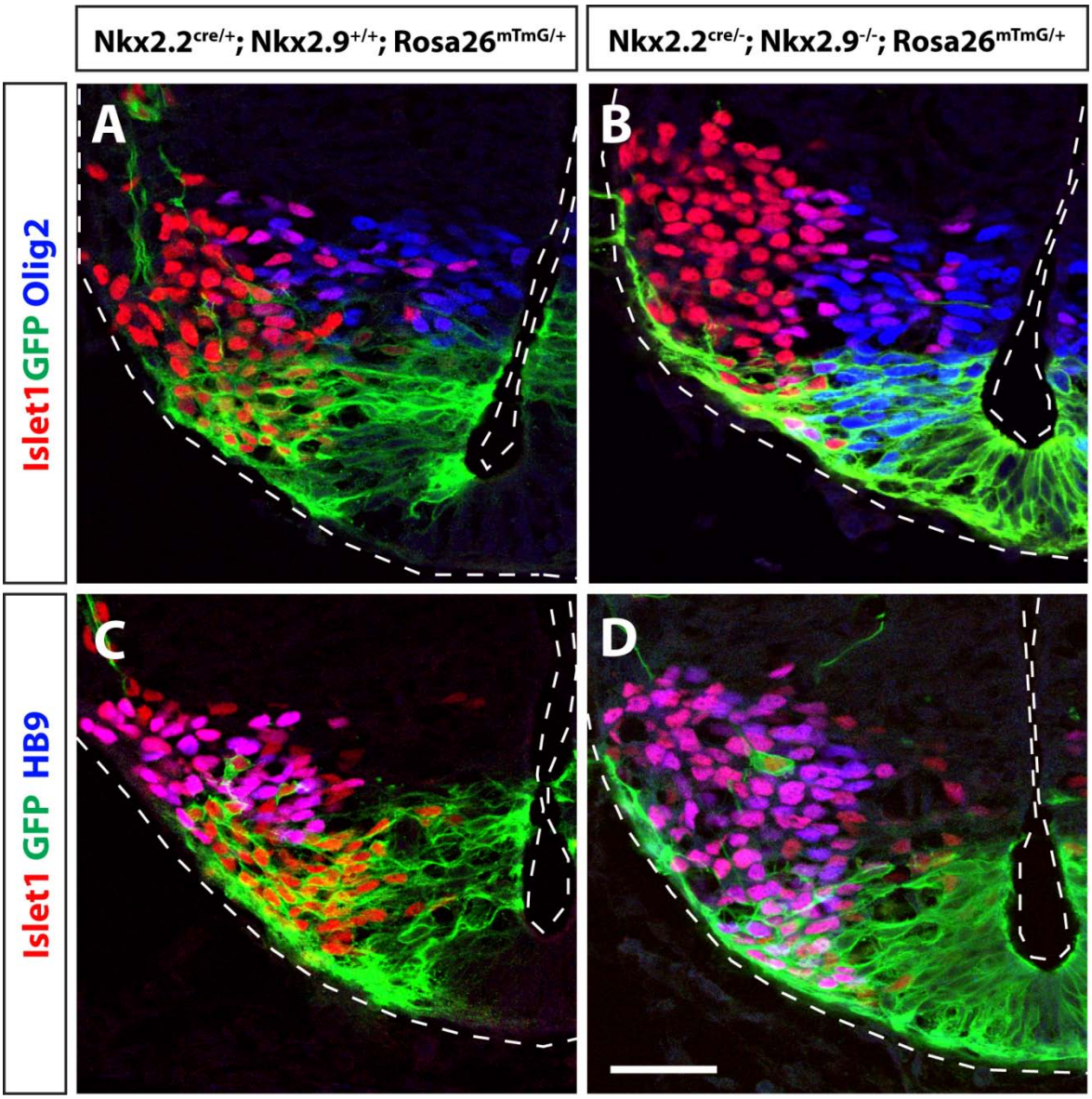

Fig.25: bvMNs transform to the sMN fate in mouse embryos lacking *Nkx2.2* and *Nkx2.9*. Transverse sections through rhombomere 7 of control *Nkx2.2$^{cre/+}$; Nkx2.9$^{+/+}$; Rosa26$^{mTmG/+}$* (A, n=3) and *Nkx2.2$^{cre/-}$; Nkx2.9$^{-/-}$; Rosa26$^{mTmG/+}$* double-null embryos (B, n=4) at E10.5 were immunostained for GFP (green), Islet1 (red), and Olig2 (blue) (A, B). In control embryos (A), the region corresponding to the p3 progenitors and the laterally located postmitotic Islet1$^+$ bvMNs expressed mGFP in their cell membrane, while Olig2$^+$ pMN progenitors and the corresponding postmitotic Islet1$^+$ sMNs did not express mGFP. In *Nkx2.2$^{cre/-}$; Nkx2.9$^{-/-}$; Rosa26$^{mTmG/+}$* double-null embryos (B), Olig2-expressing cells were present in the p3 territory and expressed GFP, confirming that progenitor cells of the Nkx2.2-lineage are transformed to Olig2-expressing cells in the absence of both Nkx2.2 and Nkx2.9 transcription factors. Transverse sections through r7 of control *Nkx2.2$^{cre/+}$; Nkx2.9$^{+/+}$; Rosa26$^{mTmG/+}$* (C, n=3) and *Nkx2.2$^{cre/-}$; Nkx2.9$^{-/-}$; Rosa26$^{mTmG/+}$* double-mutant embryos (D, n=4) at E10.5 were immunostained with antibodies against Islet1 (red), GFP (green) and Hb9 (blue) (C, D). In control embryos (C), Islet1$^+$/Hb9$^-$ bvMNs expressed GFP in their cell membrane, while Islet1$^+$/Hb9$^+$ sMNs were devoid of GFP expression. In *Nkx2.2$^{cre/-}$; Nkx2.9$^{-/-}$; Rosa26$^{mTmG/+}$* double-null embryos (D), Islet1$^+$/Hb9$^-$/GFP$^+$ bvMNs were drastically reduced in number. Interestingly, Islet1$^+$/Hb9$^+$ sMNs lying in the normal ventral position of bvMNs expressed GFP in their cell membrane confirming that cells of the Nkx2.2-lineage express Hb9 in the absence of both Nkx2.2 and Nkx2.9 transcription factors. All images were taken using a confocal microscope. The images represent only one side of the ventral hindbrain region.. The dotted lines demarcate hindbrain tissue margins. Scale bar: 25µm.

3.1.5.3 Axons of GFP$^+$ transformed cells acquire the typical pattern of sMN-like trajectories in mouse embryos lacking both Nkx2.2 and Nkx2.9 transcription factors

The *Nkx2.2$^{cre/+}$; Rosa26$^{mTmG/+}$* mouse was used to study axonal projections in detail. The consequences of the cell fate transformation in *Nkx2.2;Nkx2.9* double-null mutant embryos were identified in a direct way, analyzing the trajectories of somatic MNs which are aberrantly formed in the *Nkx2.2;Nkx2.9* double-null condition.

In wildtype situations, GFP-labeled bvMNs, expressing the pan-neuronal neurofilament antigen 2H3 (Dodd et al., 1988) along their axons, migrated dorsally and extended their axons out of the CNS at the defined dorso-lateral exit points (Fig.26, Fig.27, A, B; white arrows). In contrast, sMNs remained at ventral positions and sent their axons which also express the neurofilament antigen through ventral exit points into the periphery (Fig.26, A, B) (Niederlander and Lumsden, 1996; Sharma et al., 1998).

In *Nkx2.2;Nkx2.9* double-null mutants, the transformed GFP$^+$ sMNs did not only show altered transcriptional identity (as documented in Fig.25), but also adopted a somatic motor neuron-like behavior. Similar to control sMNs, the transformed GFP$^+$ cells settled in the ventral neural tube and extended their axonal projections into the periphery from ventral exit points (Fig.26, Fig.27). At posterior hindbrain levels of *Nkx2.2;Nkx2.9* double-null embryos, the GFP$^+$ trajectories aligned with normal sMN bundles and used the same ventral exit points to leave the CNS (Fig.26, C, D, blue arrows). Only very few neurofilament$^+$/GFP$^+$ axons were detected to utilize dorsal exit points for their exit from CNS (Fig.26, C, D; white arrows).

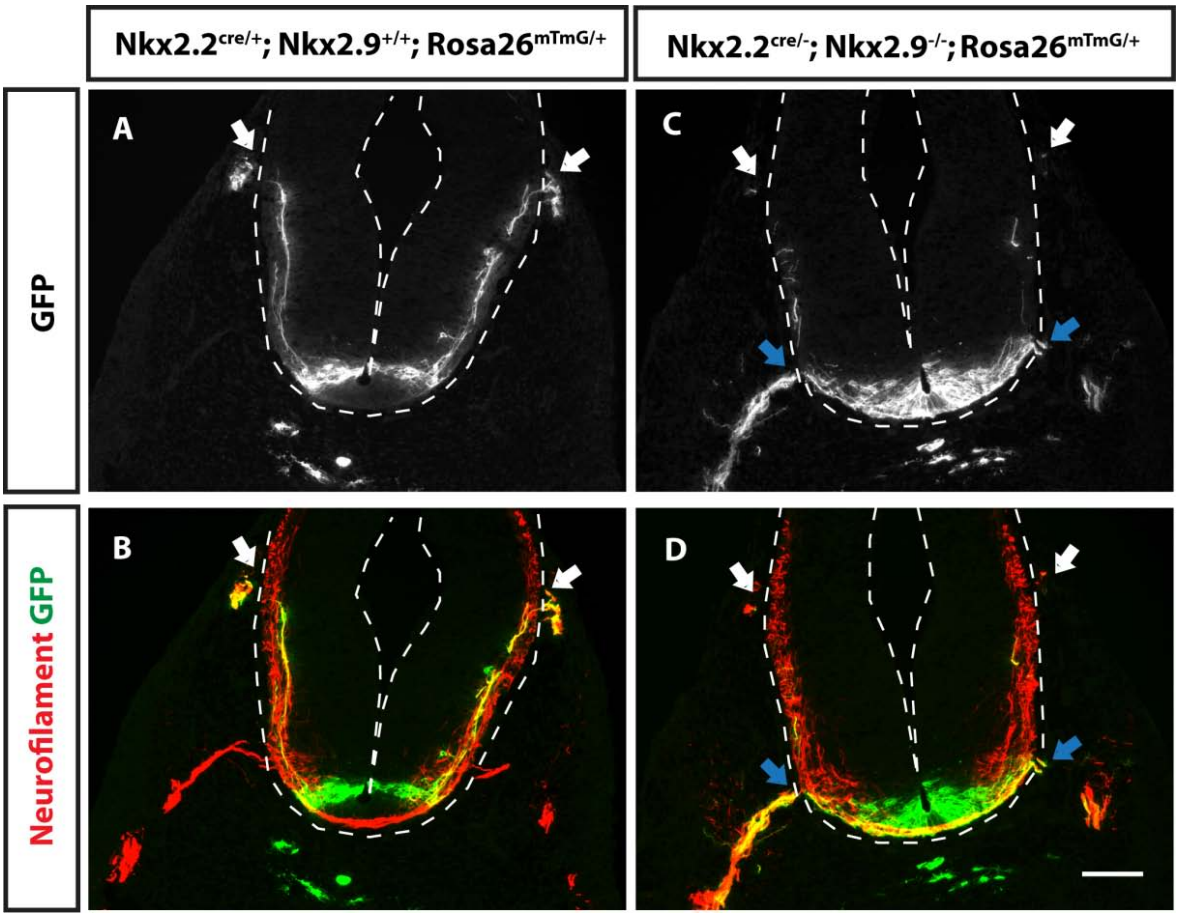

Fig.26: GFP$^+$ axons of transformed cells adopt a sMN-like trajectory pattern in mouse embryos lacking *Nkx2.2* and *Nkx2.9*. Transverse sections through rhombomere 7 level of control *Nkx2.2$^{cre/+}$; Nkx2.9$^{+/+}$; Rosa26$^{mTmG/+}$* (A, B, n=4) and *Nkx2.2$^{cre/-}$; Nkx2.9$^{-/-}$; Rosa26$^{mTmG/+}$* (C, D, n=4) embryos were immunostained with antibodies against neurofilament (red) to visualize axonal projections and GFP (green) to identify Nkx2.2-lineage cells and axons at E10.5. In control *Nkx2.2$^{cre/+}$; Nkx2.9$^{+/+}$; Rosa26$^{mTmG/+}$* embryos (A, B), neurofilament$^+$/GFP$^+$ axons of bvMNs extended dorsally and left the CNS from dorsal exit points (white arrows), while neurofilament$^+$ axons of sMNs exit the CNS ventrally (B). In *Nkx2.2$^{cre/-}$; Nkx2.9$^{-/-}$; Rosa26$^{mTmG/+}$*double-null embryos (C, D), neurofilament$^+$/GFP$^+$ axons of bvMNs were drastically reduced in number and very few, if any, exited the hindbrain dorsally (white arrows). Interestingly, in *Nkx2.2;Nkx2.9* double-knockout mutants, almost all of the neurofilament$^+$/GFP$^+$ axons stayed in a ventral position and exited the hindbrain ventrally along with other pMN-derived sMNs (blue arrows, compare C and D to the control in B). The dotted lines demarcate hindbrain tissue margins. Scale bar: 100µm.

Interestingly, at regions of the hindbrain that are usually devoid of sMN neurons and therefore lack ventral exit points, such as rhombomere 4 (Fig.27, A, B), I found evidence for ectopic ventral roots expressing neurofilament and GFP in *Nkx2.2;Nkx2.9* double-knockout mutant embryos (Fig.27, C, D, blue arrows). Despite the marked overall decrease in neurofilament$^+$/GFP$^+$ bvMN axons in *Nkx2.2;Nkx2.9* double-null mutant embryos, very few axons extended dorsally to leave the CNS from normal exit points of the facial nerve (Fig.27, C, D, white arrow).

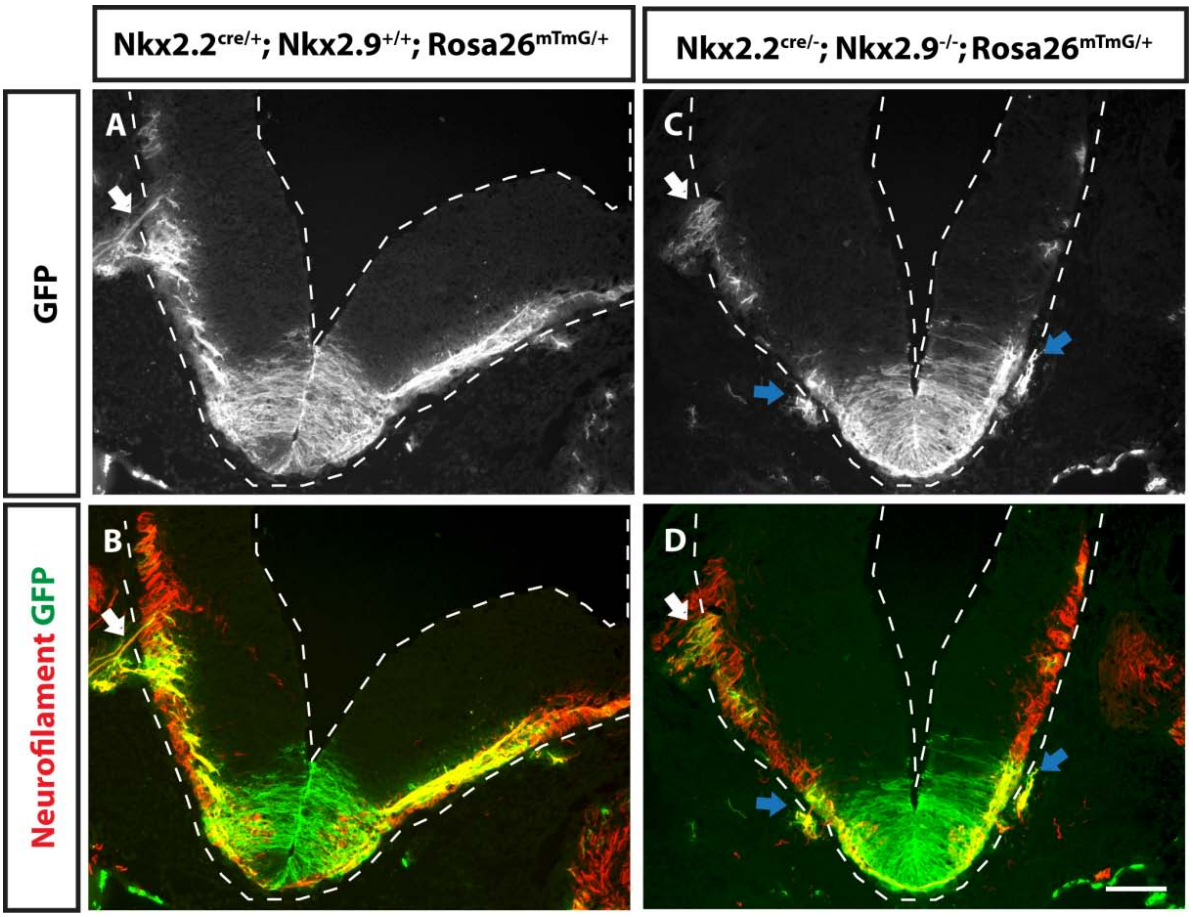

Fig.27: Ectopic GFP$^+$ ventral roots were detected in rhombomere 4 of *Nkx2.2;Nkx2.9* double-null mutants. Transverse sections through rhombomere 4 of control *Nkx2.2$^{cre/+}$; Nkx2.9$^{+/+}$; Rosa26$^{mTmG/+}$* (A, B, n=3) and *Nkx2.2$^{cre/-}$; Nkx2.9$^{-/-}$; Rosa26$^{mTmG/+}$* double-null (C, D, n=4) embryos at E10.5 were immunostained with antibodies against neurofilament (red) to visualize axonal projections and GFP (green) to identify Nkx2.2-lineage cells and axons. In *Nkx2.2$^{cre/+}$; Nkx2.9$^{+/+}$; Rosa26$^{mTmG/+}$* control embryos (A, B), neurofilament$^+$/GFP$^+$ axons of bvMNs (of the facial nerve) extended dorsally and left the CNS from dorsal exit points (white arrow), while somatic motor nerves were not formed in this rhombomere (B). Interestingly, in *Nkx2.2$^{cre/-}$; Nkx2.9$^{-/-}$; Rosa26$^{mTmG/+}$* double-null embryos, almost all of the neurofilament$^+$/GFP$^+$ axons stayed in a ventral position and formed an ectopic ventral root (C, D, blue arrows) at positions normally devoid of neurofilament$^+$ nerves that exit ventrally in control embryos (B). In addition, neurofilament$^+$/GFP$^+$ axons of bvMNs that extended dorsally were drastically reduced in number in *Nkx2.2;Nkx2.9* double-null embryos but exited the hindbrain dorsally (C, D, white arrow). The dotted lines demarcate hindbrain tissue margins. Scale bar: 100µm.

The facial nucleus was severly reduced in size but not completely eliminated in *Nkx2.2;Nkx2.9* double-null mouse embryos as demonstrated previously (Fig.12, O; Fig.13). Using the *Nkx2.2^{cre}* mouse, it was shown that residual branchial motor neurons of the defective facial nucleus co-expressed Islet1, Phox2b and GFP in *Nkx2.2;Nkx2.9* double-null embryos (Fig.28, B). This observation suggests that some bvMNs of the facial nucleus that are derived from the Nkx2.2-lineage are still formed in the absence of Nkx2.2 and Nkx2.9.

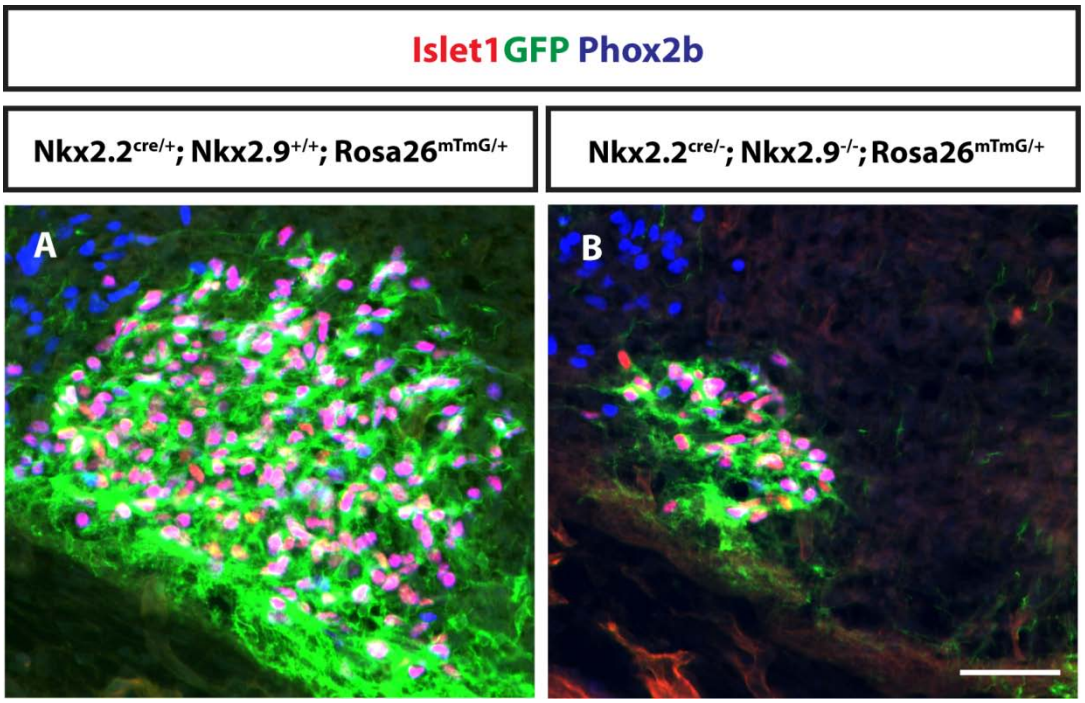

Fig.28: Residual Phox2b$^+$/Islet1$^+$ motor neurons of the defective facial nucleus expressed GFP in their cell membranes in *Nkx2.2;Nkx2.9* double-null mutant embryos. Immunohistochemistry using antibodies directed against the Islet1 (red), membrane-targeted GFP (green) and Phox2b (blue) antigens was performed on transverse sections of rhombomere 6 in *Nkx2.2$^{cre/+}$; Nkx2.9$^{+/+}$; Rosa26$^{mTmG/+}$* control and *Nkx2.2$^{cre/-}$; Nkx2.9$^{-/-}$; Rosa26$^{mTmG/+}$* double-null embryos at E12.5. Islet1$^+$/Phox2b$^+$ motor neurons of the facial nucleus expressed GFP in their cell membranes in wildtype embryos (A). In mouse embryos lacking *Nkx2.2* and *Nkx2.9* (B), the few residual Islet1$^+$/Phox2b$^+$ cells of the diminished facial nucleus also expressed membrane-targeted GFP. Scale bar: 50µm.

Finally, the analysis of GFP reporter expression in whole-mount *Nkx2.2$^{cre/-}$; Nkx2.9$^{-/-}$; Rosa26$^{mTmG/+}$* embryos at E10.5 clearly confirmed the hypothesis of cell-fate conversion in absence of the Nkx2.2 and Nkx2.9 transcription factors. The cranial and spinal roots of the branchial accessory motor nerve (XI) were completely missing in *Nkx2.2;Nkx2.9* double-null mutants based on the membrane-tagged GFP protein (Fig.29, B, green arrows marking its anterior and posterior boundaries). This result is in agreement with the previous whole-mount immunostaining of neurofilament in *Nkx2.2;Nkx2.9* double-null mutants that showed a loss of the accessory nerve (XIth) (see Fig.4 and Fig.5). The vagus motor nerve (X) was also significantly reduced with only very few GFP$^+$ axons remaining in the *Nkx2.2;Nkx2.9* double-knockout animals (Fig.29, B, red arrow). GFP- expressing axon bundles of the glossopharyngeal nerve (IX) and facial nerve (VII) appeared considerably thinner in *Nkx2.2;Nkx2.9* double-null embryos when compared to wildtype control (Fig.29, B). The motor branch of the trigeminal nerve (mandibular, V3) was not affected in the *Nkx2.2;Nkx2.9* double-null embryos (Fig.29, B, black arrow).

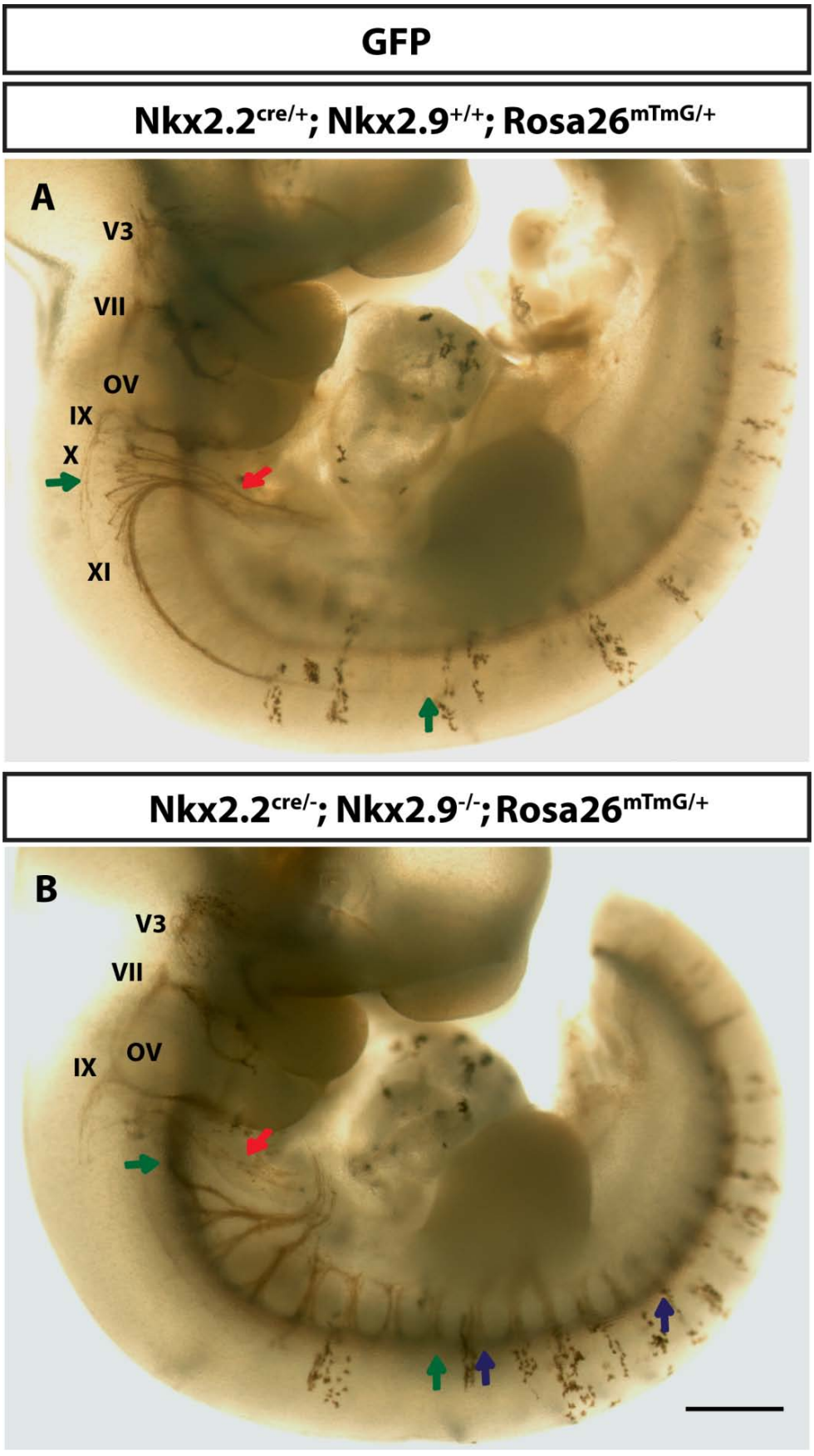
GFP
Nkx2.2cre/+; Nkx2.9+/+; Rosa26mTmG/+
A
V3
VII
OV
IX
X
XI
Nkx2.2cre/-; Nkx2.9-/-; Rosa26mTmG/+
B
V3
VII
OV
IX

Fig.29: GFP reporter expression in *Nkx2.2$^{cre/-}$; Nkx2.9$^{-/-}$; Rosa26$^{mTmG/+}$* embryos reveals a transformation of branchiovisceral motor nerves to somatic motor nerves. An Immunostaining using an antibody directed against the GFP antigen was performed on *Nkx2.2$^{cre/+}$; Nkx2.9$^{+/+}$; Rosa26$^{mTmG/+}$* control (A, n=4) and *Nkx2.2$^{cre/-}$; Nkx2.9$^{-/-}$; Rosa26$^{mTmG/+}$* double-null (B, n=4) whole-mount embryos at E10.5. In *Nkx2.2$^{cre/+}$; Nkx2.9$^{+/+}$; Rosa26$^{mTmG/+}$* control embryos (A), membrane-bound GFP expression was detected in all branchiovisceral motor nerves; the trigeminal motor nerve (V3 branch); the facial motor nerve (VII), the glossopharyngeal motor nerve (IX), the vagus motor nerve (X) (red arrow), the cranial and spinal roots of the accessory motor nerve (XI) (green arrows marking the rostral and caudal margins of the nerve). The axons of the accessory nerve (XI), which exited dorsally in control embryos, were absent in the *Nkx2.2;Nkx2.9* double-knockout embryos (B) (compare B to green arrows in A). Concurrently, at the same rostro-caudal level (green arrows in B), GFP expression was detected in ventrally-exiting hypoglossal somatic motor nerve fibers (XII) and cervical somatic motor nerves (C1- C5) of the *Nkx2.2;Nkx2.9* double-null embryo (B, green arrows), and not in control embryo (A). The vagus motor nerve (X) was drastically reduced in *Nkx2.2;Nkx2.9* double-null embryos (B, red arrow, compare to the control embryo in A). The glossopharyngeal nerve (IX) and facial nerve (VII) fibers were extremely thin in the *Nkx2.2;Nkx2.9* double-null mutant in comparison to the control, while the motor branch of the trigeminal nerve (V3) was mildly affected in the *Nkx2.2;Nkx2.9* double-knockout embryo (B). Notice also the GFP^{+} motor axons emerging ventrally corresponding to the somatic motor trajectories of the thoracic spinal cord, which are identified in the *Nkx2.2;Nkx2.9* double-null mutant embryos (B, blue arrows marking the rostral and caudal limits), and not in the control embryos (A). Scale bar: 500µm.

Interestingly, *Nkx2.2;Nkx2.9* double-null mutants but not control embryos showed GFP reporter expression in the somatic hypoglossal motor nerve (XII) exiting ventrally as well as the somatic motor nerves of the cervical region (C1-C5) (Fig.29, B, green arrows mark the rostral and caudal margins). This latter observation together with my previous findings (Fig.25) confirms that the motor nerves destined to become branchiovisceral in the wildtype hindbrain and cervical spinal cord, change their fate and become somatic motor nerves in the absence of Nkx2.2 and Nkx2.9 transcription factors.

GFP expression was also observed in somatic motor nerves of the thoracic spinal cord of *Nkx2.2;Nkx2.9* double-null mutants suggesting cell fate transformation of V3 interneurons to sMNs also in spinal cord of embryos lacking the Nkx2.2 and Nkx2.9 transcription factors (Fig.29, B, blue arrows).

In summary, using genetically mediated cell tracing of the Nkx2.2-cell lineage I showed that all bvMNs of the hindbrain and cervical spinal cord are descendants of Nkx2.2-expressing progenitor cells. In addition, I could demonstrate that in the absence of *Nkx2.2* and *Nkx2.9* cells normally fated to become bvMNs undergo a fate conversion and develop into somatic motor neurons, which show the same behavior as normal sMNs as judged by their ventral-exiting axon trajectories.

3.2 The expression pattern of the floor plate marker FoxA2 is unchanged in the hindbrain of *Nkx2.2;Nkx2.9* double-null embryos

Floor plate (FP) cells are non-neuronal cells that occupy the ventral midline of the neural tube (Del Brio et al., 2001; Jessell et al., 1989; Jessell and Dodd, 1990; Placzek and Briscoe, 2005; Rodríguez et al., 1996). *Nkx2.2*$^{-/-}$ and *Nkx2.9*$^{-/-}$ single mutants show normal floor plate development (Briscoe et al., 1999; Holz et al., 2010; Pabst et al., 2003), while mouse embryos that lack both *Nkx2.2* and *Nkx2.9* genes reveal developmental and functional defects in floor plate cells of the spinal cord (Holz et al., 2010; Lek et al., 2010). In *Nkx2.2*$^{+/-}$*;Nkx2.9*$^{-/-}$ compound mutants and most prominently in embryos lacking both, *Nkx2.2* and *Nkx2.9* genes the floor plate was significantly reduced. In addition, the defective floor plate in double-null mutant embryos exhibited a drastic loss of FP-specific proteins, such as FoxA2 and Shh, (Holz et al., 2010; Lek et al., 2010). These floor plate defects were stronger in caudal than in rostral regions of the spinal cord.

The defective floor plate in spinal cord of mutant embryos, prompted me to analyze the FP cells in hindbrain of mice lacking Nkx2.2 and Nkx2.9 transcription factors. To recognize the floor plate, the well-characterized marker FoxA2 was used (Marti et al., 1995; Ruiz i Altaba et al., 1995; Ribes et al., 2010). This is a transcription factor which is required for floor plate development (Sasaki and Hogan, 1994). Somewhat surprisingly and in contrast to the spinal cord the results revealed that the floor plate in hindbrain of *Nkx2.2;Nkx2.9* double-null embryos developed essentially normal, as it appeared indistinguishable from wildtype (Fig.30). Thus floor plate development in the hindbrain does not seem to be significantly affected by the combined loss of Nkx2.2 and Nkx2.9 proteins.

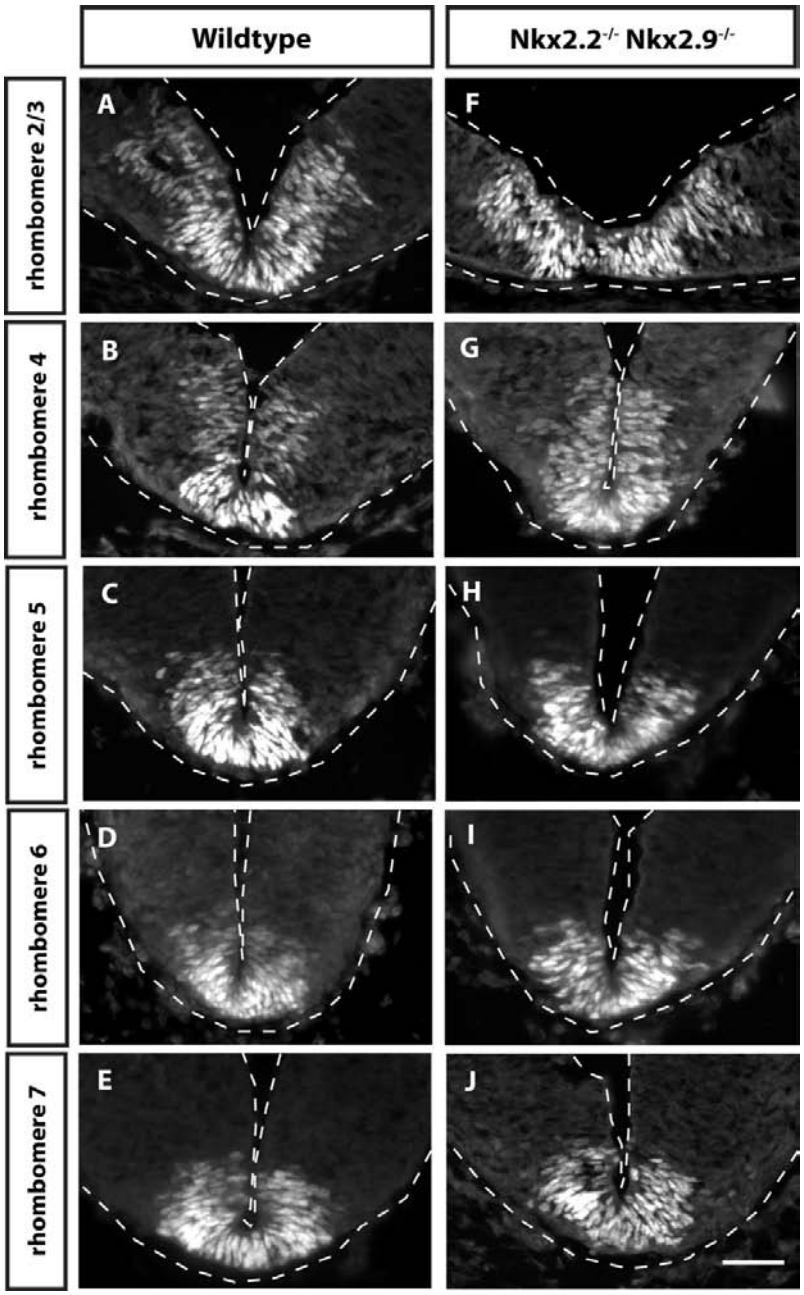

Fig.30: Normal FoxA2 expression was observed in the floor plate cells of the hindbrain in *Nkx2.2;Nkx2.9* double-null mutant embryos. An immunohistochemistry using an antibody directed against the floor plate marker FoxA2 was performed on transverse sections of the hindbrain in r2/r3 (A, F), r4 (B, G), r5 (C, H), r6 (D, I) and r7 (E, J) of wildtype (A - E, n=4) and *Nkx2.2;Nkx2.9* double-null mutant embryos (F - J, n=5) at E10.5. No changes in the $FoxA2^{+}$ expression pattern and cell number all axial levels of the hindbrain in *Nkx2.2;Nkx2.9* double-knockout mutants (F - J) in comparison to wildtype embryos (A- E). The images illustrate the ventral parts of the hindbrain with dotted lines demarcating hindbrain tissue margins. Scale bar: 50µm.

Analysis of hindbrains in control embryos of the *Nkx2.2^{cre};Rosa26^{mTmG}* mouse line revealed that expression of the GFP-reporter does not occur in the entire floor plate territory but only in some of the floor plate cells (Fig.31, A, B, C; Fig.32, A). In contrast to this pattern in the hindbrain of controls, *Nkx2.2;Nkx2.9* double-null embryos exhibited expression of the GFP-reporter throughout the entire floor plate (Fig.31, D, E, F; Fig.32, D). This expansion of the GFP pattern reflecting the *Nkx2.2* gene activity was observed at all axial levels of the mutant hindbrain (Fig.31, Fig.32 and data not shown).

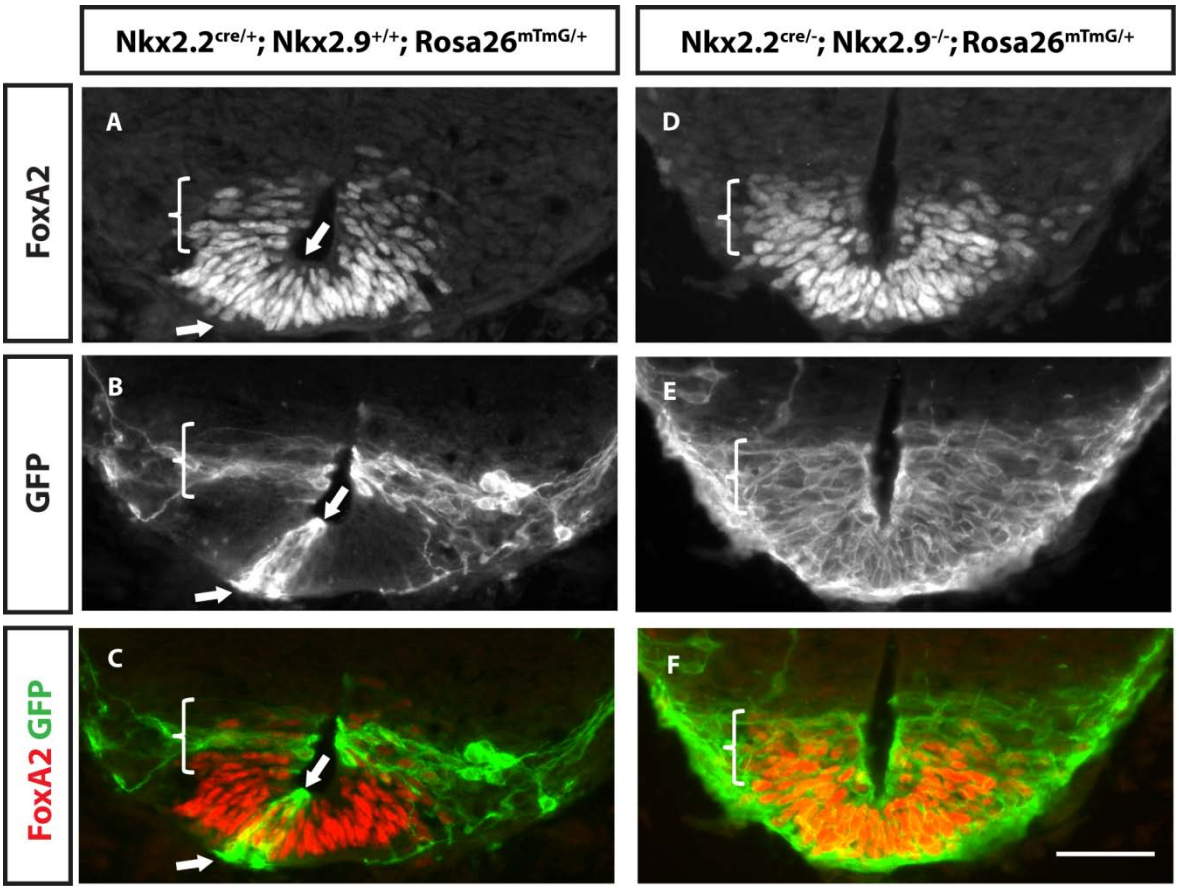

Fig.31: GFP reporter expression was detected in the entire floor plate territory in mouse embryos devoid of Nkx2.2 and Nkx2.9 transcription factors. The images represent an immunohistochemistry done on transverse sections of the hindbrain (r7) in control *Nkx2.2$^{cre/+}$; Nkx2.9$^{+/+}$; Rosa26$^{mTmG/+}$* (A - C, n=4) and *Nkx2.2$^{cre/-}$; Nkx2.9$^{-/-}$; Rosa26$^{mTmG/+}$* (D - F, n=4) embryos at E10.5. FoxA2 (A, D) and GFP (B, E) expression was shown in separate white and black images for better evaluation. In *Nkx2.2$^{cre/+}$; Nkx2.9$^{+/+}$; Rosa26$^{mTmG/+}$*control embryos, GFP-expression (green) was only detected in the cell membrane of a few FoxA2^{+} (red) floor plate cells (A – C, white arrows). In contrast, in *Nkx2.2$^{cre/-}$; Nkx2.9$^{-/-}$; Rosa26$^{mTmG/+}$* double-null mutant embryos, all FoxA2^{+} floor plate cells expressed membrane-bound GFP. Notice also the GFP expression in the cell membrane of p3 progenitors, expressing low concentrations of FoxA2, in control embryos (A – C, white bracket; see Fig.S1 in supplementary material for Nkx2.2/FoxA2 double-expression in p3 progenitor cells). In addition, in *Nkx2.2$^{cre/-}$; Nkx2.9$^{-/-}$; Rosa26$^{mTmG/+}$* double-null embryos, membrane-bound GFP expression was also detected in the cells harboring the normal region of p3 progenitors, which retain low concentrations of FoxA2 (D – F, the white bracket marks the presumptive territory of p3 cells). Scale bar: 50µm.

Analysis of the GFP reporter in *Nkx2.2*$^{-/-}$ single mutant embryos revealed GFP expression in only some floor plate cells similar to control embryos (Fig.32, A, B). In *Nkx2.2*$^{+/-}$*;Nkx2.9*$^{-/-}$ compound mutants with only one functional copy of *Nkx2.2*, most floor plate cells expressed the membrane-targeted GFP reporter (Fig.32, C). Taken together, the expression patterns of GFP in embryos with different combinations of *Nkx2.2* and *Nkx2.9* mutant alleles (Fig.32) strongly suggest that Nkx2.9 plays an important role in delimiting *Nkx2.2* gene activity to cells located dorsally to floor plate, presumably the p3 progenitors. Occasionally single cells in floor plate are found positive for the GFP reporter indicating that very few cells of the medial floor plate activate the *Nkx2.2* gene.

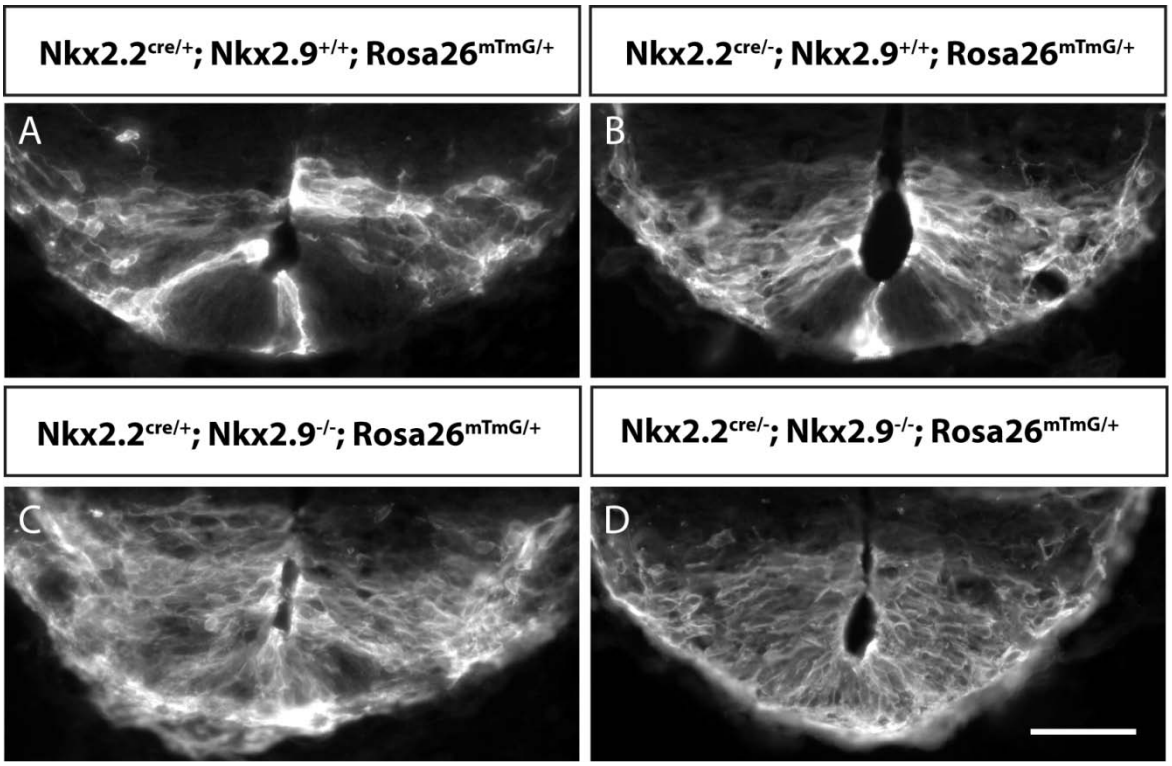

Fig.32: The expression pattern of the GFP reporter in the floor plate region of the hindbrain in *Nkx2.2* and *Nkx2.9* mutant mouse embryos. The images represent an immunohistochemistry done with an antibody directed against membrane-targeted GFP on transverse sections of the hindbrain (r7) in control *Nkx2.2*$^{cre/+}$*; Nkx2.9*$^{+/+}$*; Rosa26*$^{mTmG/+}$ (A), *Nkx2.2*$^{cre/-}$*; Nkx2.9*$^{+/+}$*; Rosa26*$^{mTmG/+}$ single mutant (B), *Nkx2.2*$^{cre/+}$*; Nkx2.9*$^{-/-}$*; Rosa26*$^{mTmG/+}$ compound mutant (C) and *Nkx2.2*$^{cre/-}$*; Nkx2.9*$^{-/-}$*; Rosa26*$^{mTmG/+}$ double-null (D) embryos at E10.5. In *Nkx2.2*$^{cre/+}$*; Nkx2.9*$^{+/+}$*; Rosa26*$^{mTmG/+}$control embryos (A) and in *Nkx2.2*$^{cre/-}$*; Nkx2.9*$^{+/+}$*; Rosa26*$^{mTmG/+}$ single mutants (B), GFP-expression was only detected in the cell membrane of a few cells in the floor plate territory. In *Nkx2.2*$^{cre/+}$*; Nkx2.9*$^{-/-}$*; Rosa26*$^{mTmG/+}$ compound embryos (C) almost all floor plate cells expressed membrane-tagged GFP while the entire floor plate region was GFP^{+} in *Nkx2.2*$^{cre/-}$*; Nkx2.9*$^{-/-}$*; Rosa26*$^{mTmG/+}$ double-null mutant embryos. Scale bar: 50µm.

3.3 The *Nkx2.2^{cre}* mouse line allows lineage tracing of serotonergic neurons

After the formation of branchiovisceral motor neurons, cells of the p3 progenitor domain in hindbrain produce serotonergic neurons (Briscoe et al., 1999; Pattyn et al., 2003a). Serotonergic neurons secrete the neurotransmitter serotonin (also called 5-HT) and play important roles in several aspects of brain development (Jacobs and Azmitia, 1992; Kiyasova and Gaspar, 2011; Lidov and Molliver, 1982; Richerson, 2004). Serotonergic neurons are generated in the hindbrain and anatomical studies showed that they send their axonal projections rostrally to innervate the midbrain and forebrain, and caudally to innervate the spinal cord (Jacobs and Azmitia, 1992). Two main cell populations of serotonergic neurons can be distinguished, a rostral cluster arising from r1-r3 and a caudal cluster produced in r5-r7. Interestingly, the rostral cell cluster can be detected substantially earlier than the caudal one (Briscoe et al., 1999; Cordes, 2005; Hendricks et al., 1999; Pattyn et al., 2003a). Importantly, no serotonergic neurons are generated in rhombomere 4 where bvMNs continue to be produced (see Phox2b flat mounts at E11.5 in Fig.6) (Lidov and Molliver, 1982; Pattyn et al., 2003a).

Nkx2.2 has been shown to be required for the development of serotonergic neurons (Briscoe et al., 1999; Pattyn et al., 2003a) as these cells are almost completely absent in *Nkx2.2$^{-/-}$* knockout animals (Briscoe et al., 1999; Pattyn et al., 2003a). Moreover, there is a close spatio-temporal relationship of the p3 domain and serotonergic precursor cells (Ding et al., 2003).

Utilizing the *Nkx2.2^{Cre};Rosa26^{mTmG}* reporter mouse, the direct link between serotonergic neurons and the Nkx2.2 cell lineage was confirmed. GFP co-expression in 5-HT-expressing serotonergic neurons in rhombomeres 2 and 7 of *Nkx2.2$^{cre/+}$;Rosa26$^{mTmG/+}$* embryos was detected (Fig.33). Note that after their generation, postmitotic 5-HT^{+}/GFP^{+} neurons leave their initial positions close to the ventricle and migrate to lateral areas (Fig.33). Reporter GFP expression was observed in all regions of the hindbrain known to generate serotonergic neurons (r1-r7) (data not shown) (Hendricks et al., 1999; Lidov and Molliver, 1982; Pattyn et al., 2003a). In summary, these results provide definitive proof that 5HT^{+} serotonergic neurons are derived from the Nkx2.2 cell lineage.

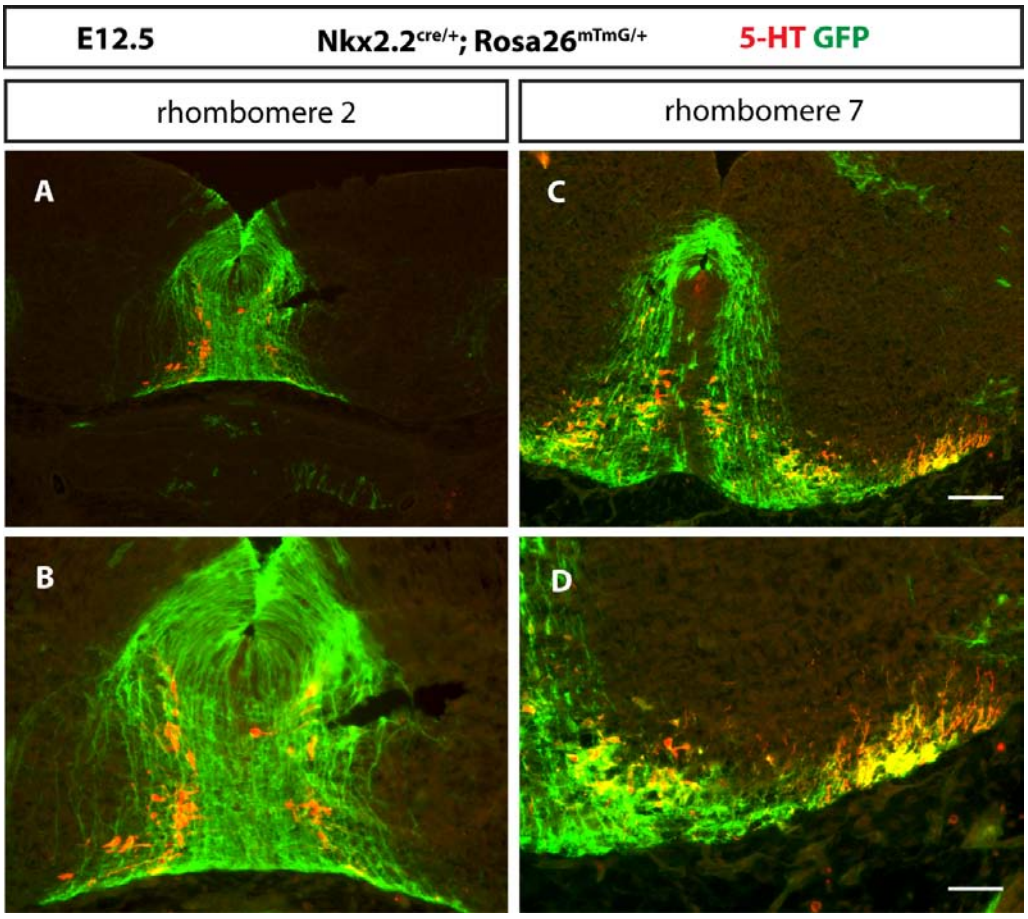

Fig.33: *Nkx2.2*^{cre} mediated reporter expression confirms that all serotonergic neurons are derived from the Nkx2.2 cell lineage. An immunostaining with antibodies directed against the 5-HT antigen (red) and membrane-bound GFP (green) on transverse sections through the hindbrain of *Nkx2.2*$^{cre/+}$*;Rosa26*$^{mTmG/+}$ embryos was performed at E12.5. 5-HT^{+} neurons (red) of the rostral (rhombomere 2, A, B) and caudal (rhombomere 7, C, D) serotonergic clusters co-express membrane-bound GFP (green) in *Nkx2.2*$^{cre/+}$*;Rosa26*$^{mTmG/+}$embryos. Notice also the GFP expression in p3 progenitors lying near the ventricle. For better evaluation, 5-HT^{+}/GFP^{+} cells in (A) and (C) are shown in a higher magnification in (B) and (D), respectively. Scale bars: (A, C) 100µm, (B, D) 50µm.

3.3.1 Analysis of the fate of serotonergic neurons in *Nkx2.2*-deficient embryos

Next, the distribution of GFP^{+} p3 cells in the absence of Nkx2.2 was analyzed during the developmental time period of serotonergic cell differentiation. As expected (Briscoe et al., 1999; Pattyn et al., 2003a), 5-HT^{+} serotonergic neurons were absent in hindbrain including rhombomere 7 (Fig. 34; data not shown) of *Nkx2.2*$^{cre/-}$*;Rosa26*$^{mTmG/+}$ mouse embryos. The GFP^{+} neurons in a lateral position of the ventral hindbrain in control embryos expressed 5-HT whereas these cells were not present in embryos lacking *Nkx2.2* (Fig.34, B, white arrows). These results suggest that serotonergic neurons are indeed not formed at their normal positions in embryos deficient for the *Nkx2.2* gene.

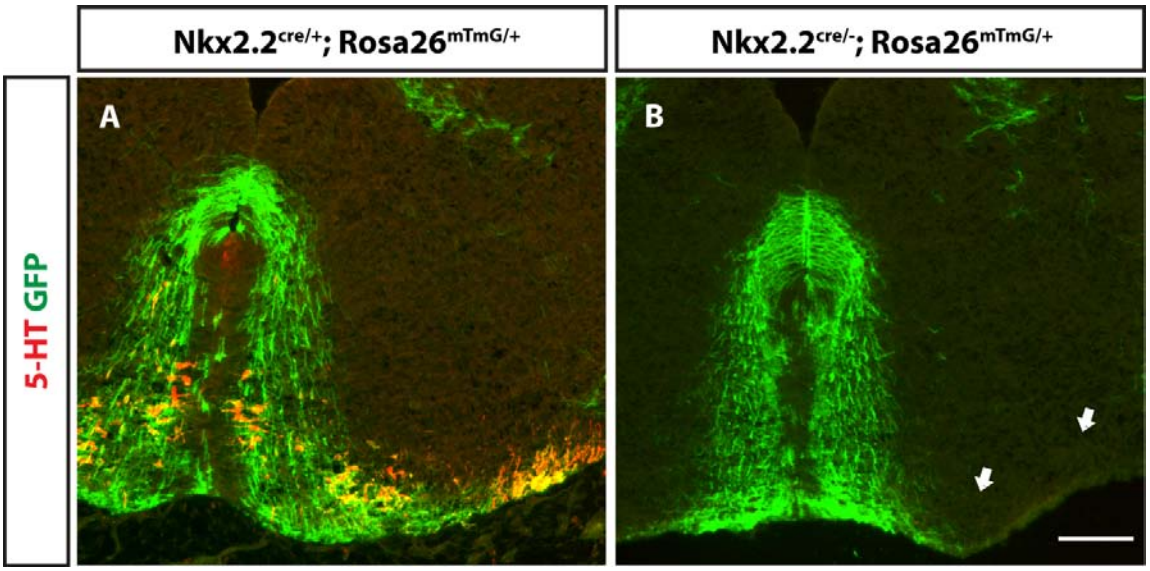

Fig.34: Serotonergic neurons are not formed in *Nkx2.2*$^{-/-}$ single mutants. The images represent transverse sections of rhombomere 7 in *Nkx2.2*$^{cre/+}$;*Rosa26*$^{mTmG/+}$ (A) control and *Nkx2.2*$^{cre/-}$;*Rosa26*$^{mTmG/+}$ (B) mutant embryos at E12.5. The sections were immunostained with antibodies directed against the serotonin antigen 5-HT (red) and membrane-bound GFP (green). 5-HT^{+}/GFP^{+} serotonergic neurons (yellow) residing in more lateral positions in the control embryos (A) are entirely missing in *Nkx2.2*$^{cre/-}$;*Rosa26*$^{mTmG/+}$ mutants (B, white arrows). Scale bar: 100µm.

3.4 *Nkx2.2;Nkx2.9* double-null mice develop severe breathing problems and die shortly after birth

Double-homozygous *Nkx2.2*$^{-/-}$;*Nkx2.9*$^{-/-}$ mutants are not viable and could only be analyzed at embryonic/fetal stages of their development. It was previously described that *Nkx2.2*$^{-/-}$ single mutant embryos show postnatal lethality, likely due to the loss of pancreatic islet cells (Sussel et al., 1998). However, it was also reported that some of these *Nkx2.2*$^{-/-}$ single mutants survive until day 8 after birth (Sussel et al., 1998; Qi et al., 2001). Adult compound *Nkx2.2*$^{+/-}$;*Nkx2.9*$^{-/-}$ mice bearing one functional *Nkx2.2* allele are viable and fertile with no apparent defects in their gross anatomy except for abnormalities in locomotion (Holz et al., 2010). In contrast, mouse embryos devoid of both *Nkx2.2* and *Nkx2.9* genes die rapidly after birth, although no apparent anatomical defects can be observed. A possible explanation for the rapid death of these animals could be the failure to breathe. To test this possibility, the breathing behavior of E18.5 fetuses was analyzed in collaboration with Prof. Dr. Swen Hülsmann at the University of Göttingen. To determine the frequency and depth of breathing plethysmographic measurements were performed in a blinded fashion to the genotype from wildtype and *Nkx2.2;Nkx2.9* mutant mouse embryos. For this purpose, viable E18.5 mouse embryos were recovered from their mother by caesarian section and used for the immediate respiratory assessment.

Plethysmographic recordings showed that 91% of the *Nkx2.2;Nkx2.9* double-null mutant embryos failed to breathe (Table.1), although some of these *Nkx2.2;Nkx2.9* double-knockout embryos showed occasionally a brief gasping. A small proportion of *Nkx2.9*$^{-/-}$ single and *Nkx2.2*$^{+/-}$*;Nkx2.9*$^{-/-}$compound mutant embryos also showed breathing inability after caesarian section.

Genotype	wildtype	*Nkx2.2*$^{-/-}$	*Nkx2.9*$^{-/-}$	*Nkx2.2*$^{+/-}$*;Nkx2.9*$^{-/-}$	*Nkx2.2*$^{-/-}$*;Nkx2.9*$^{-/-}$
Total number of analyzed embryos	10	5	13	22	11
Number of embryos that don't breathe	0	0	3	2	10
% of embryos that don't breathe	0	0	23	9	91

Table.2: *Nkx2.2;Nkx2.9* double-null mutant embryos do not breathe. Plethysmographic recordings were made from a total of 10 wildtype, 5 *Nkx2.2*$^{-/-}$, 13 *Nkx2.9*$^{-/-}$, 22 *Nkx2.2*$^{+/-}$*;Nkx2.9*$^{-/-}$ and 11 *Nkx2.2*$^{-/-}$*;Nkx2.9*$^{-/-}$ mouse embryos at E18.5. Interestingly, 91% of the mouse embryos devoid of both *Nkx2.2;Nkx2.9* genes did not breathe. Some of the embryos which were not breathing showed from time to time a gasping behavior. In addition, 23% *Nkx2.9*$^{-/-}$ single and 9% *Nkx2.2*$^{+/-}$*;Nkx2.9*$^{-/-}$ compound mutant embryos did not breathe. In contrast, all wildtype and *Nkx2.2*$^{-/-}$ single mutant embryos breathed normally.

The failure to breathe in *Nkx2.2;Nkx2.9* double-null mouse embryos could be the result of a cell-autonomous or a non-cell autonomous influence. Since there is no evidence that the main respiratory rhythm generators which are located in the mammalian hindbrain (Mellen and Thoby-Brisson, 2012; Thoby-Brisson et al., 2009) are derived from Nkx2.2 and Nkx2.9-expressing p3 progenitors (see discussion, section 4.4), a cell-autonomous effect of Nkx2.2 and Nkx2.9 is unlikely to be the reason for the breathing failure. However, non-cell autonomous influences that could result from the loss of Nkx2.2 and Nkx2.9, such as failure or disturbance in the migration pattern of cells of the main respiratory rhythm generators could not be excluded. Thus, the two main respiratory rhythm generators of the hindbrain were analyzed (Mellen and Thoby-Brisson, 2012; Thoby-Brisson et al., 2009). Specifically, characteristic molecular markers were used to visualize the retrotrapezoid nucleus (RTN) (Stornetta et al., 2006; Thoby-Brisson et al., 2009) and the pre-Bötzinger complex (preBötC) (Gray et al., 2010; Pagliardini et al., 2003) in the wildtype and *Nkx2.2;Nkx2.9* double-null hindbrain.

The chemosensitive rhythmic interneurons of the RTN originate from the dorsal dB2 domain which expresses the transcription factors, Phox2b and Lbx1 (Bouvier et al., 2010; Mulkey et al., 2004; Nattie and Li, 2002; Onimaru et al., 2008; Sieber et al., 2007; Stornetta et al., 2006; Thoby-Brisson et al., 2009). RTN cells are not related to branchiovisceral motor neurons, however, they also require the Phox2b transcription factors together with Lbx1 for their proper development (Dubreuil et al., 2008; Dubreuil et al., 2009; Pagliardini et al., 2008). Mice devoid of Phox2b or Lbx1 are unable to form an RTN and such mutants die shortly after birth due to severe respiratory defects (Dubreuil et al., 2008; Dubreuil et al., 2009; Pagliardini et al., 2008). The cells that constitute the RTN are born at dorsal positions and migrate ventrally to finally cluster in a position close to the facial motor nucleus (VII) at the pial surface of the hindbrain (Bouvier et al., 2010; Dubreuil et al., 2009; Stornetta et al., 2006; Thoby-Brisson et al., 2009). RTN interneurons are known to express the neurokinin1 receptor (NK1R) (Nattie and Li, 2002; Pagliardini et al., 2008; Thoby-Brisson et al., 2009).

Using three characteristic markers, $Phox2b^{+}/Lbx1^{+}/NK1R^{+}$ RTN cells lying ventral to the facial nucleus (VII) were identified in the hindbrain of wildtype and *Nkx2.2;Nkx2.9* double-knockout embryos. The data revealed that the molecular phenotype, the number, and the location of RTN neurons was identical in wildtypes and *Nkx2.2;Nkx2.9* double-null embryos (Fig.35).

Finally, another important breathing center of the hindbrain was analyzed, namely the pre-Bötzinger complex that resides in the ventral medulla beneath the nucleus ambiguus (NA) and is comprised of glutamatergic commissural interneurons derived from the dorsal $Dbx1^{+}$ V0 domain (Gray et al., 2010; Bouvier et al., 2010; Thoby-Brisson et al., 2009). It has been shown that cells of the pre-Bötzinger complex are expressing the neurokinin 1 receptor (NK1R) at high levels (Gray et al., 1999; Stornetta et al., 2003). Immunolabeling the preBötC showed that this respiratory center was normally formed in *Nkx2.2;Nkx2.9* double-null mice (Fig.36).

Taken together, the normal expression pattern of the marker proteins characteristic for cells of the respiratory centers suggests that both, the RTN and preBötC complex, are formed normally and are likely to be functional in *Nkx2.2;Nkx2.9* double-null embryos based on their production of the specific NK1R receptor. Thus, it seems unlikely that the breathing defect is caused by anatomical or cellular abnormalities in the known central breathing centers.

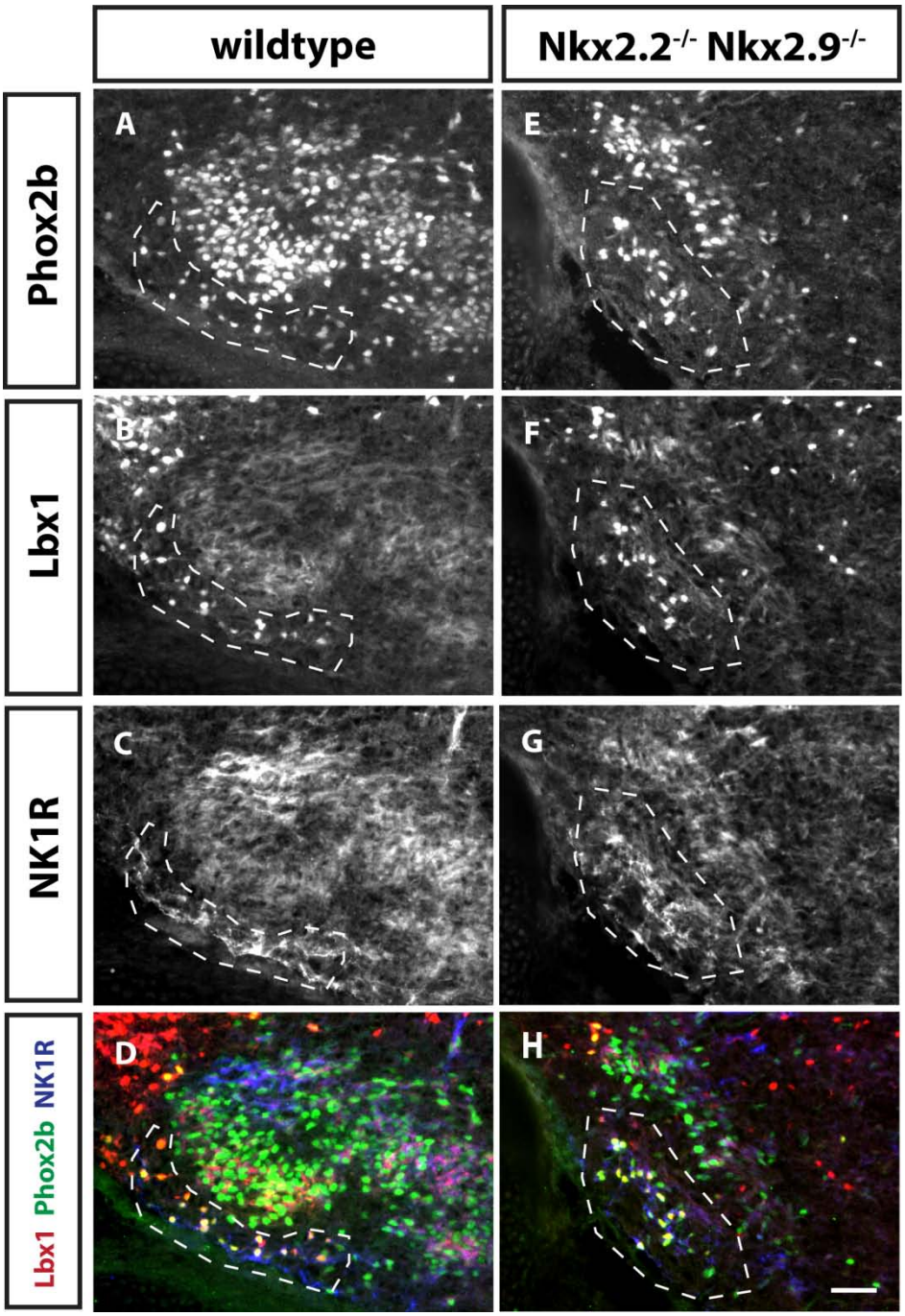

Fig.35: The retrotrapezoid nucleus (RTN) develops normally and reaches its ventral position lying below the facial motor nucleus in mutants deficient in both Nkx2.2 and Nkx2.9 transcription factors. The RTN can be distinguished by the co-expression of the molecular markers Lbx1 (red), Phox2b (green) and NK1R (blue). $Lbx1^{+}$/$Phox2b^{+}$/$NK1R^{+}$ RTN cells resided in a position ventral to the facial motor nucleus (also expressing Phox2b) in wildtype embryos (A - D, n=3). In the *Nkx2.2;Nkx2.9* double-null mutants (E - H, n=3), the RTN cells reached and settled in their normal position despite of the reduction in the facial motor nucleus (notice reduction in Phox2b-expressing cell number in the facial motor nucleus region). The images demonstrate magnifications of an immunostaining of transverse sections through the medulla of embryos at E15.5. Scale bar: 50µm.

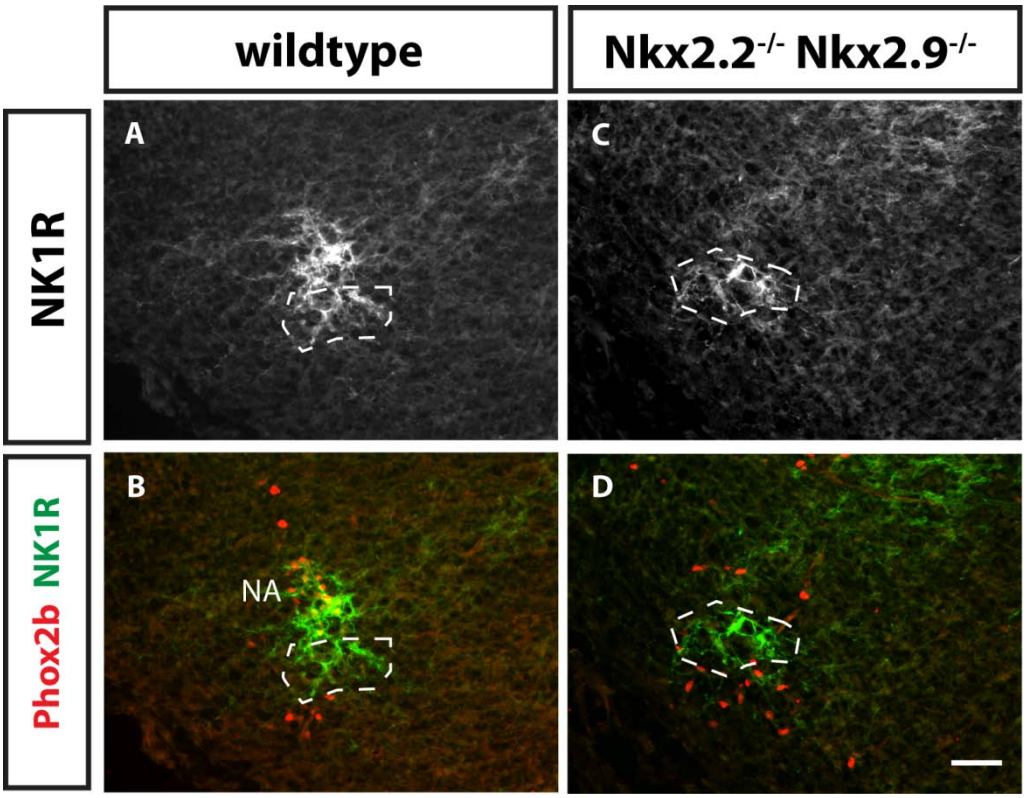

Fig.36: The pre-Bötzinger complex (preBötC) expressed the NK1R receptor in mutants lacking the *Nkx2.2* and *Nkx2.9* gene activity. In wildtype embryos, Phox2b^{+}/NK1R^{+} cells (A, B, n=4) which represent the nucleus ambiguous (NA), a branchiovisceral motor nucleus were detected which are absent in *Nkx2.2;Nkx2.9* double-null embryos (C, D, n=3). The NK1R^{+}/Phox2b^{-} cells lying immediately below the NA constitute the pre-Bötzinger complex in the wildtype (A, B). In contrast, in the *Nkx2.2;Nkx2.9* double-null mutant embryos, the NK1R^{+} cells in the preBötC area seemed to reside in their normal position and no changes in the general structure of the preBötc was observed (C, D). The images demonstrate magnifications of an immunostaining of transverse sections through the medulla of embryos at E15.5. Scale bar: 50µm.

4. Discussion

This study provides compelling evidence that the identity of p3 progenitor cells of the hindbrain is controlled by the redundant function of the Nkx2.2 and Nkx2.9 transcription factors. A requirement of Nkx2.2 and Nkx2.9 for the specification of branchiovisceral motor neurons was demonstrated. In absence of *Nkx2.2* and *Nkx2.9* gene function, the fate of motor neuron progenitors switches subtype identity from bvMN to sMN. Genetic labeling of the p3 cell lineage in the hindbrain illustrates that all branchiovisceral motor neurons are descendants of Nkx2.2^{+} progenitors and these progenitor cells undergo ventral-to-dorsal transformation of the p3 fate in mice lacking the *Nkx2.2* and *Nkx2.9* genes. This work also reveals that in absence of Nkx2.2 and Nkx2.9 transcription factors postnatal embryos die soon after birth due to severe respiratory problems, emphasizing the importance of proper *Nkx2.2* and *Nkx2.9* gene function for survival.

4.1 Nkx2.2 and Nkx2.9 function redundantly in neuronal progenitor cells to determine the branchiovisceral type of motor neurons

This work demonstrates that loss of Nkx2.2 and Nkx2.9 function in the hindbrain results in a ventral-to-dorsal transformation of progenitor cell identity. Progenitor cells of branchiovisceral motor neurons in hindbrain acquire the cell fate of somatic motor neurons in absence of Nkx2.2 and Nkx2.9 transcription factors. This transformation of cell fate confirms the role of homeodomain transcription factors to mediate Shh-dependent decisions to determine progenitor cell fate in the ventral neural tube. Previous studies showed that the loss of Shh-dependent homeodomain proteins in the ventral neural tube, such as Pax6 and Nkx6.1/Nkx6.2, caused transformation of cell identity (Ericson et al., 1997; Vallstedt et al., 2001). However, very little is known about the role of Nkx2.2 and Nkx2.9 in controlling cell fate decisions in the hindbrain. My data show that a complete fate transformation occurs in mice lacking both *Nkx2.2* and *Nkx2.9* genes, while in contrast the p3 progenitor domain in *Nkx2.2*$^{-/-}$ and *Nkx2.9*$^{-/-}$ single mutants as well as in *Nkx2.2*$^{+/-}$*;Nkx2.9*$^{-/-}$ compound mutants is mostly conserved (Fig.14). Specifically, cells expressing Olig2 entirely replace the bvMN progenitors in the p3 territory of hindbrain in *Nkx2.2;Nkx2.9* double-null embryos (Fig.14). Since there is no evidence for increased cell death in the p3 progenitor domain of *Nkx2.2;Nkx2.9* double-knockout embryos, cell fate conversion is likely to occur (Fig.16). A definite proof for this idea came from cell lineage tracings using the *Nkx2.2*^{Cre} knockin mouse. With this tool it was shown that ectopic

Olig2^{+} cells in the p3 territory expressed the GFP reporter (Fig.25). These findings are in accordance with similar studies in the spinal cord (Holz et al., 2010; Lek et al., 2010) and suggest that the correct determination of progenitor cell identity in the p3 domain requires either Nkx2.2 or Nkx2.9 or both arguing for at least partial functional redundancy between both proteins.

In previous studies it was shown that Nkx2.2 in spinal cord represses the expression of Olig2 (Novitch et al., 2001) and the generation of somatic motor neurons (Briscoe et al., 1999). Lineage tracing studies of motor neurons in the developing murine spinal cord showed that Nkx2.2 is expressed in cells that earlier during development expressed Olig2 (Dessaud et al., 2007). In addition, in the early ventral neural tube (E8.5), *Shh*-dependant Olig2 expression precedes that of Nkx2.2 in the most ventral cells of the CNS that will later develop into non-neuronal floor plate cells (Chamberlain et al., 2008; Dessaud et al., 2007; Jeong and McMahon, 2005). Hence, it is likely that expression of Olig2 is repressed by Nkx2.2 and/or Nkx2.9 in newly formed/specified p3 progenitors. My data support this view/hypothesis convincingly since Olig2 remained expressed in cells in which the transcriptional repressors Nkx2.2 and Nkx2.9 were lost and as a consequence sMNs were generated instead of bvMNs. Thus, Nkx2.2 and Nkx2.9 control the subtype identity of motor neurons in the hindbrain. Counting cells expressing the pan-motor neuronal marker Islet-1 indicated that the total number of motor neurons generated in hindbrain of *Nkx2.2;Nkx2.9* double-null mutant embryos was not changed compared to wildtype, *Nkx2.2*$^{-/-}$ and *Nkx2.9*$^{-/-}$ single, and *Nkx2.2*$^{+/-}$*;Nkx2.9*$^{-/-}$compound mutant embryos (Fig.8). However, the subtype of motor neurons was altered from branchiovisceral to somatic in rhombomeres 4 to 7. Furthermore, using cre-mediated cell lineage tracing I could convincingly demonstrate that transformed GFP^{+} motor neurons in *Nkx2.2;Nkx2.9* double-null mutants sent trajectories into the periphery via ventral exit points together with the natural somatic motor neurons in posterior rhombomeres (rhombomeres 5 and 7) (Fig.26, Fig.29). Most interestingly, in rhombomeres that usually do not produce somatic motor neurons, axons of transformed cells leave the CNS via newly formed ventral exit points (rhombomere 4) (Fig.27). As a consequence of the cell fate change in the motor neuron pool, nuclei of the accessory nerve (r7, C1-C5), vagus nerve (r7), glossopharyngeal nerve (r6) and facial nerve (r4-r5) are severely reduced or absent in *Nkx2.2/Nkx2.9* double-null embryos.

Using Nkx2.2 cre-mediated cell lineage analysis allows specific visualization of the motor component of cranial nerves in control and *Nkx2.2;Nkx2.9* double-null embryos. In this way it was shown that all posterior branchiovisceral motor nerves are missing or significantly reduced in *Nkx2.2;Nkx2.9* double-null embryos. The accessory nerve and vagus nerve are totally lost in *Nkx2.2;Nkx2.9* double-null embryos (Fig.28). The numbers of GFP^+ axonal projections of the glossopharyngeal and facial motor nerves are also severely decreased in *Nkx2.2;Nkx2.9* double-knockout embryos. In contrast, the anterior groups of bvMNs, i.e. the trigeminal motor neurons located in rhombomeres 2-3, are only mildly affected and the trigeminal motor nucleus forms normally in absence of Nkx2.2 and Nkx2.9. Projections of these rostral neurons to their peripheral targets were indistinguishable in controls and *Nkx2.2;Nkx2.9* double-null embryos. Very few ectopic $Olig2^+$ cells are present in the rostral p3 progenitor territory of *Nkx2.2;Nkx2.9* double-null embryos, indicating that the cell fate change from bvMN to sMN does not occur with high frequency in the anterior rhombomeres r2 and r3 (Fig.4-6, Fig.10, Fig.12, Fig.28, data not shown). The fact that bvMNs are normally generated in r2 of *Nkx2.2;Nkx2.9* double-knockout embryos and that some bvMNs of the facial nucleus are produced in r4/r5 and reach their final positions after extensive migration, raises the question whether a *Nkx2.2* and *Nkx2.9* independent pathway exists in rostral hindbrain that leads to the generation of motor neurons. It is reasonable to assume that other factors might be responsible for the formation of p3-derived bvMNs specifically in rhombomere 4 contributing to the facial nerve. Since p3 progenitors in r2-r3 are unaffected in *Nkx2.2;Nkx2.9* double-null mice, it seems likely that so far unknown genes regulate bvMN identity in these anterior rhombomeres. Segment identity of rhombomeres along the rostro-caudal axis is not affected in *Nkx2.2;Nkx2.9* double-knockout embryos since the rhombomere-specific expression of Hoxb1 and Hoxb4 genes shows no alterations in *Nkx2.2;Nkx2.9* double-null embryos compared to wildtype (Fig.11, data not shown). Moreover, the sensory roots and motor axons of cranial nerves derived from the anterior rhombomeres develop normally in *Nkx2.2;Nkx2.9* double-knockout mutant (Fig.4, Fig.5). Thus, a general change of regional specification along the rostro-caudal axis in hindbrain of *Nkx2.2;Nkx2.9* double-null mice is unlikely to play a role.

Thus, *Nkx2.2* and *Nkx2.9* are important for the development of bvMNs. Nkx2.2 and/or Nkx2.9 determine the p3 progenitor cells likely by suppressing the expression of Olig2 leading to the differentiation into bvMNs.

4.2 Nkx2.9 appears to be required to exclude *Nkx2.2* gene activity from medial floor plate cells

Floor plate (FP) cells occupy the ventral midline of the neural tube (Del Brio et al., 2001; Jessell et al., 1989; Jessell and Dodd, 1990; Placzek and Briscoe, 2005; Rodríguez et al., 1996) where they participate in dorso-ventral patterning of the spinal cord and play a role in axonal pathfinding of commissural interneurons (Charron et al., 2003; Colamarino and Tessier-Lavigne, 1995; Jessell, 2000; Tanabe and Jessell, 1996). Nkx2.2 and Nkx2.9 proteins are already expressed in prospective floor plate cells at early stages of development between E7.5 and E9.5 (Chamberlain et al., 2008; Holz et al., 2010; Jeong and McMahon, 2005; Lek et al., 2010; Ono et al., 2010; Pabst et al., 1998; Ribes et al., 2010).

It has been shown previously that the floor plate in the spinal cord of *Nkx2.2;Nkx2.9* double-null embryos is structurally and functionally defective (Holz et al., 2010; Lek et al., 2010). In contrast, the floor plate in hindbrain of mutant embryos shows no significant defects based on the number of $FoxA2^{+}$ cells (Fig.30, Fig.31). Interestingly, FoxA2 is also expressed in the prospective p3 domain of hindbrain in wildtype embryos at E10.5 (Fig. S1, Fig.15, Fig.31) and transformed $Olig2^{+}/FoxA2^{+}$ positive cells are detected in *Nkx2.2;Nkx2.9* double null embryos dorsal to but not within the floor plate (Fig.15, B).

In cell lineage tracings using $Nkx2.2^{cre};Rosa26^{mTmG}$ mouse embryos, very few GFP-expressing cells were found in the floor plate of hindbrain (Fig.31, Fig.32) and this sparse GFP expression pattern persisted into later developmental stages (E12.5) (data not shown). This result is somewhat surprising, since previously published data clearly demonstrated that Nkx2.2 is expressed (E8.5- E9.5) in the most ventral cells of the neural tube which will contribute to floor plate tissue during subsequent development (Chamberlain et al., 2008; Jeong and McMahon, 2005; Lek et al., 2010; Ono et al., 2010; Ribes et al., 2010). In this scenario, GFP reporter expression would be expected to accumulate in the entire floor plate territory. One explanation for the surprising result might be that cells co-expressing Nkx2.2 and FoxA2 in the prospective floor plate region early in development disappear from the floor plate territory at later developmental stages (E10.5) by migration to the prospective p3 domain. Such a morphogenetic process might contribute to the cell segregation into the floor plate domain harboring non-neuronal cells and the p3 domain consisting of neuronal progenitor cells. In this way the defined and sharp boundary between both regions may be established as described recently for zebrafish (Xiong et al.,

2013). It should be mentioned that very few GFP^{+} cells remain in the floor plate territory of *Nkx2.2^{cre};Rosa26^{mTmG}* embryos at E10.5 the reasons for which are presently unclear but may include a brief and biologically non functional activation of the Nkx2.2 gene during early neural tube development (Fig.31, Fig.32). To clarify this hypothesis further experiments need to be done with *Nkx2.2^{cre};Rosa26^{mTmG}* embryos at earlier developmental stages (E8.5 and E9.5). An antibody directed against the Cre recombinase protein might also be useful to identify cells at the onset of *Nkx2.2* gene activity in the floor plate region.

Interestingly, ectopic *Nkx2.2* gene activity reflected by GFP expression was detected in the entire territory of the FoxA2-positive floor plate which appeared morphologically normal in *Nkx2.2$^{cre/-}$;Nkx2.9$^{-/-}$;Rosa26$^{mTmG/+}$* double-null mouse embryos. This observation suggests that in absence of both Nkx2.2 and Nkx2.9 transcription factors the *Nkx2.2* gene activation expands ectopically into cells of the medial floor plate. Most of these cells do not express Nkx2.2 in wildtype embryos. *Nkx2.9* is expressed in the most ventral region of the neural tube early in development at E7.5 (Pabst et al., 1998; Holz et al., 2010), whereas Nkx2.2 is not expressed in medial floor plate but rather in p3 progenitor cells that reach their final domain at E10.5 (Fig.31, Fig.32). A possible explanation for the ectopic *Nkx2.2* gene activity in the entire floor plate region of *Nkx2.2;Nkx2.9* double-null mutants is that Nkx2.9 and/or Nkx2.2 are needed to prevent the activation of the *Nkx2.2* gene in floor plate cells. That *Nkx2.2* gene activity is suppressed in the floor plate but not in p3 progenitors of the wildtype mouse suggests that Nkx2.9, although required, may not be sufficient to switch off Nkx2.2 in the most ventral cells. An additional factor, possibly Shh or high levels of FoxA2 may play a role. It is worth mentioning that the floor plate in hindbrain of *Nkx2.2;Nkx2.9* double-null embryos appears fairly normal, despite the ectopic activation of *Nkx2.2* in floor plate territory. Thus, loss of both Nkx2.2 and Nkx2.9 transcription factors in hindbrain does not seem to lead to a fate change of the floor plate cells, whereas it does result in the transformation of branchiovisceral to somatic motor neurons. The reasons for these differences are presently unclear.

4.3 The *Nkx2.2^{Cre}* mouse line is a reliable tool for cell lineage tracing

Cell lineage tracing or fate mapping represents a powerful approach to identify and mark the progeny of a single cell in the living tissue (Kretzschmar and Watt, 2012). Using conventional tracing techniques, such as injecting cells with vital dyes (e.g. DiI) or introducing transient expression markers via cell transfections, has the intrinsic disadvantage that only snapshots of development and movement of cells are obtained at

different time points. In addition, the specificity of such conventional techniques are usually less specific than genetic cell lineage tracings by cre-mediated recombination in which the progeny of a genetically-marked cell is permanently labeled. Furthermore, genetic cell lineage tracing allows studying cell fate decisions in specific tissues/cells in the presence and absence of selected genes.

In this study, the *Nkx2.2*^{cre} mouse line was found to be a suitable tool for cell lineage tracing studies, since it reliably labeled Nkx2.2-expressing cells and their descendants (Fig.19- Fig.23). For these purposes, the *Nkx2.2*^{cre} mouse line was crossed with *Rosa26*^{mTmG} and *Rosa26*^{LacZ} reporter mice (Fig.18; Muzumdar et al., 2007; Soriano, 1999). The *Rosa26*^{mTmG} reporter was particularly important for the analysis of axonal projections, since GFP marker in this mouse strain is coupled to membranes and therefore was readily detectable in axons of recombined cells. In contrast, the *Rosa26*^{LacZ} reporter was suitable for analyzing the cell bodies of developing neurons but often failed to mark axonal projections due to preferential accumulation of β-galactosidase in the cytoplasm of somata.

Previous studies showed the double-expression of Nkx2.2 and Phox2b (Pattyn et al., 2000; Pattyn et al., 2003a) at specific rostro-caudal rhombomere levels, providing a regional link between p3 progenitors and bvMNs. Lineage tracing data provided evidence that all branchiovisceral motor neurons, including the trigeminal motor neurons which are not affected in *Nkx2.2;Nkx2.9* double-null embryos, are descendants of Nkx2.2-expressing p3 progenitors (Fig.19- Fig.23).

Furthermore, analysis of bvMN fate in *Nkx2.2;Nkx2.9* double-null embryos using the *Nkx2.2*^{cre} line proved the ventral-to-dorsal transformation in cell fate hypothesis (see section 4.1 for details) and substantiates the usefulness of the *Nkx2.2*^{cre} knockin mouse strain.

Lineage tracing of serotonergic neurons using the *Nkx2.2*^{cre} mouse confirmed that serotonergic neurons along the entire hindbrain are also descendants of the p3 progenitors (Fig.33, data not shown). Previous studies have shown the close regional relation of Nkx2.2^{+} p3 progenitors and Lmx1b^{+} serotonergic precursor cells (Ding et al., 2003). Furthermore, almost complete loss of 5-HT^{+} neurons was observed in *Nkx2.2*$^{-/-}$ knockout mice (Briscoe et al., 1999; Pattyn et al., 2003a). The *Nkx2.2*^{cre} mouse line allowed the lineage tracing of serotonergic neurons in *Nkx2.2*-deficient embryos (Fig.34, data not shown). However, the previously suggested transformation of 5-HT neurons into bvMNs

(Pattyn et al., 2003a) could neither be confirmed nor falsified since reporter expression is present in both neuronal subtypes, the bvMNs and the 5-HT neurons (Fig.34).

The analysis of *Nkx2.2^{cre};Rosa26^{mTmG}* embryos confirmed that commissural V3 interneurons of the spinal cord are indeed derived from Nkx2.2^{+} p3 progenitor cells (data not shown, Briscoe et al., 1999). Moreover, using the *Nkx2.2^{cre}* mouse line two other cell types in which *Nkx2.2* was described to be expressed during development were also labeled. These were oligodendrocytes (GFP^{+} cells close to the ventricle in Fig.23 and Fig.24, data not shown; Qi et al., 2001) and pancreatic islet cells (Fig.19, data not shown; Sussel et al., 1998).

4.4 Loss of the Nkx2.2 and Nkx2.9 transcription factors causes severe breathing problems that lead to rapid postnatal death

This study provides evidence that in the absence of both the *Nkx2.2* and *Nkx2.9* genes embryos do not breathe and die shortly after birth (Table 2). In comparison, only a very small proportion of *Nkx2.9$^{-/-}$* single and *Nkx2.2$^{+/-}$;Nkx2.9$^{-/-}$* mutants failed to breathe (Table 2). *Nkx2.2$^{-/-}$* single mutants were comparable to wildtypes and started initial breathing (Table 2).

Breathing is a motor behavior that is regulated by respiratory rhythm-generators in the hindbrain, the proper functions of which are required for survival (Mellen and Thoby-Brisson, 2012). The respiratory rhythm is described to be generated from two distinct, but functionally coupled rhythm generators: the retrotrapezoid nucleus (RTN) and the pre-Bötzinger complex (preBötC) (Mellen and Thoby-Brisson, 2012). The developmental origins of the RTN and pre-Bötzinger complex are well described (Bouvier et al., 2010; Gray et al., 2010; Mellen and Thoby-Brisson, 2012; Thoby-Brisson et al., 2009). Using genetic cell-lineage tracing it was shown that the dorsal dB2 domain gives rise to RTN neurons (Thoby-Brisson et al., 2009) and most pre-Bötzinger cells originate from Dbx1-expressing V0 progenitors (Bouvier et al., 2010; Thoby-Brisson et al., 2009). dB2-derived RTN neurons are characterized by the expression of Phox2b, a TF that is also expressed by bvMNs (see Fig.6 for dorsal Phox2b-expressing cell populations which represent, among other cells, RTN cells). Analysis of *Nkx2.2^{cre};Rosa26^{lacZ}* mice revealed that Lbx1^{+}/Phox2b^{+}/Islet1^{-} RTN cells are not derived from the p3-progenitors (data not shown). These results are in agreement with results that come from conditional Phox2b mutants which express cre recombinase from the Islet1 locus, which is expressed in all motor

neurons and therefore leads to elimination of all bvMNs (Dubreuil et al., 2009). The RTN cells in these conditional mutants retained expression of Phox2b indicating that they are not derived from bvMN progenitors (Dubreuil et al., 2009). According to these data, it is unlikely that a cell-autonomous influence of the Nkx2.2 and Nkx2.9 transcription factors accounts for the observed breathing failure in *Nkx2.2;Nkx2.9* double-null mouse embryos.

It remains possible, however, that the breathing failure in *Nkx2.2;Nkx2.9* double-null mouse embryos is a result of non-cell autonomous influence, such as developmental migration defects of cells forming the respiratory generator. A first analysis of both respiratory rhythm generators (RTN and preBötC) in *Nkx2.2;Nkx2.9* double-knockout embryos revealed no differences in the gross anatomy of these neuronal nuclei. Furthermore, the RTN and preBötC are likely to be functional, since they expressed the neurokinin (NK)1 receptor normally, a neurotransmitter receptor that is highly expressed in functional RTN and preBötC interneurons (Stornetta et al., 2003; Nattie and Li, 2002) (Fig.35, Fig.36). RTN cells localize in close proximity to the facial motor nucleus (Fig.35; Thoby-Brisson et al., 2009), raising the formal possibility that an intact facial nucleus affects dorsal to ventral migration of RTN progenitor cells. This is apparently not the case, rather, cells of the RTN were present at their normal positions in the ventral medulla of *Nkx2.2;Nkx2.9* double-null embryos where they localized at the pial surface near the defective facial nucleus (Fig.35). These results are in agreement with a previous study in which RTN cells were shown to migrate to their normal ventral positions in embryos lacking the facial motor nucleus (Dubreuil et al., 2009). Moreover, embryos containing a mutation that affects migration of facial motor neurons showed that the migration of RTN and preBötc cells was not grossly affected and their functional and anatomical characterisctics were not altered since they generated organized rhythmic output (Thoby-Brisson et al., 2012). Altogether, my own and these published results indicate that the severe reduction or loss of motor neurons (facial nucleus and nucleus ambiguus) in mouse embryos lacking *Nkx2.2* and *Nkx2.9* does not have an effect on the migration pattern of cells forming the respiratory rhythm generator. Although the immunohistochemical analysis of RTN and preBötC cells indicated no functional impairment, a detailed cellular and electrophysiological analysis (e.g calcium imaging) of these cells is needed for unambiguous results.

Serotonergic neurons have been suggested to play an important role in the control of respiratory output of neuronal nuclei implicated in the regulation of breathing (Richerson, 2004). However, our plethysmographic recordings showed that *Nkx2.2*$^{-/-}$ single mutants were able to start initial breathing (Table.2) despite their lack of serotonergic neurons (Briscoe et al.,1999; Pattyn et al., 2003a). Thus, serotonergic neurons are unlikely to be the reason for the severe breathing problems of *Nkx2.2;Nkx2.9* double-knockout mice. They are rather suggested to act as sensors of blood carbon dioxide and seem to play a role in regulating the rhythm of breathing in response to environmental challenges (Erickson et al., 2007; Richerson, 2004).

Pathfinding defects of commissural axons were previously observed in the spinal cord of *Nkx2.2;Nkx2.9* double-null embryos and are suggested to be the result of a severe floor plate defect (Holz et al., 2010). Prebötc interneurons are characterized by their commissural projections which are essential for proper bilateral synchronization of the Prebötzinger complex and the correct breathing rhythm (Tan et al., 2010). Hence, an alternative hypothesis to explain the breathing defect of *Nkx2.2;Nkx2.9* double-null animals could be the inability or disturbance of respiratory axons to cross the midline of the medulla correctly. To test for possible axon pathfinding defects in the hindbrain, anterograde labeling of commissural neurons in the Prebötc should be performed in future experiments.

Motor neurons of the nucleus ambiguus (also considered to be one of the main respiratory nuclei) send axonal projections (vagus nerve and cranial accessory nerve) that innervate laryngeal muscles which play a role in adjusting the respiratory airflow (Dutschmann and Paton, 2002; Richerson, 2004). The nucleus ambiguus is absent in mouse embryos lacking Nkx2.2 and Nkx2.9 (Fig.12, T). However, it is unlikely that loss of innervation of laryngeal muscles might be the underlying mechanism for such severe breathing problems in *Nkx2.2;Nkx2.9* double-null postnatal mice.

5. Materials and Methods

5.1 Materials

5.1.1 Standard Solutions

10x Phosphate buffered saline (PBS) (pH 7.4): 80 g NaCl, 2 g KCL, 2.4 g KH_2PO_4, 14.4 g Na_2HPO_4. ad. 1 L and autoclave. Do not adjust pH!! pH of 1xPBS should be 7.4.

4%Paraformaldehyde (PFA)/PBS: 200 ml 1xPBS, 20 g PFA, ˜800 µl 4M NaOH, dissolve at 60°C then add 250 ml 1xPBS, adjust pH to 7.4 then ad. 500ml with 1xPBS and filter-sterilize (0.45µm).

Lysis buffer: For 100 ml: 10 ml 1M TrisHCl (pH 8.5), 4 ml 5M NaCl, 2 ml 10% SDS, 1 ml 0.5M EDTA (pH 8.0), 83 ml ddH_2O.

5.1.2 Antibodies and Sera

5.1.2.1 Primary Antibodies

Antibody (clone) name/Order number	Antigen	Host Species	Isotype	Dilution	Source/Company
Phox2b (H-20)	Phox2b	goat	Polyclonal IgG	1:500	Santa Cruz Biotechnology
Phox2b	Phox2b	rabbit	Polyclonal IgG	1:500	Prof.Dr.Jean-François Brunet (Pattyn et al., 1997)
81.5C10	MNR2/Hb9	mouse	IgG1	1:400	DSHB
2H3	Neurofilament (165 kDa)	mouse	IgG1	c- 1:800; s- 1:20	DSHB
74.5A5	Nkx2.2	mouse	IgG2b	c- 1:1000; s- 1:70	DSHB
F55A10	Nkx6.1	mouse	IgG1	1:800	DSHB
40.2D6	Islet-1 homeobox	mouse	IgG1	1:600	DSHB
39.4D5	Islet-1&2 homeobox	mouse	IgG2b	1:600; E14.5 and above 1:300)	DSHB
4C7	HNF3b/FoxA2	mouse	IgG1	1:400	DSHB
GFP (MAB3580)	GFP	mouse	IgG1	1:800	Millipore
GFP (A-11122)	GFP	rabbit	Polyclonal IgG	1:2000	Molecular probes
Olig2 (18953)	Olig2	rabbit	Polyclonal IgG	1:400	IBL
Lbx1	Lbx1	guinea pig	Polyclonal IgG	1:16000	Prof.Dr.Carmen Birchmeier (Müller et al., 2002)
Hoxb1 (PRB-231P)	Hoxb1	rabbit	Polyclonal IgG	1:200	Covance
ß-galactosidase (#559761)	ß-galactosidase	rabbit	Polyclonal IgG	1:10000	Cappel

active caspase 3 (ab2302)	active caspase 3 peptide	rabbit	Polyclonal IgG	1:300	Abcam
NCAM-L1 (C-20)	NCAM L1	goat	Polyclonal IgG	1:500	Santa Cruz Biotechnology
5HT (s5545)	Serotonin	rabbit	Polyclonal	1:5000	Sigma
NK1R (s8305)	NK1R	rabbit	Polyclonal IgG	1:5000	Sigma
AP-conjugated anti-digoxigenin (DIG)	DIG	sheep	IgG, Fab fragments	1:2000	Roche

Table 3: List of primary antibodies used in this study. c: concentrate, s: supernatant. DSHB: Developmental Studies Hybridoma Bank, the University of Iowa.

5.1.2.2 Secondary Antibodies:

Antibody name/Order number	Isotype	Host Species	Conjugate/ Flourochrome	Dilution	Source / Company
anti-mouse (115-545-205)	IgG1	goat	Alexa Fluor® 488	1:600	Jackson Immunoresearch
anti-mouse (115-165-205)	IgG1	goat	Cy3	1:300	Jackson Immunoresearch
anti-mouse (115-605-205)	IgG1	goat	Alexa Fluor® 647	1:300	Jackson Immunoresearch
anti-mouse (115-545-207)	IgG2b	goat	Alexa Fluor® 488	1:600	Jackson Immunoresearch
anti-mouse (115-165-207)	IgG2b	goat	Cy3	1:300	Jackson Immunoresearch
anti-mouse (115-605-207)	IgG2b	goat	Alexa Fluor® 647	1:600	Jackson Immunoresearch
anti-rabbit (711-175-152)	IgG	donkey	Cy5	1:300	Jackson Immunoresearch
anti-rabbit (711-546-152)	IgG	donkey	Alexa Fluor® 488	1:600	Jackson Immunoresearch
anti-guinea pig (706-165-148)	IgG	donkey	Cy3	1:300	Jackson Immunoresearch
anti-goat (705-165-147)	IgG	donkey	Cy3	1:300	Jackson Immunoresearch
anti-goat	IgG	donkey	Alexa Fluor® 647	1:800	Invitrogen
anti-goat (705-035-033)	IgG	donkey	HRP	1:600	Jackson Immunoresearch
anti-rabbit (711-035-152)	IgG	donkey	HRP	1:600	Jackson Immunoresearch
anti-mouse (115-035-205)	IgG1	goat	HRP	1:600	Jackson Immunoresearch

Table 4: List of secondary antibodies used in this study. HRP: horseradish peroxidase, Cy: Cyanine.

5.1.3 Sera and Blocking solutions

Normal sera (all sera were heat-inactivated before storage and use): donkey serum, goat serum, horse serum and sheep serum (Millipore Chemical).

Blocking reagent (#1096176, Roche).

5.2 Methods

5.2.1 Mouse strains and generation of mouse embryos

Nkx2.9-deficient (Pabst et al., 2003), *Nkx2.2*-deficient (Sussel et al., 1998), *Nkx2.2*^{cre} (this mouse was generated in the group of Prof.Dr.Hans-Henning Arnold by Dr.Andreas Holz), *Rosa26*^{mTmG} (Muzumdar et al., 2007), *Rosa26*^{LacZ} (Soriano, 1999) and wildtype mice were used in this study. Mice of mixed C57BL/6J/129Sv/CD1 backgrounds were used in this study. The *Nkx2.9*$^{-/-}$ single mutant mouse was generated by disrupting the *Nkx2.9* gene and replacing it by the *LacZ* gene (Pabst et al., 2003). The *Nkx2.2*$^{-/-}$ single mutant mouse was generated by replacing the *Nkx2.2* open reading frame by a PGK-neomycin cassette (Sussel et al., 1998). The *Nkx2.2*^{cre} mouse was generated by replacing the entire endogenous *Nkx2.2* gene by the *Cre recombinase* ORF (this mouse was generated in the group of Prof.Dr.Hans-Henning Arnold by Dr.Andreas Holz). *Nkx2.2* null mutant mice die shortly after birth due to severe hyperglycemia because of loss of islet cells of the pancreas (Sussel et al., 1998). Mouse embryos with the *Nkx2.2*$^{+/-}$*;Nkx2.9*$^{-/-}$ genotype, containing one *Nkx2.2* allele, develop into adults and show no anatomical defects, but the majority display an abnormal locomotion (i.e. hopping gate) (Holz et al., 2010). The abnormal locomotion is most probably the result of a defect in the function of central pattern generators of the spinal cord (Holz et al., 2010). *Nkx2.2;Nkx2.9* double-null mutant embryos were obtained by crossing *Nkx2.2*$^{+/-}$*;Nkx2.9*$^{-/-}$ compound mutant mice. Mouse embryos of all *Nkx2.2;Nkx2.9* genotype combinations develop until birth suggesting that the *Nkx2.2* and *Nkx2.9* genes are not embryonic lethal. *Nkx2.2;Nkx2.9* double-null embryos die shortly after birth because of breathing defects (see results section 3.4 for more details). The morning of detection of the vaginal plug was considered as gestational age 0.5.

5.2.2 Preparation of embryos, isolation of DNA and genotyping of transgenic mice

Embryos were dissected out and stored in 1x PBS before usage for experiments. Extra-embryonic membranes were isolated and digested overnight with lysis buffer containing Proteinase K at 56°C. To isolate DNA, 100 µl of the lysate was mixed with 100 µl isopropanol and centrifuged at 13000 rpm for 10 min. The supernatant was discarded and the pellet was left to dry for a maximum of 5 minutes. Finally, the pellet was resuspended in 10mM Tris (pH 8.0). DNA was dissolved at 60°C for 2 hours and used for genotyping using the polymerase chain reaction (PCR) method. Genotyping of mice and embryos of the *Nkx2.9, Nkx2.2, Nkx2.2*^{cre}, *Rosa26*^{mTmG} and *Rosa26*^{LacZ} mouse lines was based on the

PCR programs described in Table 5. The primer sequences used for genotyping and the expected sizes of PCR products for the different mouse lines are listed in Table 6.

Mouse strain	Primer	Initial denaturing	Denaturing	Annealing	Elongation	Cycle number
Nkx2.9	2.9 10332 2.9 10623 KO 258	94°C 10 min	94°C 30 sec	60°C 30 sec	72°C 45 sec	35
Nkx2.2	Nkx2.2 #6 sense Nkx2.2 #7 AS Nkx2.2 mut#1 AS	94°C 10 min	94°C 30 sec	60°C 30 sec	72°C 45 sec	35
Nkx2.2^{cre}	Nkx2.2 #26 sense Nkx2.2 #27 AS iCre #3 AS	94°C 10 min	94°C 30 sec	57°C 30 sec	72°C 30 sec	35
Rosa26^{mTmG}	Rosa 10 Rosa 11 PCMV#2 AS	94°C 10 min	94°C 30 sec	58°C 30 sec	72°C 45 sec	35
Rosa26^{LacZ}	Rosa26R #1 Rosa26R #2 Rosa26R #3	94°C 10 min	94°C 30 sec	57°C 30 sec	72°C 30 sec	35

Table 5: PCR protocols used for genotyping of the different transgenic mouse lines analyzed in this study are listed in this table. PCR: polymerase chain reaction

Mouse strain	Primer name	Primer Sequence	Expected fragment size
Nkx2.9	2.9 10332 2.9 10623 KO 258	5'-ACC ACC GCT ACA AGC TGA AGC 5'-GGT GGT GCT AAG TGC TGG TAG 5'-AGC TCA TTC CTC CCA CTC ATG	Wildtype allele (291 bp) Mutant allele (400 bp)
Nkx2.2	Nkx2.2 #6 sense Nkx2.2 #7 AS Nkx2.2 mut#1 AS	5'-TTC CAA AGG CAC CAC AAA TCG C 5'-GGT CTT GGG AGT CAA GTG GAT GAA G 5'-TGA AGA ACG AGA TCA GCA GCC TCT	Wildtype allele (399 bp) Mutant allele (310 bp)
Nkx2.2^{cre}	Nkx2.2 #26 sense Nkx2.2 #27 AS iCre #3 AS	5'- TGC TTT CCG AGA AGA GAG AGG CA 5'- TTG TCG CTG CTG TCG TAG AAA GG 5'- ACA GTC AGC AGG TTG GAG ACT TTC CTC	Wildtype allele (450 bp) Mutant allele (290 bp)
Rosa26^{mTmG}	Rosa 10 Rosa 11 PCMV#2 AS	5'- CTC TGC TGC CTC CTG GCT TCT 5'- CGA GGC GGA TCA CAA GCA ATA 5'- TCA ATG GGC GGG GGT CGT T	Wildtype allele (330 bp) Mutant allele (250 bp)
Rosa26^{LacZ}	Rosa26R #1 Rosa26R #2 Rosa26R #3	5´−AAAGTCGCTCT- GAGTTGTTAT 5´−GCGAAGAGTTTGTCCTCAACC 5´−GGAGCGGGAGAAATG GATATG	Wildtype allele (500 bp) Mutant allele (250 bp)

Table 6: The sequence of primers used for genotyping the different transgenic mouse lines and the expected PCR product fragment sizes are listed in this table.

5.2.3 Cryosections

16 µm sections were made on a Cryostat (Leica, Jung Frigocut 2800E) at -18°C. Sections were thaw mounted onto SuperFrost Plus slides (Fisher Scientific) and the slides were stored at -20°C until use.

5.2.4 Immunohistochemistry on sections

Embryos were recovered and fixed for 60-120 min (depending on the age of the embryo: E10.5 and E11.5, 60 min; E12.5, 90 min; older than E12.5, 120 min) in 4% PFA/ PBS at 4°C. Embryos were washed several times and overnight with PBS at 4°C. Embryos were cryoprotected using 25% sucrose/PBS at 4°C for 48 hours (until embryos sank to the bottom of the well). Afterwards, embryos were embedded in TissueTek O.C.T. compound (Sakura) and stored at -80°C. Cryosections were prepared and stored at -20°C (see section 5.2.3). Sections were thawed, encircled with a PAP pen (Daido Sangyo Co.) and dried for 5 min. Then, sections were postfixed using 4% PFA/PBS at RT for 10 min. Sections were washed 3x with PBS (5 min each). Tissue was permeabilized at RT with 1% Tween-20 (Merck) and 1% Triton-X100 (Biorad) in PBS for 30 min. Sections were then washed 3x with PBS. Blocking solution (5% heat-inactivated normal serum from the host species of the secondary antibody in PBS) was added to the slides for one to two hours at RT in 5% blocking serum in PBS. Slides were incubated overnight with primary antibodies diluted in blocking solution at 4°C. The next day, slides were washed 3x with PBS (5 min each) and then the appropriate secondary antibodies diluted in PBS were added and incubated at RT for 2 hours. Slides were washed 3x with PBS (5 min each). DAPI (stock: 1mg/ml; Molecular Probes) diluted 1:1000 in PBS was added (counterstaining) at RT for 10 min. Again, the slides were washed 3x with PBS (5 min each). Finally, 2-3 drops Fluoro-gel (containing Tris buffer, Electron microscope Sciences) and a coverslip were added. Slides were left to dry over night and stored at 4°C until imaging.

5.2.5 In-situ hybridization on sections with Digoxigenin-labeled riboprobes

5.2.5.1 Preparation of the digoxigenin- labeled Peripherin riboprobe

Peripherin cDNA (1.8 kb) subcloned in the pKS vector was obtained from Prof.Dr.Marie-Madeleine Portier (Collège de France). In order to synthesize an antisense riboprobe of the *Peripherin* gene, the pKs-peripherin vector was linearized as follows: 5 µg of plasmid DNA were linearized with the ClaI enzyme (New England Biolabs) in a 50 µl restriction digest volume. To perform the Phenol extraction: 50µl of 10 mM Tris pH 8.0 was added to

the linearized DNA mix. Then, 100µl phenol:chloroform mix (1:1; Roth) were added and mixed well. The mix was then centrifuged at 13,000 rpm for 5 min at RT. The aqueous upper phase was transferred to a new eppendorf tube and 100µl of chloroform was added and mixed well. The mixture was centrifuged again at 13.000 rpm for 5 min at RT. The aqueous upper phase was transferred to a new eppendorf tube. DNA was precipitated by adding 10µl of 3M Sodium acetate (pH 5.2) and 250 µl icecold ethanol. DNA was precipitated for 30-60 min at -80°C. Afterwards, the probe was centrifuged at 13.000 rpm for 15 min at 4°C and the supernatant was decanted. The pellet was washed with 80% cold ethanol and centrifuged at 13.000 rpm for 15 min at 4°C. The supernatant was decanted and pellet was left to dry for 5 min. The pellet was resuspended in 33µl RNase-free H_2O (pH 7.0). In vitro transcription was performed to generate the antisense digoxigenin (DIG)-labeled riboprobe (DIG-RNA labeling Kit from Roche) as follows: 10µl of the Peripherin DNA probe (which corresponds to about 1µg DNA), 4µl 5x in vitro transcription buffer, 1 µl DTT, 2µl 10x DIG-UTP labeling mix, 1µl H_2O. The mixture was vortexed and 2 µl of the T7- RNA Polymerase (40-80 units) was added to produce an anti-sense probe. The mixture was mixed and incubated at 37°C for 2 hours (In-vitro transcription). The reaction was inactivated by adding 1 µl of 500µM EDTA (pH 8.0). Then, RNA was precipitated by adding 2.4µl LiCl and 75µl cold ethanol and storing at -80°C for a minimum of 30 min. Then, the mix was centrifuged at 13,000 rpm for 15 min at 4°C. The supernatant was decanted. The pellet was washed with 80% cold ethanol and centrifuged at 13,000 rpm for 15 min at 4°C. The supernatant was decanted and the pellet was left to dry for about 5 min. The RNA was then resuspended in 50µl RNase-free H_2O. The RNA sample was checked to determine the quality and yield of the generated digoxigenin-labeled Peripherin antisense riboprobe.

5.2.5.2 In-situ hybridization on sections procedure

This protocol is described in (Holz et al., 1996) and modifications appeared in (Oldstone et al., 1999) and (Zagrebelsky et al., 2005).

Embryos were recovered and fixed for 60-120 min (depending on the age of the embryo: E10.5 and E11.5, 60 min; E12.5, 90 min; older than E12.5, 120 min) in 4% PFA/ PBS at 4°C. Embryos were washed several times and overnight with PBS at 4°C. Embryos were cryoprotected using 25% sucrose/PBS at 4°C for 48 hours (until embryos sank to the bottom of the well). Afterwards, embryos were embedded in TissueTek O.C.T. compound (Sakura) and stored at -80°C. Cryosections were prepared and stored at -20°C (see section 5.2.3). Sections were thawed, encircled carefully with a PAP pen (Daido Sangyo Co.) and

were dried for 5 min. Postfixation by adding 4% PFA/PBS for 10 min at RT. washed 3x with PBS (5 min each). Acetylation was performed by adding: 140 µl tri-ethanolamine (SIGMA T-1377; final concentration: 0.1 M) and 25 µl acetic anhydride (final concentration: 0.25 %) to 10 ml H2O right before use (mixed well) and then adding 1 ml of the Acetylation solution to each slide for 10 min. Slides were washed 3x with PBS (each 5 min). Sections were permeabilized with 0.5 % Triton-X 100 in PBS for 10 min then washed 3x with PBS (each 5 min). Sections were pre-equilibrated in 5x SSC for 5 min. Prehybridization was performed by adding the hybridization solution (without probe) for 1 hour at RT. The hybridization solution consisted of: 50% Formamide (F9037 Bioreagent for molecular biology, Sigma), 5x SSC, 2% Blocking reagent solution (section 5.1.3). After prehybridization, the solution was exchanged with hybridization solution containing the denatured probe. For the hybridization solution, the riboprobe was denatured in autoclaved ddH2O at 80°C for 5 min and placed on ice. Then, about 30-50 ng riboprobe/ml hybridization solution was used which usually corresponds to 0.5 to 1 µl of a standard digoxygenin-riboprobe synthesis reaction. The sections were hybridized in a sealed humid chamber over night at 68°C. The next day, the slides were washed 2x in 2x SSC at room temperature (each 10 min). The slides were then washed 2x in 0.2x SSC at 68°C (for 30 min each). Then, slides were briefly washed in 2x SSC at RT. Immunological detection was carried out at RT. First, the slides were briefly equilibrated with Maleic acid buffer and then Blocked with Blocking solution for 1 hour. During the slide blocking duration, a parallel pre-absorption of the sheep anti-digoxigenin AP antibody was performed by diluting the antibody in Blocking solution (1:2000) (the anti-DIG AP antibody is produced in sheep; see table 3) and leaving the blocking/DIG-antibody solution at room temperature while blocking the tissue slides (60 – 120 min). The slides were then washed 2x with maleic acid buffer (each 30 minutes) and then left in maleic acid buffer over night at 4°C. The next day, slides were equilibrated 2x for 10 min with alkaline phosphatase buffer (100 mM Tris pH 9.5; 100 mM NaCl; 50 mM MgCl2). Then, the substrate was prepared by using the pre-prepared BCIP/NBT solution from Roche. Staining reaction was allowed for 30 min up to overnight in a light-protected box. Color reaction was stopped by incubation in 10 mM Tris pH7.5/ 25 mM EDTA for 1 hour. Counterstaining was done by incubating the slides with (1:1000) DAPI solution in PBS (Stock solution: 1 mg/ml in PBS; Molecular Probes) for 10 minutes. Finally, the slides were washed 3x in PBS and embedded in Fluoro-gel (containing Tris buffer, Electron microscope Sciences) and a coverslip was added.

Solutions

20x SSC, pH 7.0: For 1 liter: 175.3 g NaCl (Final: 3 M), 88.25 g tri-Sodium citrate dihydrate (Final: 0.3 M), adjust the pH to 7.0 with about 500 µl (!) conc. HCl and autoclave.

Maleic acid buffer, pH 7.5: For 1 liter: 11.6 g Maleic acid, 8.75 g NaCl, adjust pH to 7.5 with approximally 8 g NaOH pellets and finally 10 M NaOH and autoclave.

Blocking solution: (2 % BM, 5 % Sheep serum) in maleic acid buffer.

10 % BM solution (w/v): weight 10 g blocking reagent (see 5.1.3) and fill up to 100 ml with maleic acid buffer then autoclave, aliquot and store at -20°C.

5.2.6 Whole-mount Immunohistochemistry

5.2.6.1 Whole-mount Immunohistochemistry (Neurofilament, NCAM-L1 and Hoxb1)

This method was applied for whole-mount immunohistochemistry with antibodies directed against the Neurofilament, NCAM-L1 and Hoxb1 antigens.

Preparation and Fixation of Embryos: After the embryos were obtained, they were fixed in freshly prepared Methanol/DMSO (4:1) at 4°C overnight. The next day, the embryos were transferred into freshly prepared methanol/DMSO/H_2O_2 (4:1:1) at RT for 5 to 10 hours. The embryos were the n stored in 100% methanol at -20 °C until use.

Immunohistochemistry procedure: Embryos were rehydrated by adding 1 ml 50% methanol/PBS and incubating for 30 min at RT. Then, 1 ml PBS was added and incubated for 30 min. (These steps and all next steps were done with rocking). 1 ml blocking solution was added and incubated for 1 hour (this was done twice) (Blocking solution: 5% heat-inactivated normal serum of the host species of the secondary antibody in PBST (0.1% Tween20 in PBS)). 0.5 ml of the primary antibody diluted in the appropriate blocking solution was added and incubated with the embryos overnight at 4°C. The next day, embryos were washed with 1 ml PBST: 2x for 1 hour at 4°C and then 6x 30 minutes at RT. Then, 0.5 ml of the secondary antibody diluted in the appropriate blocking solution was incubated with the embryos overnight at 4°C. The next day, embryos were washed with 1 ml PBST: 2x for 1 hour at 4°C and then 6x 30 minutes at RT. Then, the DAB (3,3'diaminobenzidine tetrahydrochloride) solution was prepared by dissolving a DAB-tablet (Sigma) in 10 ml PBST and sterile-filtering the solution (0.45µm filter). The embryos were transferred into a 24-well plate and 1 ml DAB solution was added to each

well. The embryos were incubated for 30 minutes in the dark at RT. Then, 1 µl 30% H_2O_2 was added to each well (to reach a final concentration of 0.03% H_2O_2) and the embryos were incubated in the dark for a maximum of 10 min. (The signal usually came in the first few minutes and the reaction was stopped in order to avoid background by washing 2x with 1 ml of PBS as soon as a clear signal was observed). The embryos were then incubated in PBS at 4°C until imaging.

5.2.6.2 Whole-mount Immunohistochemistry (membrane-targeted GFP)

This method was applied for whole-mount immunohistochemistry with an antibody directed against the GFP protein. This protocol is described in (Huber et al., 2005).

Fixation of embryos: embryos older than E12.5 were eviscerated before fixation. Embryos were fixed for 24 hours at 4°C in 4% PFA/PBS in microcentrifuge tubes with screw caps (rotating). Embryos were then rinsed 3x in PBS and bleached for 24 hours in Dent's bleach (1 part H2O2: 2 parts Dent's Fix) at 4°C (at this step the microcentrifuge tubes were not completely filled since gas production due to H2O2 might push the lid open). Embryos were rinsed 5x in MeOH and then fixed in Dent's Fix (1 part DMSO: 4 parts MeOH) for at least 24 hrs at 4°C and were finally stored in this solution until use.

Whole-mount immunohistochemistry procedure: embryos were rinsed 3x in PBS then washed 3x in PBS (each 1 hour). The primary antibody in blocking solution (5% heat-inactivated normal horse serum, 75% PBS, 20% DMSO) was added and incubated at RT 3-5 days (rotating). Embryos were rinsed 3x in PBS and then washed 5x in PBS (each 1 hour). Secondary antibody in blocking solution was added and incubated at RT for 2 days (rotating). Embryos were rinsed 3x in PBS and then washed 5x in PBS (each 1 hour). Finally, the DAB (3,3'diaminobenzidine tetrahydrochloride) solution was prepared by dissolving a DAB- tablet (Sigma) in 10 ml PBS and sterile-filtering the solution (0.45µm filter). The embryos were transferred into a 24-well plate and 1 ml DAB solution was added to each well. The embryos were incubated for 30 minutes in the dark at RT. Then, 1 µl 30% H_2O_2 was added to each well (to reach a final concentration of 0.03% H_2O_2) and the embryos were incubated in the dark for a maximum of 10 min. (The signal usually came in the first few minutes and the reaction was stopped in order to avoid background by washing 2x with 1 ml of PBS as soon as a clear signal was observed). The embryos were then incubated in PBS at 4°C until imaging.

Clearing of embryos: 1/2 of PBS was withdrawn, replaced with MeOH and left standing for 10 min. Embryos were then washed 3x with MeOH (each 20 min). Then 1/2 of MeOH was withdrawn, replaced with BABB (1 part Benzyl alcohol : 2 parts benzyl benzoate) and left standing for 10 min. Embryos were the cleared in 100% BABB (10 min) then stored in 100% BABB at 4°C.

5.2.7 Image acquisition and analysis

Whole-mount embryo images were acquired using a Nikon Stereomicroscope SMZ1000. Images of in-situ hybridization sections were acquired using a Leica Leitz DMRBE microscope. Immunohistochemical sections images were acquired using an Axioplan 2 fluorescent microscope (Zeiss). Confocal images were acquired using the Olympus BX61W1 FluoView 1000 (FV1000) confocal laser scanning biological microscope (40x oil immersion objective, 1.3 NA). Images were edited and modified using the Adope PhotoShop 6.0 and Adope Illustrator CS5 programs. Cell counting was performed using the Adope Photoshop CS5 program. The programs Excel 2007 and GraphPad Instat3 for the ANOVA test were used for statistical analysis.

6. References

Alexander, T., Nolte, C. and Krumlauf, R. (2009) Hox genes and Segementation of the Hindbrain and Axial Skeleton. *Annu.Rev.Cell.Biol*. 25:431-456.

Arber, S., Han, B., Mendelsohn, M., Smith, M., Jessell, T.M., and Sockanathan , S. (1999) Requirement for the homeobox gene Hb9 in the consolidation of motor neuron identity. *Neuron* 23, 659-674.

Auclair, F., Valdes, N. and Marchand, R. (1996). Rhombomere-specific origin of branchial and visceral motoneurons of the facial nerve in the rat embryo. *J. Comp. Neurol.* 369, 451-461.

Barrow, J. R., Stadler, H. S. and Capecchi, M. R. (2000) Roles of Hoxa1 and Hoxa2 in patterning the early hindbrain of the mouse. *Development* 127, 933–944.

Barlow, L. (2002) Cranial Nerve Development: Placodal Neurons Ride the Crest. *Current Biology* 12, 171-173.

Bell, E., Wingate, R.J.T. and Lumsden, A. (1999) Homeotic Transformation of Rhombomere Identity after Localized *Hoxb1* Missexpression. *Science* 284, 2168-2171.

Bravo-Ambrosio, A. and Kaprielian, Z. (2011). Crossing the border: molecular control of motor axon exit. *Int. J. Mol. Sci.* 12, 8539-8561.

Bravo-Ambrosio, A., Mastick, G., Kaprielian, Z. (2012) Motor axon exit from the mammalian spinal cord is controlled by the homeodomain protein Nkx2.9 via Robo-Slit signaling. *Development* 139, 1435-1446.

Brichta, AM., Callister, RJ., Peterson, EH. (1987) Quantitative analysis of cervical musculature in rats: histochemical composition and motor pool organization. I. Muscles of the spinal accessory complex. *J Comp Neurol* 255:351–368.

Briscoe, J., Sussel, L., Serup, P., Hartigan-O'Connor, D., Jessell, T.M., Rubenstein, J.L. and Ericson, J. (1999) Homeobox gene Nkx2.2 and specification of neuronal identity by graded Sonic hedgehog signaling. *Nature* 398, 622-627.

Briscoe, J. & Ericson, J. (1999) The specification of neuronal identity by graded Sonic hedgehog signalling. *Semin. Cell Dev. Biol.* 10, 353–362.

Briscoe, J., Pierani, A., Jessell, T.M. and Ericson, J. (2000) A homeodomain code specifies progenitor cell identity and neuronal fate in the ventral neural tube. *Cell* 101, 435-445.

Bruce, L.L., Kingsley, J., Nichols, D.H., and Fritzsch, B. (1997). The development of vestibulocochlear efferents and cochlear afferents in mice. *Int. J. Dev. Neurosci.* 15, 671–692.

Chandrasekhar, A. (2004). Turning heads: development of vertebrate branchiomotor neurons. *Dev. Dyn.* 229, 143-161.

Chamberlain, C.E., Jeong, J., Guo, C., Allen, B.L. and McMahon, A.P. (2008) Notochord-derived Shh concentrates in close association with the apically positioned basal body in neural target cells and forms a dynamic gradient during neural patterning. *Development* 135, 1097-1106.

Champagnat, J. and Fortin, G. (1997) Primordial respiratory-like rhythm generation in the vertebrate embryo. *Trends Neurosci.* 20, 119-124.

Charron, F., Stein, E., Joeng, J., McMahon, A.P. and Tessier-Lavigne, M. (2003) The morphogen Sonic hedgehog Is an Axonal Chemoattractant that Collaborates with Netrin-1 in Midline Axon Guidance. *Cell* 113, 11-23.

Colamarino, S.A. and Tessier-Lavigne, M. (1995) The role of the floor plate in axon guidance. *Annu. Rev. Neurosci.* 18, 497-529.

Cordes, S.P. (2001) Molecular genetics of cranial nerve development in mouse. *Nat.Rev. Neurosci*. 2, 611-623.

Cordes SP. (2005) Molecular genetics of the early development of hindbrain serotonergic neurons. *Clin Genet.* 68, 487-494.

Dauger, S., Pattyn, A., Lofaso, F., Gaultier, C., Goridis, C., Gallego, J. and Brunet, JF. (2003) Phox2b controls the development of peripheral chemorecep- tors and afferent visceral pathways. *Development* 130, 6635-6642.

Del brio, M.A, Riera, P., Peruzzo, B. and Rodríguez, E.M. (2001) Hindbrain Floor Plate of the Rat: Ultrastructural Changes Occurring During Development. *Micro.Res. and Tech.* 52, 615-626.

Dessaud, E., Yang, L. L., Hill, K., Cox, B., Ulloa, F., Ribeiro, A., Mynett, A., Novitch, B. G. and Briscoe, J. (2007). Interpretation of the sonic hedgehog morphogen gradient by a temporal adaptation mechanism. *Nature* 450, 717- 720.

Dillon, A.K., Fujita, S.C, Matise, M.P, Jarjour, A.A., Kennedy, T.E., Kollmus, H., Arnold, H.H., Weiner, J.A., Sanes, J.R. and Kaprielian, Z. (2005) Molecular Control of Spinal Accessory Motor Neuron/Axon Development in the Mouse Spinal Cord. *Jour.Neurosci*. 25, 10119-10130.

Ding, Y.-Q., Marklund, U., Yuan, W., Yin, J., Wegman, L., Ericson, J., Deneris, E., Johnson, R.L. & Chen, Z.-F. (2003) Lmx1b is essential for the development of serotonergic neurons. *Nat. Neurosci.*, 9, 933-938.

Dodd, J., Morton, S. B., Karagogeos, D., Yamamoto, M. and Jessell, T. M. (1988). Spatial regulation of axonal glycoprotein expression on subsets of embryonic spinal neurons. *Neuron* 1, 105-116.

Dubreuil, V., Hirsch, M.R., Pattyn, A., Brunet, J-F. and Goridis, C. (2000) The Phox2b transcription factor coordinately regulates neuronal cell cycle exit and identity. *Development* 127, 5191-5201.

Dubreuil, V., Hirsch. M.R., Jouve, C., Brunet, J.F. and Goridis, C. (2002) The role of Phox2b in synchronizing pan-neuronal and type-specific aspects of neurogenesis. *Development*, 129, 5241-5253.

Dubreuil, V., Thoby-Brisson, M., Rallu, M., Persson, K., Pattyn, A., Birchmeier, C., Brunet. J.F., Fortin. G. and Goridis, C. (2009) Defective respiratory rhythmogenesis and loss of central chemosensitivity in Phox2b mutants targeting retrotrapezoid nucleus neurons. *J Neurosci*, 29, 14836-14846.

Dubreuil, V., Ramanantsoa, N., Trochet, D., Vaubourg, V., Amiel, J., Gallego, J., Brunet, J.F. and Goridis, C. (2008) A human mutation in Phox2b causes lack of CO2 chemosensitivity, fatal central apnea, and specific loss of parafacial neurons. *Proc Natl Acad Sci USA*, 105, 1067-1072.

Ericson, J., Thor, S., Edlund, T., Jessell, T.M., and Yamada, T. (1992) Early stages of motor neuron differentiation revealed by expression of homeobox gene Islet-1. *Science* 256, 1555-1560.

Ericson, J., Rashbass, P., Schedl, A., Brenner-Morton, S., Kawakami, A., van Heyningen, V., Jessell, T.M. and Briscoe, J. (1997) Pax6 controls progenitor cell identity and neuronal fate in response to graded Shh signaling. *Cell* 90, 169-180.

Erickson, J.T., Shafer, G., Rossetti, M.D., Wilson, C.G. and Deneris, E.S. (2007) Arrest of 5HT neuron differentiation delays respiratory maturation and impairs neonatal homeostatic responses to environmental challenges. *Res.Phy. and Neuro*. 159, 85-101.

Escurat, M., Djabali, K., Gumpel, M., Gros, F. and Portier, M.M. (1990) Differential expression of two neuronal intermediate-filament proteins, peripherin and low-molecular-mass neurofilament protein (NF-L), during the development of the rat. *J.Neurosci*. 10, 764-784.

Fritzsch B. (1996) Development of the labyrinthine efferent system. *Ann N Y Acad Sci*. 781, 21–33.

Garel, S., Garcia-Dominguez, M. and Charnay, P. (2000) Control of the migratory pathway of facial branchiomotor neurones. *Development*. 127, 5297–5307.

Gaufo, G.O., Flodby, P. and Capecchi, M.R. (2000) Hoxb1 controls effectors of sonic hedgehog and Mash1 signaling pathways. *Development* 127, 5343-5354.

Gaufo, G.O., Wu S. and Capecchi, M.R. (2003) Contribution of Hox genes to the diversity of the hindbrain sensory system. *Development* 131, 1259-1266.

Goddard, J.M., Rossel, M., Manley, N.R. and Capecchi, M.R. (1996). Mice with targeted disruption of Hoxb-1 fail to form the motor nucleus of the VIIth nerve. *Development* 122, 3217-3228.

Gottschall, J., Zenker, W., Neuhuber, W., Mysicka, A. and Muntener, M. (1980) The sternomastoid muscle of the rat and its innervation. *Anat Embryol (Berl)* 160, 285-300.

Gilland, E. and Baker, R. (1993) Conservation of neuroepithelial and mesodermal segments in the embryonic vertebrate head. *Acta Anat* 148, 110-123.

Gray, P.A., Rekling, J.C., Bocchiaro, C.M. and Feldman, J.L. (1999) Modulation of respiratory frequency by peptidergic input to rhythmogenic neurons in the preBötzinger complex. *Science* 286, 1566-1568.

Gray, P.A. (2008) Transcription factors and the genetic organization of brain stem respiratory neurons. *J Appl Physiol* 104, 1513-1521.

Gray, P.A., Hayes, J.A., Ling, G.Y., Llona, I.,Tupa, S., D. Picardo, M.C., Ross, S.E., Hirata, T., Corbin, J.G., Eugenín, J. and A. Del Negro, C. (2010) Developmental Origin of PreBötzinger Complex Respiratory Neurons. *J. Neurosci*. 30, 14883–14895.

Gown, A.M. and Willingham, M.C. (2002) Improved detection of apoptotic cells in archival paraffin sections: immunohistochemistry using antibodies to cleaved caspase 3. *J Histochem Cytochem* 50, 449-454.

Guthrie, S., Muchamore, I., Kuroiwa, A., Marshall, H., Krumlauf, R. and Lumsden, A. (1992) Neuroectodermal autonomy of Hox-2.9 expression revealed by rhombomere transpositions. *Nature* 356, 157-159.

Guthrie, S. (2007). Patterning and axon guidance of cranial motor neurons. *Nat.Rev. Neurosci*. 8, 859-871.

Hartigan, D.J. and Rubenstein, J.L.R. (1996) The cDNA sequence of murine Nkx2.2. *Gene* 168, 271-272.

Hendricks, T., Francis, N., Fyodorov, D. and Deneris, E.S. (1999) The ETS domain factor Pet-1 is an early and precise marker of central serotonin neurons and interacts with a conserved element in serotonergic genes. *J. Neurosci*. 19, 10348-10356.

Hirsch, M.R., Glover, J.C., Dufour, H.D., Brunet, J.F. and Goridis, C. (2007) Forced expression of Phox2 homeodomain transcription factors induces a branchio-visceromotor axonal phenotype. *Dev Biol*, 303, 687-702.

Holz, A., Schaeren-Wiemers, N., Schaefer, C., Pott, U., Colello, R.J., Schwab, M.E. (1996) Molecular and developmental characterization of novel cDNAs of the myelin-associated/oligodendrocytic basic protein. *J Neurosci*, 16, 467-477.

Holz, A., Kollmus, H., Ryge J., Niederkofler, V., Dias, J., Ericson, J., Stoeckli, ET., Kiehn, O. and Arnold, H.H. (2010) The transcription factors Nkx2.2 and Nkx2.9 play a novel role in floor plate development and commissural axon guidance. *Development* 137, 4249-60.

Huber, A. and Huettl, RE. (2011) Cranial nerve fasciculation and Schwann cell migration are impaired after loss of Npn-1. *Developmental Biology* 359, 230-241.

Huber, A.B., Kania, A., Tran, T.S., Gu, C., De Marco Garcia, N., Lieberam, I., Johnson, D., Jessell, T.M., Ginty, D.D., Kolodkin, A.L. (2005) Distinct roles for secreted semaphorin signaling in spinal motor axon guidance. *Neuron* 48, 949-964.

Jacobs, B.L. and Azmitia, E.C. (1992) Structure and function of the brain serotonin system. *Physiol Rev* 72, 165–229.

Jacob, J., Tiveron, M.C., Brunet, J.F., and Guthrie, S. (2000). Role of the target in the pathfinding of facial visceral motor axons. *Mol. Cell. Neurosci*. 16, 14-26.

Jacob, J., Hacker A. and Guthrie, S. (2001) Mechanisms and molecules in motor neuron specification and axon pathfinding. *Bioassays*. 23, 582-595.

Jacob, J., Ferri, A.L., Milton, C., Prin, F., Pla, P., Lin, W., Gavalas, A., Ang, S.L., and Briscoe, J. (2007) Transcriptional repression coordinates the temporal switch from motor to serotonergic neurogenesis. *Nat.Neuro.* 10, 1433-1439.

Jessell, T.M., Bovolenta, P., Placzek, M., Tessier-Lavigne, M. and Dodd, J. (1989) Polarity and patterning in the neural tube: the origin and function of the floor plate. *Ciba Found Symp*. 144, 255-276.

Jessell, T.M. and Dodd, J. (1990) Floor plate-derived signals and the control of neural cell pattern in vertebrates. *Harvey Lect.*86, 87-128.

Jessell, T.M. (2000) Neuronal specification in the spinal cord: inductive signals and transcriptional codes. *Nat.Rev.Genet*. 1, 20-29.

Jeong, J. and McMahon, A.P. (2005) Growth and pattern of the mammalian neural tube are governed by partially overlapping feedback activities of the hedgehog antagonists patched 1 and Hhip1. *Development* 132, 143-154.

Kandel, E.R., Schwartz, J.H. and Jessell, TM. (2000) Principles of neural science. 4. New York: McGraw Hill.

Kiyasova, V. and Gaspar, P. (2011) Development of raphe serotonin neurons from specification to guidance. *Eur. Jour. Neuro*, 34, 1553-1562.

Kretzschmar, K. and Watt, F.M. (2012) Lineage Tracing. *Cell* 148, 33-45.

Krumlauf R. (1994) Hox genes in vertebrate development. *Cell* 78, 191-201.

Lek, M., Dias, J.M., Marklund, U., Uhde, C.W., Kurdija S., Lei, Q., Sussel, L., Rubenstein, J.L., Matise, M.P., Arnold, H.H., Jessell, T.M. and Ericson, J. (2010) A homeodomain feedback circuit underlies step-function interpretation of a Shh morphogen gradient during ventral neural patterning. *Development* 137, 4051-4060.

Lidov, H.G. and Molliver, M.E. (1982) Immunohistochemical study of the development of serotonergic neurons in the rat CNS. *Brain Res. Bull*. 9, 559-604.

Litingtung, Y. and Chiang, C. (2000) Control of Shh activity and signaling in the neural tube. *Dev. Dyn.* 219, 143-154.

Lucki, I. (1998) The spectrum of behaviors influenced by serotonin. *Biol. Psychiatry* 3, 151-162.

Lumsden, A. and Keynes, R. (1989) Segmental patterns of neuronal development in the chick hindbrain. *Nature* 337, 424-428.

Marti, E., Takada, R., Bumcrot, D.A., Sasaki, H. and McMahon, A.P. (1995) Distribution of Sonic hedgehog peptides in the developing chick and mouse embryo. *Development* 121, 2537-2547.

Manzanares, M., Trainor, P.A., Nonchev, S., Ariza-McNaughton, L., Brodie, J., Gould, A., Marshall, H., Morrison, A., Kwan, C.T., Sham, M.H., Wilkinson, D.G. and Krumlauf, R. (1999) The role of kreisler in segmentation during hindbrain development. *Dev. Biol.* 211, 220-237.

McKay, I.J., Muchamore, I., Krumlauf, R., Maden, M., Lumsden, A. and Lewis, J. (1994) The kreisler mouse: a hindbrain segmentation mutant that lacks two rhombomeres. *Development* 120, 2199-2211.

Mellen, N.M. and Thoby-Brisson, M. (2012) Respiratory circuits: development, function and models. *Curr. Op. in Neuro.* 22:1-10.

Mizuguchi, R., Sugimori, M., Takebayashi, H., Kosako, H., Nagao, M., Yoshida, S., Nabeshima, Y., Shimamura, K., and Nakafuku, M. (2001). Combinatorial roles of olig2 and neurogenin2 in the coordinated induction of pan-neuronal and subtype-specific properties of motoneurons. *Neuron 31*, 757-771.

Muhr, J., Andersson, E., Persson, M., Jessell, T.M., and Ericson, J. (2001). Groucho-mediated transcriptional repression establishes progenitor cell pattern and neuronal fate in the ventral neural tube. *Cell* 104, 861-873.

Mulkey DK, Stornetta RL, Weston MC, Simmons JR, Parker A, Bayliss DA, Guyenet PG (2004) Respiratory control by ventral surface chemoreceptor neurons in rats. *Nat Neurosci* 7, 1360-1369.

Müller, T., Brohmann, H., Pierani, A., Heppenstall, P.A., Lewin, G.R., Jessell, T.M., and Birchmeier, C. (2002) The Homeodomain Factor Lbx1 Distinguishes Two Major Programs of Neuronal Differentiation in the Dorsal Spinal Cord. *Neuron* 34, 551–562.

Müller, M., Jabs, N., Lorke, D,E., Fritzsch, B., and Sander M. (2003) Nkx6.1 controls migration and axon pathfinding of cranial branchio-motoneurons. *Development* 130, 5815-5826.

Murphy, P., Davidson, D.R. and Hill, R.E. (1989) Segment-specific expression of a homeobox-containing gene in the mouse hindbrain. *Nature* 341, 156-159.

Muzumdar, M.D., Tasic, B., Miyamichi, K., Li, L. and Luo, L. (2007). A global double-fluorescent Cre reporter mouse. *Genesis* 45, 593-605.

Nattie, E.E. and Li, A. (2002) Substance P-saporin lesion of neurons with NK1 receptors in one chemoreceptor site in rats decreases ventilation and chemosensitivity. *J Physiol* 544:603-616.

Niederlander, C., and Lumsden, A. (1996). Late emigrating neural crest cells migrate specifically to the exit points of cranial branchiomotor nerves. *Development* 122, 2367-2374.

Novitch, B., Chen, A.I., and Jessell, T.M. (2001) Coordinate regulation of motor neuron subtype identity and pan-neural properties by the bHLH repressor Olig2. *Neuron* 31, 773-789.

Oldstone, M.B., Lewicki, H., Thomas, D., Tishon, A., Dales, S., Patterson, J., Manchester, M., Homann, D., Naniche, D. and Holz, A. (1999) Measles virus infection in a transgenic model: virus-induced immunosuppression and central nervous system disease. *Cell* 98, 629-640.

Ong, C.K., and Chong, V.F.H. (2010). The glossopharyngeal, vagus and spinal accessory nerves. *European journal of radiology*, 74, 359-367.

Onimaru, H., Ikeda, K. and Kawakami, K. (2008) CO2-sensitive preinspiratory neurons of the parafacial respiratory group express Phox2b in the neona-tal rat. *J Neurosci* 28, 12845–12850.

Ono, Y., Nakatani, T., Minaki, Y. and Kumai, M. (2010) The basic helix-loop-helix transcription factor Nato3 controls neurogenic activity in mesencephalic floor plate cells. *Development* 137, 1897-906.

Orban, P. C., Chui, D., Marth, J. D. (1992) Tissue- and site-specific DNA recombination in transgenic mice. *Proc. Natl Acad. Sci. USA* 89 (15): 6861 – 6865.

Pabst, O., Herbrand, H. and Arnold, H.H. (1998) Nkx2.9 is a novel homeobox transcription factor which demarcates ventral domains in the developing mouse CNS. *Mech. Dev.* 73, 85-93.

Pabst, O., Herbrand, H., Takuma, N. and Arnold, H.H. (2000) NKX2 gene expression in neuroectoderm but not in mesendodermally derived structures depends on sonic hedghog in mouse embryos. *Dev.Genes Evol*. 210, 47-50.

Pabst, O., Rummlies, J., Winter, B. and Arnold, H.H. (2003) Targeted disruption of the homeobox gene Nkx2.9 reveals a role in development of the spinal accessory nerve. *Development* 130, 1193-1202.

Pagliardini, S., Ren, J. and Greer, J.J. (2003) Ontogeny of the pre-Bötzinger complex in perinatal rats. *J Neurosci* 23, 9575-9584.

Pagliardini, S., Ren, J., Gray, P.A., Vandunk, C., Gross, M., Goulding, M. and Greer JJ. (2008) Central respiratory rhythmogenesis is abnormal in Lbx1- deficient mice. *J Neurosci* 28, 11030-11041.

Pattyn, A., Morin, X., Cremer, H., Goridis, C. and Brunet, J.F. (1997) Expression and interactions of the two closely related homeobox genes Phox2a and Phox2b during neurogenesis. *Development* 124, 4065-4075.

Pattyn, A., Hirsch, M., Goridis, C. and Brunet, J.F. (2000) Control of hindbrain motor neuron differentiation by the homeobox gene Phox2b. *Development* 127, 1349-1358.

Pattyn, A., Vallstedt, A., Dias, J.M., Samad, O.A., Krumlauf, R., Rijli, F.M., Brunet, J.F. and Ericson, J. (2003a). Coordinated temporal and spatial control of motor neuron and serotonergic neuron generation from a common pool of CNS progenitors. *Genes Dev*. 17, 729-737.

Pattyn, A., Vallstedt, A., Dias, J.M., Sander, M. and Ericson, J. (2003b) Complementary roles for Nkx6 and Nkx2 class proteins in the establishment of motoneuron identity in the hindbrain. *Development* 130, 4149-4159.

Pfaff, S.L., Mendelsohn, M., Stewart, C.L., Edlund, T. and Jessell, T.M. (1996) Requirement for LIM homeobox gene *Isl1* in motor neuron generation reveals a motor neuron-dependent step in interneuron differentiation. *Cell* 84, 309-320.

Placzek, M. and Briscoe, J. (2005) The floor plate: multiple cells, multiple signals. *Nat.Rev.Neurosci*. 6, 230-240.

Price, M., Lazzaro, D., Pohl, T., Mattei, M.G., Ruther, U., Olivo, J.C., Duboule, D. and DiLauro, R. (1992) Regional expression of the homeobox gene Nkx2.2 in the developing mammalian forebrain. *Neuron* 8, 241-255.

Ribes, V., Balaskas, N., Sasai, N., Cruz, C., Dessaud, E., Cayuso, J., Tozer, S., Yang, L.L., Novitch, B., Marti, E., Briscoe, J. (2010) Distinct Sonic hedgehog signaling dynamics specify floor plate and ventral neuronal progenitors in the vertebrate neural tube. *Genes Dev.* 24, 1186-1200.

Richerson, G.B. (2004) Serotonergic neurons as carbon dioxide sensors that maintain pH homeostasis. *Nat.Rev.Neurosci*. 5, 449-461.

Rodríguez E.M., Del Brío León, M.A., Riera, P., Menendez, J. and Schoebitz, K. (1996) The floor plate of the hindbrain is a highly specialized gland. Immunocytochemical and ultrastructural characteristics. *Dev.Brain.Res.* 97, 153-168.

Rossel, M. and Capecchi, M.R. (1999) Mice mutant for both Hoxa1 and Hoxb1 show extensive remodeling of the hindbrain and defects in craniofacial development. *Development* 126, 5027-5040.

Ruiz i Altaba, A., Placzek, M., Baldassare, M., Dodd, J. and Jessell, T.M. (1995) Early stages of notochord and floor plate development in the chick embryo defined by normal and induced expression of HNF-3 beta. *Dev. Biol.* 170, 299-313.

Ryan, S., Blyth, P., Duggan, N., Wild, M. and Al-Ali S. (2007) Is the cranial accessory nerve really a portion of the accessory nerve? Anatomy of the cranial nerves in the jugular foramen. *Anat Sci Int*; 82, 1-7.

Sasaki, H. and Hogan, B.L. (1994) HNF-3 beta as a regulator of floor plate development. *Cell* 76, 103-115.

Sander, M., Paydar, S., Ericson, J., Briscoe, J., Berber, E., German, M., Jessell, T. M. and Rubenstein, J. L. (2000). Ventral neural patterning by Nkx homeobox genes: Nkx6.1 controls somatic motor neuron and ventral interneuron fates. *Genes Dev.* 14, 2134-2139.

Shirasaki, R. & Pfaff, S. L. (2002) Transcriptional codes and the control of neuronal identity. *Annu. Rev. Neurosci.* 25, 251-281.

Schneider-Maunoury, S., Seitanidou, T., Charnay, P. and Lumsden, A. (1997). Segmental and neuronal architecture of the hindbrain of Krox-20 mouse mutants. *Development* 124, 1215-1226.

Schubert, W. and Kaprielian, Z. (2001) Identification and characterization of a cell surface marker for embryonic rat spinal accessory motor neurons. *J. Comp. Neurol.* 439, 368-383.

Snider, W.D. and Palavali, V. (1990) Early axon and dendritic outgrowth of spinal accessory motor neurons studied with DiI in fixed tissues. *J. Comp. Neurol.* 297, 227-238.

Sieber, M.A., Storm, R., Martinez-de-la-Torre, M., Müller, T., Wende, H., Reuter, K., Vasyutina, E. and Birchmeier C. (2007) Lbx1 acts as a selector gene in the fate determination of somatosensory and viscerosensory relay neu- rons in the hindbrain. *J Neurosci* 27: 4902-4909.

Sharma, K., Sheng, H.Z., Lettieri, K., Li H., Karavanov, A., Potter, S., Westphal, H. and Pfaff, S.L. (1998) LIM homeodomain factors *Lhx3* and *Lhx4* assign subtype identities for motor neurons. *Cell* 95, 817-828.

Song, M.R. (2007) Moving Cell Bodies: Understanding the Migratory Mechanism of Facial Motor Neurons. *Arch Pharm Res* 30, 1273-1282.

Song, M.R., Shirasaki, R., Cai, C.-L., Ruiz, E., Evans, S.M., Lee S.-K. and Pfaff S. (2006) T-Box transcription factor Tbx20 regulates a genetic program for cranial motor neuron cell body migration. *Development* 133, 4945-4955.

Soriano, P. (1999). Generalized lacZ expression with the ROSA26 Cre reporter strain. *Nat. Genet.* 21, 70-71.

Stornetta, R.L., Rosin, D.L., Wang, H., Sevigny, C.P., Weston, M.C. and Guyenet, P.G. (2003) A group of glutamatergic interneurons expressing high levels of both neurokinin-1 receptors and somatostatin identifies the region of the pre-Botzinger complex. *J Comp Neurol* 455, 499-512.

Stornetta, R.L., Moreira, T.S., Takakura, A.C., Kang, B.J., Chang, D.A., West, G.H., Brunet, J.F., Mulkey, D.K., Bayliss, D.A. and Guyenet, P.G. (2006) Expression of Phox2b by brainstem neurons involved in chemosensory integration in the adult rat. *J Neurosci* 26, 10305-10314.

Strähle, U., Lam, C.S., Ertzer, R. and Rastegar, S. (2004) Vertebrate floor plate specification: variations of common themes. *Trends Genet*. 20, 155-162.

Studer, M., Lumsden, A., Ariza-Mcnaughton, L., Bradley, A. and Krumlauf, R. (1996) Altered segmental identity and abnormal migration of motor neurons in mice lacking *Hoxb-1*. *Nature* 384, 630-634.

Sussel, L., Kalamaras, J., Hartigan-O'Connor, D.J., Meneses, J.J., Pedersen, R.A., Rubenstein, J.L. and German, M.S. (1998) Mice lacking the homeodomain transcription factor Nkx2.2 have diabetes due to arrested differentiation of pancreatic beta cells. *Development* 125, 2213-2221.

Tan, W., Pagliardini, S., Yang, P., Janczewski, W.A. and Feldman, J.L. (2010) Projections of preBötzinger Complex neurons in adult rats. *J. Comp. Neurol.* 518, 1862-1878.

Tanabe, Y. and Jessell, T.M. (1996) Diversity and pattern in the developing spinal cord. *Science* 274, 1115-1123.

Takebayashi, H., Yoshida, S., Sugimori, M., Kosako, H., Kominami, R., Nakafuku, M., and Nabeshima, Y. (2000) Dynamic expression of basic helix-loop-helix Olig family members: implication of Olig2 in neuron and oligodendrocyte differentiation and identification of a new member, Olig3. *Mech. Dev.* 99, 143-148.

Thaler, J., Harrison, K., Sharma, K., Lettieri, K., Kehrl, J. and Pfaff, S.L. (1999) Active suppression of interneuron programs within developing motor neurons revealed by analysis of homeodomain factor HB9. *Neuron* 23, 675-687.

Thoby-Brisson, M., Karle´n, M., Wu, N., Charnay, P., Champagnat, J. and Fortin, G. (2009) Genetic identification of an embryonic parafacial oscillator coupling to the pre-Bötzinger complex. *Nat Neurosci* 12, 1028-1035.

Thoby-Brisson M, Bouvier, J., Glasco, D.M., Stewart, M.E., Dean, C., Murdoch, J.N., Champagnat, J., Fortin, G. and Chandrasekhar, A. (2012) Brainstem Respiratory Oscillators Develop Independently of Neuronal Migration Defects in the Wnt/PCP Mouse Mutant looptail. *Plos One* 7, 1-12.

Tiveron, M.C., Pattyn, A., Hirsch, M.R. and Brunet, J.F. (2003). Role of Phox2b and Mash1 in the generation of the vestibular efferent nucleus. *Dev. Biol.* 260, 46-57.

Vallstedt, A., Muhr, J., Pattyn, A., Pierani, A., Mendelsohn, M., Sander, M., Jessell, T.M. and Ericson, J. (2001) Different levels of repressor activity assign redundant and specific roles to Nkx6 genes in motor neuron and interneuron specification. *Neuron* 31, 743-755.

Wentworth, L.E. and Hinds, J.W. (1978) Early motor neuron formation in the cervical spinal cord of the mouse: an electron microscopic, serial section analysis. *J Comp Neurol* 177:611-634.

Wilkinson, D.G., Bhatt, S., Cook, M., Boncinelli, E. and Krumlauf, R. (1989) Segmental expression of Hox-2 homoeobox-containing genes in the developing mouse hindbrain. *Nature* 341, 405-409.

Xiong, F., Tentner, A.R., Huang, P., Gelas, A., Mosaliganti, K.R., Souhait, L., Rannou, N., Swinburne, I.A., Obholzer, N.D., Cowgill, P.D., Schier, A.F. and Megason, S.G. (2013) Specified Neural Progenitors Sort to Form Sharp Domains after Noisy Shh Signaling. *Cell* 153, 550-561.

Yamada, T., Pfaff, S. L., Edlund, T. and Jessell, T. M. (1993) Control of cell pattern in the neural tube: motor neuron induction by diffusible factors from notochord and floor plate. *Cell* 73, 673-686.

Zagrebelsky, M., Holz, A., Dechant, G., Barde, Y.A., Bonhoeffer, T. and Korte, M. (2005) The p75 neurotrophin receptor negatively modulates dendrite complexity and spine density in hippocampal neurons. *J Neurosci.* 25, 9989-9999.

Zhang, L., Yoshimura, Y., Hatta, T., and Otani, H. (2000). Reconstructing the pathway of the tensor veli palatini motor nerve during early mouse development. *Anat. Embryol. (Berl.)* 201, 235-244.

Zhang, Y., Narayan, S., Geiman, E., Lanuza, G. M., Velasquez, T., Shanks, B., Akay, T., Dyck, J., Pearson, K., Gosgnach, S., Fan, C.M. and Goulding, M. (2008) V3 spinal neurons establish a robust and balanced locomotor rhythm during walking. *Neuron* 60, 84-96.

Zhou, Q. and Anderson, D.J. (2002) The bHLH transcription factors OLIG2 and OLIG1 couple neuronal and glial subtype specification. *Cell* 109, 61-73.

7. Supplementary Material

7.1 Supplementary Figures

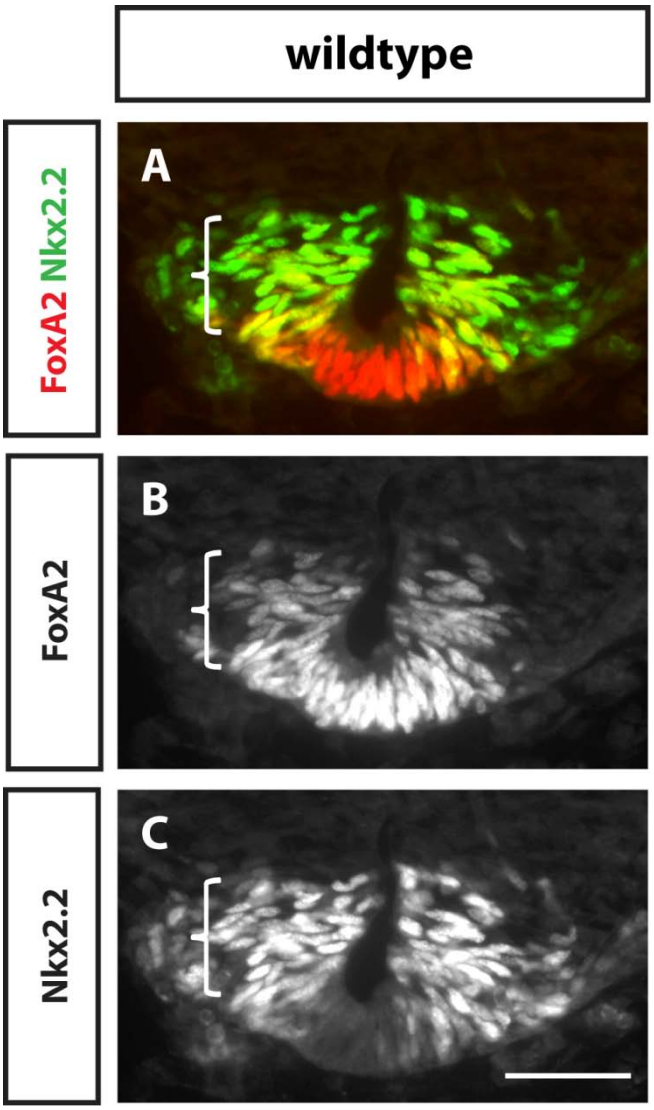

Fig.S1: FoxA2 and Nkx2.2 are co-expressed in p3 progenitor cells of the hindbrain in E10.5 wildtype mouse embryos. An immunohistochemistry was performed on a transverse section in r7 of a wildtype embryo with antibodies directed against the Nkx2.2 (green) and the FoxA2 (red) transcription factors. FoxA2 is expressed in midline floor plate cells (red) and is co-expressed with Nkx2.2 in the p3 progenitor domain cells (yellow). The bracket marks the p3 progenitor domain. Scale bar: 50µm.

7.2 List of Figures

7.3 Frequently used abbreviations

bvMNs	branchiovisceral motor neurons
sMNs	somatic motor neurons
GFP	green fluorescent protein
RTN	retrotrapezoid nucleus
preBötC	pre-Bötzinger complex
FGF	fibroblast growth factors
PG	paralogous groups
Shh	Sonic hedgehog
TF	transcription factor
r	rhombomere
CNS	central nervous system
C	cervical
FBM	facial branchial motor
SAN	spinal accessory nerve
A/P	antero-posterior
ORF	open reading frame
Cre	Cre recombinase
FP	floor plate

7.4 Acknowledgements

First and foremost, I wish to thank Allah, for blessing me with health and patience to complete this work. I would like to express my appreciation and gratitude to my mentor Prof. Dr. Hans-Henning Arnold for providing the great opportunity to work on this interesting research project as well as for his continuous encouragement, advice and support throughout this study. I am extremely grateful for his critical comments that have added much to this work. I am also thankful to Prof. Dr. Martin Korte and Prof. Dr. Reinhard Köster for their unhesitant consent to be members of the examination committee. My gratitude goes to my supervisor Dr. Andreas Holz for his ongoing support and guidance in the laboratory, for the fruitful scientific discussions and for critically reading my thesis. The *Nkx2.2*^{cre} knockin mouse used in this study was kindly generated by Dr. Andreas Holz. I would like to thank Dr. Franz Vauti for conducting the ES cell transfer needed for generating the *Nkx2.2*^{cre} knockin mouse. Special thanks go to Jana Pravemann for the open-book preparations and for her help in many aspects. I am greatly thankful to all present and past members of the cell and Molecular Biology Department, in particular Alex Wolf, Iris Linde, Dr. Barbara Winter, Franziska Resch, Dr. Astrid Buchberger, Gabriele Erxleben and Dr. Ines Lahmann for their technical assistance, genotyping mice, sharing expertise, words of encouragement and mainly for the pleasant working atmosphere. Furthermore, I would like to thank the members of the "Zentrale Einrichtung für Tierhaltung" especially Claudia Schulze for taking care of our mice. I also wish to thank the Cellular Neurobiology group for granting me access to the fluorescent microscope. My sincere appreciation goes to Dr. Marta Zagrebelsky for giving us the opportunity and helping us to take images on the confocal microscope. I thank Prof. Dr. Carmen Birchmeier for the Lbx1 antibody, Prof. Dr. Jean-François Brunet for the Phox2b antibody and Prof. Dr. Marie-Madeleine Portier for the cDNA of Peripherin. I wish to thank Prof. Dr. Swen Hülsmann from the University of Göttingen for the plethysmographic measurements of our mouse embryos. A special thanks go to my family in Germany for making me feel home. Words cannot express how grateful I am to my grandmother Amal and my aunt Arfaa for their continuous care and love. I am grateful to my friends in Jordan, especially Aziza, for their ongoing support. I would like to express my deepest appreciation to my beloved parents, Ghaleb and Asmaa, and my lovely sister Rania, who supported me in every step during my study even though they were miles away. Their prayer for me, their encouragement and love was what sustained me thus far. I am appreciative from all my heart of my soul mate Bashar who supported me with his positive energy in every aspect. Bashar and my mother Asmaa incented me to strive towards my goals. I would like to dedicate this work in loving memory of my mother Asmaa, may Allah have mercy on her. Finally, this work was supported by a grant of the Deutsche Forschungsgemeinschaft (DFG).